

**Preparation and Characterization of Mixed Metal Oxides as  
Solid Catalysts for Transesterification of Triglycerides**

**A Thesis  
Submitted in the fulfillment of the requirement for the  
Degree of**

**Doctor of Philosophy  
by**

**Mandeep Kaur  
(Regn. No. 900909014)**



**Under the supervision of  
Dr. Amjad Ali  
*Associate professor***

**SCHOOL OF CHEMISTRY AND BIOCHEMISTRY  
THAPAR UNIVERSITY  
PATIALA – 147004  
October – 2014**

## **ACKNOWLEDGEMENTS**

*It is always hard to look back and try to remember all of those kind individuals who have helped me during my Ph.D. I would like to say 'thank you' to all of them.*

*Foremost, I would like to express my sincere gratitude to my mentor Dr. Amjad Ali, School of Chemistry and Biochemistry, Thapar University, Patiala for the continuous support of my Ph.D. study and research, for his patience, motivation, enthusiasm, and immense knowledge. His guidance helped me in all the time of research and writing of this thesis. I could not have imagined having a better advisor and mentor for my Ph.D. study. He supported me throughout my work with patience and knowledge whilst allowing me the room to work in my own way. He has always been a pillar of support and constant source of inspiration. His commitment and sense of mission has molded my work to provide it direction and substance.*

*I am extremely thankful to the Director, Thapar University, Dean (Research & Sponsored Projects), Head and other faculty members of School of Chemistry & Biochemistry for extending the opportunity to undertake this doctoral research.*

*I am highly obliged to Dr. Arvind Kumar and Dr. Indrajit Mukhopadhyay from CSMCRI-Bhavnagar, Gujarat for directing my study through their valuable inputs. I am grateful to Dr. K. J. Prathap, Technion Israel Institute of Technology, Israel, Dr. Tejwant Singh, Kyushu University, Japan, Dr. Yogesh Kumar, KAUST, Saudi Arabia, Dr. B. P. Tripathi, Leibniz-Institut für Polymerforschung, Dresden, Germany & Amrita Ghosh, Biefeld University, Germany for having faith in me. I am thankful to Dr. Harsh Manchanda and Dr. S. B. S. Mishra from NIT, Jalandhar for enormous encourage and support.*

*I would be failing in my duties if I do not mention University Grants Commission (UGC), New Delhi for providing fellowship and the members of the doctoral committee for monitoring my research work from time to time and giving their valuable suggestions.*

*I would like to acknowledge Dr. B. Sreedhar, IICT Hyderabad for XPS analysis and Mr. Avtar Singh, Mr. Dinesh Sharma and Mr. Jagtar Singh Panjab University, Chandigarh for their ingenious skills of carrying out NMR, SEM, TEM and XRD. In lab-I have been aided for many years in running the equipment by Mr. Chander Singh, a fine technician.*

*This journey would not have been the same without my seniors, Dr. Dinesh Kumar, Dr. Joginder Singh, Dr. Nirankar Singh, Dr. Vishal Mutreja, Dr. Pawan Upadhyay, Ahmad Firoz and*

*Dr. Madhu Katiyar, and my very special friends Rupinder Makkar, Rajwant Kaur, Gurpreet Kaur, Sandeep Kaur, Navjot Kaur, Abida, Alka Sharma, Poonam Bhatia, Pankil, Gurdeep Kaur, Rishu Jain, Tapsi Nagpal, Mani Mahajan, Rohit Singh, Inderpreet Singh, Bhupender Pal, Akul Sen Gupta, Ankush Sharma, Rajesh Kumar, Sandeep Kumar, K. Munnusamy, Anjan Das, Prasantha Bera, S. Sarvanan, Chandu Madankar, Tamal Roy, Sivashunmugam Sankaranarayanan, Thillai Sivakumar, Murugnathan Packriswamy, Arpan Shah, Srinivasan Rao, Siddharth Mohan, Sidharth and Samir Dharmadhikari. They were always there for me.*

*At the same time, I would express thanks to my beloved family, my mother, my elder brother, my sister-in-law and my little sister for their infinite patience and unending support. Their continual warm care make me grow up happily, their unselfish dedication make my life without worries, and their unwavering supporting make me devote all my efforts to studies.*

*Hope my dear father has a peace life in the heaven.*

*Last but not the least; I am thankful to the Almighty, who has provided me sound health and strength to complete this work. What I am and what I would be I owe to the Almighty for leading me the path of Light and Success.*

*Words are forgotten.....*

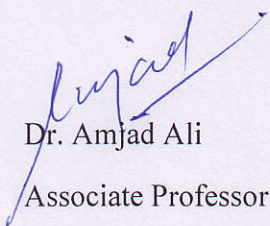
*Memories are remembered.....*

*Mandeep Kaur*

*Mandeep Kaur*

## **CERTIFICATE**

This is to certify that thesis entitled "PREPARATION AND CHARACTERIZATION OF MIXED METAL OXIDES AS SOLID CATALYSTS FOR TRANSESTERIFICATION OF TRIGLYCERIDES", being submitted by Mandeep Kaur, to the School of Chemistry and Biochemistry, Thapar University, Patiala for the award of degree of DOCTOR OF PHILOSOPHY, is a record of bonafide research work carried out by her. Ms. Mandeep Kaur has worked under my guidance and supervision and has fulfilled the requirements for the submission of this thesis, which to my knowledge has reached the requisite standard. The results embodied in the thesis have not been submitted in part or full to any other University or Institute for the award of any degree or diploma.



Dr. Amjad Ali

Associate Professor

School of Chemistry and Biochemistry,

Thapar University, Patiala.

---

---

# CONTENTS

| Chapter   | Title  | Page Number |
|-----------|--|-------------|
|           | List of abbreviations  | i           |
|           | List of symbols  | ii          |
|           | List of figures  | iii         |
|           | List of tables   | vii         |
|           | Abstract   | ix          |
| <b>1.</b> | <b>Introduction and literature review</b>  |             |
| 1.1       | Introduction   | 1           |
| 1.2       | Biodiesel  | 2           |
| 1.3       | Feedstock for biodiesel production   | 3           |
| 1.4       | Alcohols used for biodiesel production   | 6           |
| 1.5       | Catalysis  | 7           |
| 1.5.1     | Homogeneous base catalyst  | 7           |
| 1.5.2     | Homogeneous acid catalyst  | 10          |
| 1.6       | Heterogeneous catalyst   | 13          |
| 1.6.1     | Single metal oxides catalysts  | 14          |
| 1.6.2     | Mixed metal oxides catalysts   | 15          |
| 1.6.1.2   | Basic mixed metal oxide catalysts  | 17          |
| 1.6.1.2   | Acidic mixed metal oxide catalysts   | 21          |
| 1.7       | Conclusions  | 24          |
| 1.8       | Objectives   | 25          |
|           | References   | 26          |
| <b>2.</b> | <b>Materials and methods</b>   |             |
| 2.1       | Chemicals  | 40          |
| 2.2       | Chemical analysis of vegetable oils  | 40          |
| 2.3       | Fatty acid composition of vegetable oils   | 41          |
| 2.4       | Thin layer chromatography (TLC)  | 41          |
| 2.5       | Instruments  | 42          |
|           | References   | 46          |
| <b>3.</b> | <b>Potassium Fluoride Impregnated CaO/NiO: An Efficient Heterogeneous Catalyst for Transesterification of Waste cottonseed oil</b> |             |
| 3.1       | Introduction   | 47          |
| 3.2       | Experimental section   | 48          |
| 3.2.1     | Catalyst preparation   | 48          |
| 3.2.2     | Transesterification of waste cottonseed oil  | 48          |

---

---

---

|           |   |    |
|-----------|---|----|
| 3.2.3     | Reaction kinetics   | 48 |
| 3.3       | Results and discussions   | 49 |
| 3.3.1     | Catalyst characterization   | 49 |
| 3.3.1.1   | SEM and TEM analysis  | 49 |
| 3.3.1.2   | BET surface area and Basic strength   | 50 |
| 3.3.1.3   | Powder X-ray diffraction study  | 51 |
| 3.3.2     | FAMEs characterization by <sup>1</sup> H NMR  | 52 |
| 3.4       | Catalytic activity of KF/CaO/NiO  | 54 |
| 3.4.1     | Effect of Impregnated KF Concentration and catalyst concentration on FAMEs yield                                    | 55 |
| 3.4.2     | Effect of Reaction Temperature and molar ratio on FAMEs yield   | 56 |
| 3.5       | Effect of FFA on catalyst activity  | 57 |
| 3.6       | Reusability of the catalyst   | 58 |
| 3.7       | Kinetic study   | 60 |
| 3.8       | Physicochemical properties of the FAMEs   | 61 |
| 3.9       | Conclusions   | 62 |
|           | References  | 63 |
| <b>4.</b> | <b>Ethanolysis of Waste cottonseed oil over Lithium Impregnated Calcium oxide: Kinetics and Reusability studies</b> |    |
| 4.1       | Introduction  | 66 |
| 4.2       | Experimental section  | 66 |
| 4.2.1     | Catalyst preparation  | 66 |
| 4.2.2     | Transesterification of waste cottonseed oil   | 66 |
| 4.3       | Results and discussion  | 67 |
| 4.3.1     | Catalyst characterization   | 67 |
| 4.3.1.1   | BET surface area and basic strength   | 67 |
| 4.3.1.2   | Powder X-ray diffraction  | 67 |
| 4.3.1.3   | SEM and TEM analysis  | 68 |
| 4.3.2     | FAMEs and FAEEs characterization by <sup>1</sup> HNMR   | 69 |
| 4.4       | Catalytic activity  | 72 |
| 4.4.1     | Effect of Impregnated lithium ion concentration and catalyst concentration  | 72 |
| 4.4.2     | Effect of reaction temperature  | 73 |
| 4.4.3     | Effect of ethanol/oil molar ratio   | 74 |
| 4.5       | Effect of the FFA on catalyst activity  | 75 |
| 4.5       | Catalyst Reusability and Homogeneous contribution   | 76 |
| 4.6       | Kinetic study   | 79 |
| 4.7       | Physicochemical properties of FAEEs   | 80 |

---

---

|           |  |     |
|-----------|--|-----|
| 4.8       | Conclusions  | 81  |
|           | References   | 82  |
| <b>5.</b> | <b>An Efficient and Reusable Li/NiO Heterogeneous Catalyst for Ethanolysis of Waste Cottonseed oil</b>       |     |
| 5.1       | Introduction   | 85  |
| 5.2       | Experimental section   | 85  |
| 5.2.1     | Catalyst preparation   | 85  |
| 5.2.2     | Transesterification reaction   | 86  |
| 5.3       | Results and discussion   | 86  |
| 5.3.1     | Catalyst characterization  | 86  |
| 5.3.1.1   | FESEM and HRTEM analysis   | 86  |
| 5.3.1.2   | Powder X-ray diffraction study   | 88  |
| 5.3.1.3   | BET surface area and basic strength study  | 88  |
| 5.3.1.4   | XPS study  | 89  |
| 5.3.2     | Influence of reaction conditions on ethanolysis of WCO   | 90  |
| 5.4       | Effect of FFA on catalyst activity   | 93  |
| 5.5       | Evaluation of the recyclability and homogeneous contribution   | 94  |
| 5.6       | Kinetic study  | 97  |
| 5.7       | Proposed mechanism for transesterification   | 97  |
| 5.8       | Conclusions  | 99  |
|           | References   | 100 |
| <b>6.</b> | <b>Tungsten Supported Ti/SiO<sub>2</sub> Nanoflowers: Mesoporous Solid Catalyst for Biodiesel Production</b> |     |
| 6.1       | Introduction   | 104 |
| 6.2       | Experimental section   | 105 |
| 6.2.1     | Catalyst preparation   | 105 |
| 6.2.2     | Transesterification reaction   | 105 |
| 6.3       | Results and discussion   | 106 |
| 6.3.1     | Catalyst characterization  | 106 |
| 6.3.1.1   | Powder X-ray diffraction study   | 106 |
| 6.3.1.2   | BET surface area study   | 107 |
| 6.3.1.3   | FESEM analysis   | 109 |
| 6.3.1.4   | HRTEM analysis   | 110 |
| 6.3.1.5   | XPS study  | 111 |
| 6.3.1.6   | TPD analysis   | 112 |
| 6.3.2     | Catalytic activity   | 113 |
| 6.4       | Effect of FFA on catalyst activity   | 116 |
| 6.5       | Evaluation of the recyclability and homogeneous contribution   | 117 |

---

---

|           |  |     |
|-----------|--|-----|
| 6.6       | Kinetic study  | 120 |
| 6.7       | Conclusions  | 121 |
|           | References   | 122 |
| <b>7.</b> | <b>Na/CaO/Fe<sub>3</sub>O<sub>4</sub> as Nano Magnetic Catalyst for the Ethanolysis and Methanolysis of Waste cottonseed oil</b> |     |
| 7.1       | Introduction   | 125 |
| 7.2       | Experimental section   | 125 |
| 7.2.1     | Catalyst preparation   | 125 |
| 7.2.2     | Transesterification reaction   | 126 |
| 7.3       | Results and discussion   | 126 |
| 7.3.1     | Catalyst characterization  | 126 |
| 7.3.1.1   | BET surface area and Basic strength  | 126 |
| 7.3.1.2   | Powder XRD study   | 127 |
| 7.3.1.3   | FESEM and HRTEM study  | 128 |
| 7.4       | Catalytic activity   | 130 |
| 7.5       | Effect of FFA on catalyst activity   | 133 |
| 7.6       | Catalyst Reusability and Homogeneous contribution  | 134 |
| 7.7       | Kinetic study  | 136 |
| 7.8       | Conclusions  | 138 |
|           | References   | 139 |
| <b>8.</b> | <b>Conclusions, Future Perspective and Scope</b>   |     |
| 8.1       | Introduction   | 140 |
| 8.2       | Conclusions from present studies   | 140 |
| 8.3       | Futuristic aspects   | 143 |
|           | <b>List of publications</b>  | 144 |

---

---

## **List of Abbreviations**

| <b>Abbreviation</b> | <b>Description</b>                                       |
|---------------------|--|
| <b>FAMEs</b>        | Fatty acid methyl esters                                 |
| <b>FAEEs</b>        | Fatty acid ethyl esters                                  |
| <b>FAAEs</b>        | Fatty acid alkyl esters                                  |
| <b>FFAs</b>         | Free fatty acids   |
| <b>MeOH</b>         | Methanol   |
| <b>EtOH</b>         | Ethanol  |
| <b>MO</b>           | Methyl Oleate  |
| <b>FESEM</b>        | Field emission scanning electron microscope              |
| <b>HRTEM</b>        | High resolution transmission electron microscopy         |
| <b>EDX</b>          | Energy Dispersive X-ray                                  |
| <b>BJH</b>          | Barret-Joyner-Halenda                                    |
| <b>BET</b>          | Brunauer- Emmett-Teller                                  |
| <b>FT-IR</b>        | Fourier transform infra red                              |
| <b>XRD</b>          | X-ray diffraction  |
| <b>TPD</b>          | Temperature programmed desorption                        |
| <b>FT-NMR</b>       | Fourier transform nuclear magnetic resonance             |
| <b>GC-MS</b>        | Gas chromatography mass spectrometry                     |
| <b>TLC</b>          | Thin layer chromatography                                |
| <b>JCPDS</b>        | Joint Committee on Powder Diffraction Standards          |
| <b>ICDD</b>         | International centre for data diffraction                |
| <b>cSt</b>          | Centistokes  |
| <b>ASTM</b>         | American Society for Testing and Materials               |
| <b>ISO</b>          | European International Organization for Standardizations |
| <b>mL</b>           | Milli liter  |
| <b>s</b>            | second   |
| <b>min</b>          | minute   |
| <b>mg</b>           | Milligram  |
| <b>g</b>            | gram   |
| <b>mol</b>          | mole   |
| <b>m/m</b>          | Mole by mole   |
| <b>v/v</b>          | Volume by volume   |
| <b>w/w</b>          | Weight by weight   |
| <b>wt%</b>          | Weight percentage  |
| <b>nm</b>           | Nano meter   |
| <b>ppm</b>          | Parts per million  |
| <b>NR</b>           | Not reported   |
| <b>NF</b>           | Not found  |

---

---

## **List of Symbols**

| <b>Symbol</b>  | <b>Description</b> |
|----------------|--------------------|
| Å              | Angstrom           |
| μ              | Micro              |
| α              | Alpha              |
| γ              | Gamma              |
| %              | Percentage         |
| R <sub>f</sub> | Retention factor   |
| ν              | Frequency          |
| H <sub>+</sub> | Basic strength     |
| °              | Degree             |

---

---

## **List of Figures**

- Fig. 1.1.** Different catalytic processes for biodiesel production.
- Fig. 1.2.** Mechanism of base catalyzed transesterification of triglycerides.
- Fig. 1.3.** Process flow diagram for production of biodiesel via base catalyzed transesterification of triglycerides.
- Fig. 1.4.** Saponification reaction of produced fatty acid alkyl esters.
- Fig. 1.5.** Mechanism of acid catalysed transesterification of vegetable oils.
- Fig. 1.6.** Process flow diagram for production of biodiesel via acid catalyzed transesterification of triglycerides.
- Fig. 1.7.** Mechanism for solid base catalyzed transesterification.
- Fig. 1.8.** Conventional flow sheet for biodiesel production from biomass feedstock based on Esterfif™ process.
- Fig. 2.1.** Setup for transesterification.
- Fig. 3.1.** a) SEM image of 20-KF/CaO/NiO-700 and b) TEM image of 20-KF/CaO/NiO-700.
- Fig. 3.2.** Comparative powder XRD patterns of CaO, NiO, KF, 5-CaO/NiO and 5-25 wt% KF impregnated CaO/NiO-700.
- Fig. 3.3.** Comparison of the <sup>1</sup>H NMR spectra of a) waste cottonseed oil and b) FAMEs.
- Fig. 3.4.** Comparison of <sup>13</sup>C-NMR spectra of a) waste cottonseed oil and b) FAMEs.
- Fig. 3.5.** Effect of a) KF concentration in CaO/NiO and b) catalyst concentration on transesterification of WCO.
- Fig. 3.6.** Effect of a) reaction temperature and b) MeOH/oil molar ratio on transesterification of WCO.
- Fig. 3.7.** Effect of added FFA (Palmitic acid) on the catalyst activity for the transesterification of WCO.
- Fig. 3.8.** Effect of reusability on the FAMEs yield for the transesterification of WCO.
- Fig. 3.9.** Comparison for <sup>1</sup>H NMR of a) waste cottonseed oil b) FAMEs with 48.6 % conversion c) FAMEs with > 98 % conversion.
- Fig. 3.10.** a) Plot of a)  $-\ln(1-X_{me})$  versus reaction time (t) at different temperatures.
- Fig. 4.1.** Comparison of powder XRD patterns of commercially available CaO and 0.5-5 wt% Li impregnated CaO.

---

**Fig. 4.2.** a) SEM and b) TEM images of 3-Li /CaO catalyst.

**Fig. 4.3.** Comparison of the  $^1\text{H}$  NMR spectra of a) waste cottonseed oil b) FAMES and c) FAEEs.

**Fig. 4.4.** Comparison of  $^{13}\text{C}$ -NMR spectra of a) waste cottonseed oil b) FAMES and (c) FAEEs.

**Fig. 4.5.** Effect of a) lithium ion concentration and b) catalyst concentration on transesterification of WCO.

**Fig. 4.6.** Effect of reaction temperature on transesterification of WCO.

**Fig. 4.7.** Effect of ethanol/oil molar ratio on transesterification of WCO.

**Fig. 4.8.** Effect of FFA on 3-Li/CaO catalyzed ethanolysis and methanolysis of various triglycerides.

**Fig. 4.9.** Reusability studies of 3-Li/CaO catalyst towards the ethanolysis of waste cottonseed oil.

**Fig. 4.10.** Comparison of powder XRD patterns of a) Fresh 3-Li/CaO and b) Reused 3-Li/CaO catalysts.

**Fig. 4.11.** Plots of a)  $-\ln(1-X_{ee})$  versus reaction time 't' at different temperatures.

**Fig. 5.1.** a) FESEM image and b) HRTEM image of 5-Li/NiO-600 catalyst.

**Fig. 5.2.** Comparison of powder XRD patterns of a) 0-6 wt% Li impregnated NiO calcined at 600 °C and b) 5-Li/NiO calcined in the range 300-900 °C.

**Fig. 5.3.** XPS spectra for a) nickel b) lithium and c) oxygen in 5-Li/NiO-600.

**Fig. 5.4.** Effect of a) lithium ion concentration in Li/NiO and b) catalyst concentration on ethanolysis of WCO.

**Fig. 5.5.** Effect of a) reaction temperature and b) ethanol/oil molar ratio on ethanolysis of WCO.

**Fig. 5.6.** Effect of FFAs on Li/NiO catalyzed ethanolysis of WCO, KO and JO.

**Fig. 5.7.** Reusability of 5-Li/NiO-600 catalyst.

**Fig. 5.8.** Comparison of powder XRD patterns of 5-Li/NiO-600 a) fresh and, b) after 8th cycle.

**Fig. 5.9.** Plots of a)  $-\ln(1-X_{ee})$  versus reaction time 't' at different temperatures.

**Fig. 5.10.** I) Proposed mechanism for Li/NiO transesterification of WCO and II) Comparison of FTIR spectra of a) neat WCO b) WCO adsorbed over Li/NiO c) neat ethanol and d) ethanol adsorbed over Li/NiO.

**Fig. 6.1.** Comparison of the powder XRD patterns of  $\text{Ti/SiO}_2$ ,  $\text{WO}_3$  and 5-25 wt% W impregnated  $\text{Ti/SiO}_2$ -700.

---

**Fig. 6.2.** a) N<sub>2</sub> adsorption-desorption isotherms and b) pore size distribution curve of 0-25 wt% W impregnated Ti/SiO<sub>2</sub>-700.

**Fig. 6.3.** FESEM images of 20-W/Ti/SiO<sub>2</sub> prepared at a) 500 °C b) 600 °C and c) 700 °C calcination temperature, and d) EDS pattern of 20-W/Ti/SiO<sub>2</sub>.

**Fig. 6.4.** HRTEM Images of 20-W/Ti/SiO<sub>2</sub> a-b) Dark spots signifies the presence of tungsten on the support c) lattice fringes of mesoporous petals and d) SAED pattern for prepared catalyst.

**Fig. 6.5.** XPS spectra of a) tungsten b) oxygen c) titanium and d) silicon in W/Ti/SiO<sub>2</sub> Catalyst.

**Fig. 6.6.** Effect of a) tungsten concentration in Ti/SiO<sub>2</sub> and b) catalyst concentration on methanolysis of WCO.

**Fig. 6.7.** Effect of a) reaction temperature and b) methanol/oil molar ratio on methanolysis of WCO.

**Fig. 6.8.** Effect of added FFA (Palmitic acid) on W/Ti/SiO<sub>2</sub> catalyzed methanolysis of WCO.

**Fig. 6.9.** Reusability of 20-W/Ti/SiO<sub>2</sub>.

**Fig. 6.10.** Comparison of the powder XRD patterns of a) fresh and b) reused 20-W/Ti/SiO<sub>2</sub>.

**Fig. 6.11.** a) A plot of  $-\ln(1-X_{me})$  versus reaction time (t) at different temperatures and b) Arrhenius plot for methanolysis of WCO in presence of 20-W/Ti/SiO<sub>2</sub>.

**Fig. 7.1.** Comparative powder XRD patterns of Fe<sub>3</sub>O<sub>4</sub>, 1-5 wt% Na impregnated CaO/Fe<sub>3</sub>O<sub>4</sub>-600.

**Fig. 7.2.** FESEM images of a) Fe<sub>3</sub>O<sub>4</sub> and b) 4-Na/CaO/Fe<sub>3</sub>O<sub>4</sub>-600.

**Fig. 7.3.** HRTEM images of a) Fe<sub>3</sub>O<sub>4</sub> and b) 4-Na/CaO/Fe<sub>3</sub>O<sub>4</sub>-600 particles and particle size distribution for c) Fe<sub>3</sub>O<sub>4</sub> and d) 4-Na/CaO/Fe<sub>3</sub>O<sub>4</sub>-600.

**Fig. 7.4.** Effect of catalyst concentration on 4-Na/CaO/Fe<sub>3</sub>O<sub>4</sub>-600 catalyzed a) methanolysis and b) ethanolysis of WCO.

**Fig. 7.5.** Effect of reaction temperature on 4-Na/CaO/Fe<sub>3</sub>O<sub>4</sub>-600 catalyzed a) methanolysis and b) ethanolysis of WCO.

**Fig. 7.6.** Effect of alcohol to oil molar ratio on 4-Na/CaO/Fe<sub>3</sub>O<sub>4</sub>-600 catalyzed a) methanolysis and b) ethanolysis of WCO.

**Fig. 7.7.** Effect of FFA on 4-Na/CaO/Fe<sub>3</sub>O<sub>4</sub>-600 catalyzed methanolysis and ethanolysis of various triglycerides.

**Fig. 7.8.** Separation of Na/CaO/Fe<sub>3</sub>O<sub>4</sub>-600 catalyst from product using magnet.

**Fig. 7.9.** Reusability of 4-Na/CaO/Fe<sub>3</sub>O<sub>4</sub>-600 catalyst.

---

**Fig. 7.10.** Comparative powder XRD patterns of a) fresh and b) reused (after 7th cycle) Na/CaO/Fe<sub>3</sub>O<sub>4</sub>-600 catalyst.

**Fig. 7.11.** Plots of a)  $-\ln(1-X_{me})$  and b)  $-\ln(1-X_{ee})$  versus time at different temperatures.

**Fig. 7.12.** Arrhenius plot for the transesterification of WCO with methanol and ethanol.

---

## **List of Tables**

**Table 1.1.** The properties of different triglyceride.

**Table 1.2.** Specification of biodiesel as per ASTM D6751 and EN 14214.

**Table 1.3.** Activity of different homogeneous base catalysts used for transesterification of triglycerides.

**Table 1.4.** Activity of different homogeneous acid catalysts used for transesterification of vegetable oils.

**Table 1.5.** Single metal oxides catalysts for transesterification of triglycerides.

**Table 1.6.** Literature reported basic mixed metal oxide catalysts for transesterification of triglycerides by impregnation and sol gel method.

**Table 1.7.** Literature reported basic mixed metal oxide catalysts for transesterification of triglycerides by co-precipitation method.

**Table 1.8.** Literature reported acidic mixed metal oxide catalysts for transesterification of triglycerides.

**Table 1.9.** Problems and possible solutions related with the application of solid catalysts for biodiesel production.

**Table 2.1.** The chemical analysis of vegetable oils used for transesterification.

**Table 2.2.** Fatty acid composition of vegetable oils employed for the transesterification in present thesis.

**Table 3.1.** Comparisons of the specific surface area, basic strength, basicity, rate of reaction and TOF of 5-25 wt% KF impregnated CaO/NiO-700.

**Table 3.2.** Comparison of reaction conditions of literature reported heterogeneous catalysts used for methanolysis with present catalyst.

**Table 3.3.** Physicochemical properties of the FAMEs prepared from WCO.

**Table 4.1.** Comparison of BET surface area and basic strength of CaO with 3-Li/CaO catalyst.

**Table 4.2.** Composition of waste cotton seed oil derived FAEEs by GC-MS technique.

**Table 4.3.** Comparison of BET surface area, basic strength and crystallite size of fresh and reused 3-Li/CaO catalyst.

**Table 4.4.** Physicochemical properties of waste cottonseed oil derived FAEEs.

---

**Table 5.1.** Comparison of BET surface area, lattice parameters, magnetic susceptibility, basic strength ( $H_{\text{L}}$ ), basicity and turn over frequency (TOF) of prepared catalysts.

**Table 5.2.** Comparison of reaction conditions of literature reported heterogeneous catalysts used for ethanolysis with present catalyst.

**Table 6.1.** Comparison of BET surface area, pore volume, pore size and crystallite size of 0-25 wt% tungsten impregnated Ti/SiO<sub>2</sub>.

**Table 6.2.** NH<sub>3</sub>-TPD measurements of 0-25 wt% tungsten impregnated Ti/SiO<sub>2</sub> catalysts.

**Table 6.3.** Metal ion concentration (ppm) in FAMEs after every catalytic cycle.

**Table 7.1.** Comparisons of the BET surface area, basic strength, basicity and TOF for 0-5 wt% Na impregnated CaO/Fe<sub>3</sub>O<sub>4</sub>.

---

## **Abstract**

Energy consumption is essential for the human survival and major portion of the human energy requirement is coming from the non renewable sources such as fossil fuel. In this contest biodiesel has gained significant attention in recent past as renewable alternate for conventional diesel fuel. Chemically, biodiesel is mono alkyl esters of fatty acids which are produced via transesterification of triglycerides in presence of heterogeneous, homogeneous or enzyme catalysts.

Traditional homogeneous basic catalysts (NaOH and KOH) are highly effective for industrial scale biodiesel production as they could catalyze the reaction under ambient reaction conditions. However, this process yielded catalyst contaminated biodiesel and glycerol and huge quantity of effluents are generated during their purification. Additionally, homogeneous alkali catalyst due to their sensitivity towards moisture and free fatty acids (FFA) could not be used for the transesterification of waste cottonseed oil and required FFA and moisture free costlier refined oil. In order to circumvent the problem associated with homogeneous catalyst, development of reusable heterogeneous catalysts has gained significant attention in recent past.

In present thesis, mixed metal oxides such as KF/CaO/NiO, Li/CaO, Li/NiO, W/Ti/SiO<sub>2</sub> and Na/CaO/Fe<sub>3</sub>O<sub>4</sub> were prepared and characterized by powder XRD, BET surface area, FESEM, HRTEM, TPD and Hammett indicators studies. These catalysts were successfully employed for the transesterification of waste cooking (cottonseed) oil to produce biodiesel. CaO/NiO impregnated with 20 wt% KF was found to have the basic strength of  $15.0 < H_{-} < 18.4$  and required 4 h to yield the complete transesterification of waste cottonseed oil (> 98% FAMES yield) with methanol under optimized reaction conditions. Further, reusability study of the catalyst has demonstrated that it was able to catalyze four catalytic cycles without significant loss in activity.

To improve the reusability, stability and surface area, tungsten impregnated Ti/SiO<sub>2</sub> in flower shape was prepared. The complete conversion of waste cooking oil into FAME was achieved in 3 h with 30:1 methanol to oil molar ratio. The catalyst was successfully recycled five times with lesser (< 5 ppm) metal ion leaching.

In order to perform the ethanolsis as well as methanolysis of waste cooking oil and non edible oils (karanja and jatropha oil), Li/CaO and Li/NiO catalysts were prepared by wet chemical

---

method. The Li/CaO catalyst under optimal reaction conditions of ethanol/oil molar ratio of 12:1, catalyst to oil weight fraction of 5% and 65 °C reaction temperature, yielded 98 % fatty acid ethyl esters in 2.5 h of reaction duration. The catalyst was recovered and reused in four catalytic runs but with partial loss in activity during successive catalytic cycles. In order to further enhance the catalytic efficiency, Li impregnated NiO was prepared. The magnetic susceptibility measurement of Li/NiO catalyst supported the formation of Ni(III) upon lithium impregnation. The catalyst was found to be effective for the ethanolysis of vegetable oils having up to 8.4 wt% free fatty acids. During reusability experiments, Li/NiO catalyst was able to catalyze seven reaction cycles without major loss in activity.

In order to achieve the easy separation of the heterogeneous catalyst from the reaction mixture, Na/CaO/Fe<sub>3</sub>O<sub>4</sub> magnetic catalyst was prepared by wet impregnation method. The prepared catalyst has been successfully employed as heterogeneous catalyst for the transesterification of waste cotton seed oil with methanol and ethanol. The catalysts was removed from the reaction mixture by magnetic separation and reused in seven catalytic runs without significant loss in the activity.

Although partial leaching of the metal ions from the catalysts was observed but leached metal ions did not show any significant homogeneous contribution, and hence, all catalysts have shown true heterogeneous mode of action. The transesterification reaction catalyzed by all catalysts has followed (pseudo) first order kinetic equation and activation energy was observed > 25 kJ/mol to support that reactions were chemically controlled and not by diffusion/mass transfer limitations. Few physicochemical properties of prepared FAMES and FAEEs have also been studied and compared with EN 14214 and ASTM D standard values.

*Keywords:* Transesterification, Triglycerides, Ethanolysis, Methanolysis, Biodiesel, Powder X-ray diffraction, BET surface area, N<sub>2</sub> adsorption desorption isotherm, Field emission scanning electron microscope, High resolution transmission electron microscope, and <sup>1</sup>H & <sup>13</sup>C Nuclear magnetic resonance.

---

**Introduction and Literature Review**

---

|            | <b>Contents</b>                               | <b>Page</b> |
|------------|---|-------------|
| <b>1.1</b> | <b>Introduction</b>                           | 1           |
| <b>1.2</b> | <b>Biodiesel</b>                              | 2           |
| <b>1.3</b> | <b>Feedstock for biodiesel production</b>     | 3           |
| <b>1.4</b> | <b>Alcohols used for biodiesel production</b> | 6           |
| <b>1.5</b> | <b>Catalysis</b>                              | 7           |
|            | 1.5.1 Homogeneous base catalyst               | 7           |
|            | 1.5.2 Homogeneous acid catalyst               | 10          |
| <b>1.6</b> | <b>Heterogeneous catalyst</b>                 | 13          |
|            | 1.6.1 Single metal oxides                     | 14          |
|            | 1.6.2 Mixed metal oxides catalysts            | 15          |
|            | 1.6.1.1 Basic mixed metal oxide catalysts     | 17          |
|            | 1.6.1.2 Acidic mixed metal oxide catalysts    | 21          |
| <b>1.7</b> | <b>Conclusions</b>                            | 24          |
| <b>1.8</b> | <b>Objectives</b>                             | 25          |
|            | <b>References</b>                             | 26          |

---

## Abstract

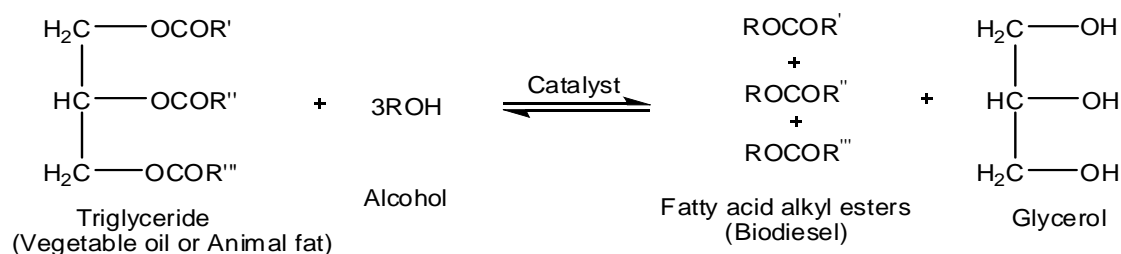
Energy crisis and environmental degradation, due to excessive use of fossil fuels, are the main reasons for the search of alternative renewable fuel such as biodiesel in recent past. Chemically biodiesel is alkyl esters of fatty acids which are prepared *via* transesterification of vegetable oils and animal fats in the presence of alkali catalyst. Biodiesel has several advantages over conventional diesel fuel as they are derived from renewable resources, free from aromatic compounds, causes lower emissions of carbon monoxide, particulate matters, sulphur compounds and greenhouse gases due to its closed carbon dioxide cycle. In spite of several advantages, biodiesel has not gained the desired popularity for commercial application in India owing to its high production cost and lack of the availability of the sufficient feedstock. Both the problems could be avoided by using fats, non-edible (*e.g.*, jatropha and karanja oils) and waste cooking oils as feedstocks for biodiesel production. The presence of relatively high amount of free fatty acids (usually 3-10 wt%) in such feedstocks leads to the formation of soap instead of biodiesel when homogeneous alkali catalyst is used for their transesterification. In order to utilize high free fatty acid (FFA) containing feedstock for biodiesel production, there is a need to develop FFA resistance heterogeneous catalysts for the transesterification process.

In recent past solid catalysts have been extensively studied for the biodiesel production and still a lot of research activities are directed across the globe towards the development of ideal solid acid or base catalyst for the biodiesel production. In this chapter, latest work on the development of heterogeneous catalyst for biodiesel production has been reviewed.

*Keywords:* Biodiesel, Mixed metal oxides, Transesterification, Heterogeneous catalyst, Triglycerides

## 1.1 Introduction

Nowadays, vegetable oil (VO) derived biodiesel has emerged as a renewable and greener replacement for the petro based diesel fuel. Biodiesel, chemically fatty acid methyl or ethyl esters (FAMES/FAEEs), is mainly produced *via* transesterification of triglycerides with methanol or ethanol in presence of homogeneous catalyst as shown in Scheme 1. Glycerol, an important molecule for the pharma and cosmetic industry, is a byproduct of this reaction.



**Scheme 1. Transesterification of triglycerides with alcohol to form alkyl esters of fatty acids (biodiesel) in the presence of acid, base or enzyme as catalyst. R', R'' and R''' are the straight hydrocarbon chains of fatty acids, usually having 14-20 carbon atoms.**

A variety of feedstocks including vegetable oils, animal fats, algal oil, and waste greases can be used as feedstock for biodiesel production in the presence of chemical or biocatalyst (Karatay and Dönmez, 2011; Rasoul-Amini et al., 2011; Chisti and Yan, 2011; Abou-Shanab et al., 2011; Montefrio et al., 2010; Hernandez et al., 2010; Brunet et al., 2012). Homogenous alkali catalyst such as NaOH and KOH have been used frequently for industrial scale biodiesel production as they catalyze the reaction at faster rate and requires mild reaction conditions. However, the same catalyst yielded biodiesel and glycerol contaminated with catalyst and leads to the formation of soap if free fatty acids (FFAs) and moisture contents are greater than 0.5% and 0.3% (w/w), respectively.

The biodiesel production cost is mainly determined by the feedstock price and due to this reason application of costly refined oil for biodiesel production is not encouraged. Moreover, application of edible oils for biodiesel production has been discouraged by Indian Government to augment their continuously increasing demand. Use of cheap non-edible and waste cooking oils as feedstock could be advantageous, as it could not only solve the waste management problem but also avoid fuel *vs* food situation. However, such feedstock usually possesses high FFA

contents and their transesterification by homogeneous alkali catalyst lead to the formation of soap instead of biodiesel. Usually transesterification of high FFA containing feedstock is carried out in two steps *viz.*, (i) esterification of FFA in concentrated mineral acid (e.g. H<sub>2</sub>SO<sub>4</sub>, HCl, etc.) catalyzed reaction followed by (ii) transesterification of ester rich oil with alkali catalyst. The homogeneous acid-catalyzed process often implies concentrated acids such as, sulfonic, sulfuric, hydrochloric acid, etc., required a high alcohol to oil molar ratio (30 to 120), high reaction temperature and acid neutralization prior to the alkali catalyzed transesterification which generate huge amount of the industrial effluents (Wahan et al., 2008). Acid catalysts are highly corrosive in nature and hence this process demand sophisticated acid resistance reactors for the reaction (Yan and Lin, 2009; Demirbas, 2009). More recently, there has been an increased research activity directed toward the development of heterogeneous catalysts for the transesterification reaction as they form uncontaminated products, are recyclable, has low sensitivity toward FFAs and moisture content, and do not corrode the reaction vessel.

### 1.2 Biodiesel

Rudolph Diesel invented diesel engine in 1893 and run it with peanut oil. The fossil fuel was discovered in early 1900s and diesel fuel was found to be more cost effective as well as efficient for the diesel engines. Moreover, the direct use of vegetable oil is avoided due to its high viscosity (42 cSt) in comparison to the diesel fuel (< 4 cSt) (Goering et al., 1982). High viscosity resulted poor flow of fuel in the engine combustion chamber and inefficient mixing with air. Further, relatively high molecular of VOs causes the poor atomization, and carbon deposition due to incomplete fuel burning. In order to reduce the viscosity and improve the performance, VOs could be chemically transformed into monoalkyl esters *via* transesterification reaction. Monoalkyl esters have less molecular weight (~ one third of VO) as well viscosity (< 5 cSt) than VO and found to have better flow properties even at low temperatures. First transesterification reaction of VO was conducted as early as 1853 by E. Duffy and J. Patrick, many years before the invention of first diesel engine.

Fuel crisis in 1990s, recent spiraling crude oil prices, and environmental concerns have renewed the interest in renewable fuel such as biodiesel. Moreover, use of biodiesel reduces the engine emissions of unburned hydrocarbons (68%), particulars (40%), carbon monoxide (44%), sulfur oxide (100%), and polycyclic aromatic hydrocarbons (80-90%) (Wu and Leung, 2011; Leduc et

al., 2009). Up to 20% (v/v) blend of conventional diesel fuel and biodiesel (known as B20) does not demand any modification in current diesel engine and few countries (Brazil, US, Canada, UK, Hong Kong, Norway) have made the policy for the use of B5 (5% biodiesel in conventional diesel fuel) in conventional diesel engines.

### 1.3 Feedstock for biodiesel production

Biodiesel could be produced from any triglyceride available in geographical region. In general, there are three major biodiesel feedstock categories: oilseeds, animal fats, and various low-value materials such as used cooking oils and greases.

Traditional oilseed feedstocks for biodiesel production predominately include soybean, rapeseed/canola, palm, corn, sunflower, cottonseed, peanut, and coconut oils (Table 1). In India due to the shortage of edible oils, application of non edible and waste cooking oils is encouraged for biodiesel product and non-edible oil such as *Jatropha* oil has attracted considerable interest as a feedstock for biodiesel production (Orthofer, 2005). The *Jatropha* tree is a perennial poisonous oilseed shrub belonging to the Euphorbiaceae family whose seeds contain 30-35 wt% oil. *Jatropha* plant is found in tropical and subtropical regions of Central America, Africa and Indian subcontinent. The primary fatty acid found in *Jatropha* oil is linoleic, followed by oleic, palmitic and stearic acids. Another non-edible feedstock of Indian origin is *Pongamia pinnata* (Karanja or Honge), that grows fast in humid and subtropical environments. The oil content of Karanja kernels ranges between 30-40 wt%. The primary fatty acid found in Karanja oil is oleic acid, followed by linoleic, palmitic, and stearic acids (Kumar and Sharma, 2011; Meher et al., 2006). The low temperature operability of the corresponding methyl esters is superior to that of *Jatropha* oil methyl esters. *Madhuca indica*, commonly known as Mahua, is a tropical tree found largely in the central and northern plains and forests of India. Mahua oil is characterized by high FFA content of around 20 wt % and a relatively high percentage of saturated fatty acids such as palmitic (17.8 wt%) and stearic (14.0 wt%) acids (Orthofer, 2005). The remaining fatty acids are primarily distributed among unsaturated components such as oleic (46.3 wt%) and linoleic (17.9 wt%) acids (Moser and Vaughn, 2010).

Used or waste frying or cooking oil is primarily obtained from the restaurant industry and may cost up to 60% less than commodity vegetable oils, depending on the source and availability. Waste oils may include a variety of low value materials such as used cooking or frying oils,

vegetable oil soapstocks, acid oils and tall oil. Waste oils are normally characterized by relatively high FFA and water contents and presence of various solid materials that must be removed by filtration prior to the transesterification reaction.

Animal fats may include materials from a variety of domesticated animals, such as cows, chickens, pigs, and other animals such as fish. Fats are normally characterized by a greater percentage of saturated fatty acids in comparison to vegetable oils (Table 1.1). Fats being the waste products, of food processing industry are normally less expensive than edible vegetable oils, and thus constitute a cost effective feedstocks for biodiesel production (Wen et al., 2010). As a result of low polyunsaturated fatty acid content in fats, the corresponding methyl esters display excellent oxidative stability, (69 h at 110°C in case of beef tallow) but poor cold flow properties (Soriano et al., 2005; Josh and Pegg, 2007; Ahmad, 2009).

**Table 1.1. The properties of different triglyceride (Talebian-Kiakalaieh et al., 2013)**

| Triglyceride sources     | Country          | Fatty acid composition<br>*Cn:x                        | Density<br>(g/cm <sup>3</sup> ) | Flash point<br>(°C) | Viscosity<br>(at 40°C) | Acid Value<br>(MJ kg <sup>-1</sup> ) |
|--------------------------|------------------|--|---------------------------------|---------------------|------------------------|--------------------------------------|
| <b>Soybean</b>           | USA, Argentina   | C16:0, C18:1, C18:2                                    | 0.91                            | 254                 | 32.9                   | 0.2                                  |
| <b>Rapeseed</b>          | Germany          | C16:0, C18:0, C18:1, C18:2                             | 0.91                            | 246                 | 35.1                   | 0.92                                 |
| <b>Sunflower</b>         | Brazil           | C16:0, C18:0, C18:1, C18:2                             | 0.92                            | 274                 | 32.6                   | NF                                   |
| <b>Palm</b>              | Costa Rica       | C16:0, C18:0, C18:1, C18:2                             | 0.92                            | 267                 | 39.6                   | 0.1                                  |
| <b>Corn</b>              | USA              | C16:0, C18:0, C18:1, C18:2, C18:3                      | 0.91                            | 277                 | 34.9                   | NF                                   |
| <b>Camelina</b>          | USA              | C16:0, C18:0, C18:1, C18:2, C18:3, C20:0, C20:1, C20:2 | 0.91                            | NF                  | NF                     | 0.76                                 |
| <b>Canola</b>            | Canada           | C16:0, C18:0, C18:1, C18:2, C18:3                      | NF                              | NF                  | 38.2                   | 0.4                                  |
| <b>Cotton</b>            | Canada, Cambodia | C16:0, C18:0, C18:1, C18:2                             | 0.91                            | 234                 | 18.2                   | NF                                   |
| <b>Jatropha curcas</b>   | India            | C16:0, C16:1, C18:0, C18:1, C18:2                      | 0.92                            | 225                 | 29.4                   | 28                                   |
| <b>Pongamina pinnata</b> | India            | C16:0, C18:0, C18:1, C18:2, C18:3                      | 0.91                            | 205                 | 27.8                   | 5.06                                 |
| <b>Palanga</b>           | India            | C16:0, C18:0, C18:1, C18:2                             | 0.90                            | 221                 | 72.0                   | 44                                   |
| <b>Nile tilapia</b>      | South east Asia  | C16:0, C18:1, C20:5, C22:6, other acids                | 0.91                            | NF                  | 32.1                   | 2.81                                 |
| <b>Animal fat</b>        | USA              | C14:0, C16:0, C16:1, C17:0, C18:0, C18:1, C18:2        | 0.92                            | NF                  | NF                     | NF                                   |

\*Cn : x, 'n' indicates the number of carbons and 'x' number of  $-C=C-$  bonds in the Fatty acid alkyl esters; NF = Not found.

The chemical composition of biodiesel depends upon the fatty acid composition of the precursor triglycerides. Broadly fatty acid could be divided in two categories named as saturated and unsaturated fatty acids. Saturated fatty acids have more thermal stability, viscosity but poor cold flow properties. On the other hand unsaturated fatty acids are less stable but due the low freezing point they have better cold flow properties. Increased viscosity can cause fuel operation and atomization problem (Ahmad, 2009), thus increasing tendency of injector chocking, sticking of moving parts, plugging of fuel filter, etc. The prepared alkyl esters can be used as fuel in diesel engines only when they satisfy the standard values accepted for biodiesel. The literature reported specifications of biodiesel as per ASTM D 6751 and EN 14214 standards are given in Table 1.2.

**Table 1.2. Specification of biodiesel as per ASTM D6751 and EN 14214 (Moser, 2009).**

| Property   | Test methods and limits |            |                 |          |
|--|-------------------------|------------|-----------------|----------|
|  | ASTM D6751              | Limits     | EN 14214        | Limits   |
| <i>Density at 15 °C (kg/m<sup>3</sup>)</i>             | NR                      | NR         | EN ISO 3675     | 860-900  |
| <i>Kinematic viscosity at 15 °C (mm<sup>2</sup>/s)</i> | D445                    | 1.9-6.0    | EN ISO 3104     | 3.5-5.0  |
| <i>Cetane number (min)</i>                             | D613                    | 47         | EN ISO 5165     | 51       |
| <i>Flash point (°C)</i>                                | D93                     | 93         | EN ISO<br>3679  | 101.0    |
| <i>Copper strip corrosion</i>                          | D130                    | No. 3 max. | EN ISO 2160     | Class 1  |
| <i>Cloud point (°C)</i>                                | D2500                   | Report     | NR              | NR       |
| <i>Oxidation stability at 110 °C (h)</i>               | NR                      | NR         | EN 14112        | 6        |
| <i>Acid value (mg KOH/g)</i>                           | D664                    | 0.5 max    | EN 14104        | 0.5 max  |
| <i>Iodine value</i>                                    | NR                      | NR         | EN 14111        | 120 max  |
| <i>Polyunsaturated (P4 double bonds)</i>               | NR                      | NR         | EN 14103        | 1 max    |
| <i>Water and sediment (vol%)</i>                       | D2709                   | 0.05 max   | NR              | NR       |
| <i>Water content (mg/kg)</i>                           | NR                      | NR         | EN ISO<br>12937 | 500 max  |
| <i>Ester content % (m/m)</i>                           | NR                      | NR         | EN 14103        | 96.5 min |
| <i>Free glycerol % (m/m)</i>                           | D6584                   | 0.02 max   | EN 14105        | 0.02     |
| <i>Total glycerol % (m/m)</i>                          | D6584                   | 0.24 max   | EN 14105        | 0.25 max |
| <i>Methanol content % (m/m)</i>                        | NR                      | NR         | EN 14110        | 0.2 max  |
| <i>Monoglyceride content % (m/m)</i>                   | NR                      | NR         | EN 14105        | 0.8 max  |
| <i>Diglyceride content % (m/m)</i>                     | NR                      | NR         | EN 14105        | 0.2 max  |
| <i>Triglyceride content % (m/m)</i>                    | NR                      | NR         | EN 14105        | 0.2 max  |
| <i>Metals (mg/kg)</i>                                  | NR                      | NR         | EN 14108        | 5 max    |
| <i>Total contamination (mg/kg)</i>                     | NR                      | NR         | EN 12662        | 24 max   |

NR = Not reported

### **1.4 Alcohols used for biodiesel production**

For biodiesel production use of short alkyl chain alcohols such as methanol, ethanol, propanol and butanol, are recommended. Among these alcohols, methanol due to its high reactivity, wide availability and cost effectiveness is preferred and used in commercial scale biodiesel production plants. Due to its lower density, fatty acid methyl esters, produced in methanolysis separate out easily from glycerol. Although methanol is highly toxic and manufactured from the refining of the crude oil and hence, biodiesel thus produced would not be having 100% renewable carbon atoms. Renewable methanol or biomethanol could be produced from biomass, either by fermentation or thermal conversion; however its production cost is much higher than commercial methanol (Amigum et al., 2010).

Recently, an increased interest has been shown by the researchers towards the application of ethanol for biodiesel production. Bioethanol is mainly produced from the plant sources and hence fatty acid ethyl esters (FAEEs) would be having 100% renewable carbon atoms. The main disadvantage associated with the use of ethanol is its high production cost, slow reactivity and difficulty of FAEEs separation from glycerol.

### **1.5 Catalysis**

Transesterification reaction can be carried out using catalytic or non-catalytic approach (Fig. 1.1). In case of non-catalytic process, energy intensive supercritical conditions (high temperature and high pressure) are required (Mamoru et al., 2001; Orcaire et al., 2006; Niza et al., 2013; Saka and Kusdiana, 2001). In catalytic processes, homogeneous acid and base catalysts, due to low cost and readily availability are used for commercial biodiesel production (Atapour and Kariminia, 2011; Demirbas, 2011).

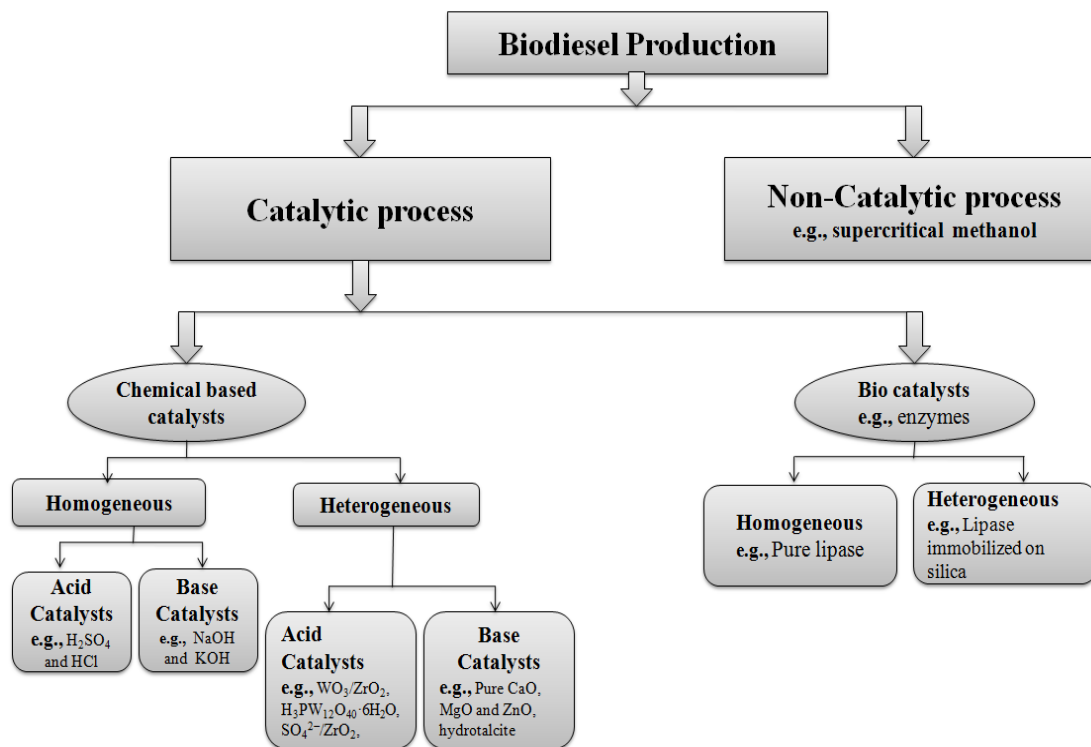


Fig. 1.1. Different catalytic processes for biodiesel production (Refaat, 2011)

### 1.5.1 Homogeneous Base Catalyst

The transesterification process is frequently catalyzed by a variety of homogeneous base catalysts such as sodium and potassium alkoxides, hydroxides (Freedman et al., 1986; Schwab et al., 1987; Stavarache et al., 2005; Meher et al., 2006), and carbonates (Varghaa and Truterb, 2005). Alkaline metal alkoxides (sodium methoxide) are the most active catalysts, since they give high yields (98%) in a short reaction time (30 min) at 0.5 molar concentration (Schuchardta et al., 1998).

As shown in Fig. 1.2, In first step, strong nucleophile (alkoxide ion) and conjugate acid (BH<sup>+</sup>) has formed due to the reaction between catalyst (NaOH, KOH) and alcohol (MeOH, EtOH). In second step, alkoxide ion attacks on the carbonyl carbon of triglyceride to form an intermediate as shown in step 2. This intermediate rearranges to give one molecule of fatty acid ester and diglyceride anion in step 3. Diglyceride anion further reacts with conjugate acid (BH<sup>+</sup>) to yield diglycerides molecules which follow the similar mechanism to yield two more ester molecules and glycerol as by product.



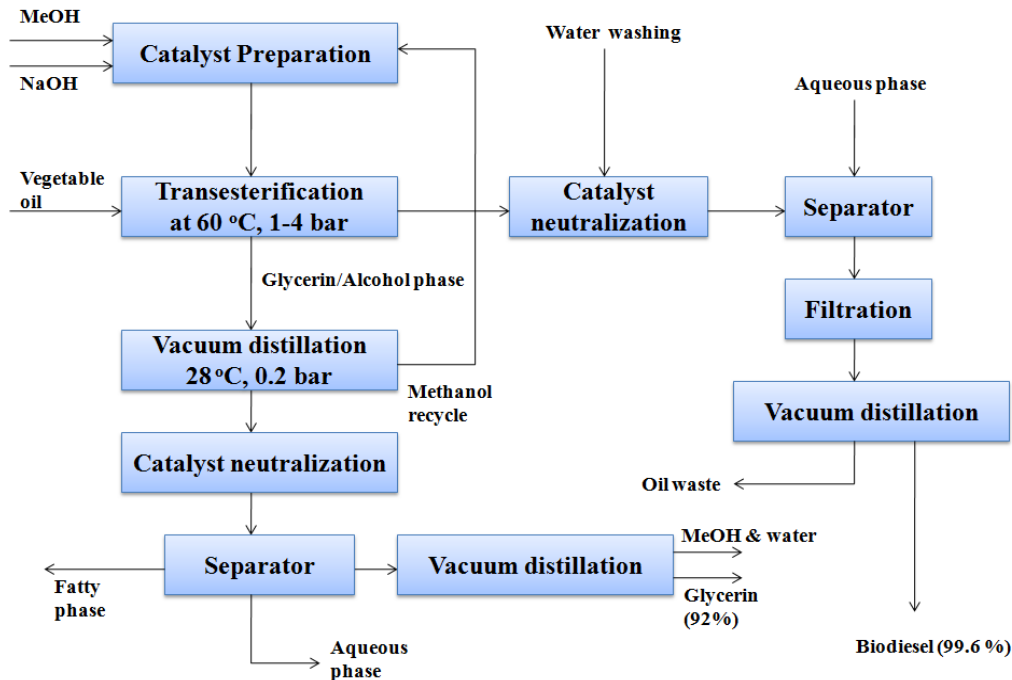


**Fig. 1.3. Process flow diagram for production of biodiesel via base catalyzed transesterification of triglycerides (Helwani et al., 2009)**

The major problem associated with the application of homogeneous base are their deactivation by FFA and water by saponification as shown in Fig 1.4. Thus in order to prevent catalyst deactivation, base catalyzed transesterification demand FFA (< 0.5 wt%) and moisture content (< 0.3 wt%) free refined vegetable oils as feedstock.

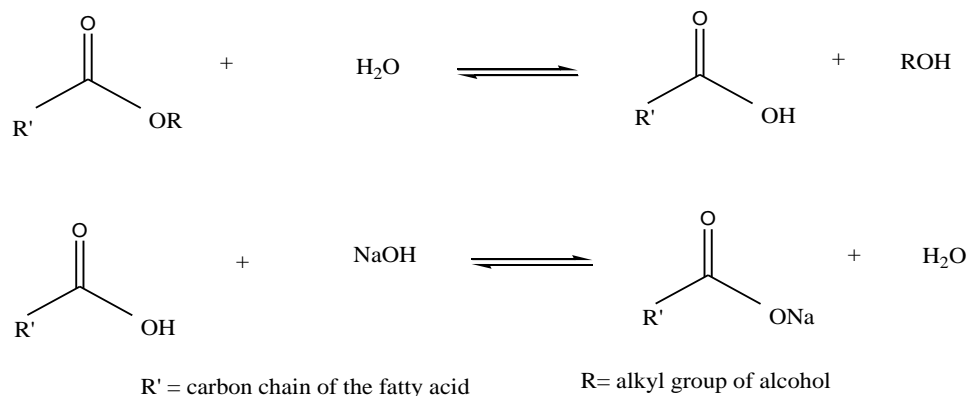


**Fig. 1.4. Saponification reaction of produced fatty acid alkyl esters (Mbaraka and Shank, 2006).**

Saponification not only reduces the ester yield, but also deactivates the alkaline catalyst and makes separation of glycerol from methyl ester difficult due to the formation of emulsion. Few literature reported homogeneous alkali catalysts along with their reaction conditions are compared in Table 1.3.

**Table 1.3. Activity of different homogeneous base catalysts used for transesterification of triglycerides.**

| Catalyst                 | Triglycerides | Reaction conditions |          |                      |                         | Yield | Ref.                   |
|--------------------------|---------------|---------------------|----------|----------------------|-------------------------|-------|------------------------|
|                          |               | Temp (°C)           | Time (h) | MeOH/oil Molar ratio | Catalytic Amount (wt %) |       |                        |
| <b>KOH</b>               | Sunflower     | 25                  | 60       | 6:1                  | 1.3                     | 98.4  | Warabi et al., 2004    |
| <b>NaOH</b>              | Waste cooking | 70                  | 0.5      | 7.5:1                | 1.1                     | 85.3  | Leung et al., 2006     |
| <b>NaOH</b>              | Soybean       | 45                  | 0.3      | 6:1                  | 0.3                     | 100   | Ji et al., 2006        |
| <b>KOCH<sub>3</sub></b>  | Canola        | 40                  | 0.5      | 4.5                  | 0.7                     | 96    | Singh et al., 2006     |
| <b>KOH</b>               | Karanja       | 65                  | 2        | 6:1                  | 1.0                     | 98    | Meher et al., 2006     |
| <b>NaOCH<sub>3</sub></b> | Canola        | 50                  | 0.5      | 6:1                  | 0.6                     | 94.2  | Singh et al., 2006     |
| <b>NaOCH<sub>3</sub></b> | Safflower     | 60                  | 2        | 6:1                  | 1.2                     | 98    | Rashid and Anwar, 2008 |
| <b>KOCH<sub>3</sub></b>  | Safflower     | 60                  | 2        | 6:1                  | 1.5                     | 98    | Rashid and Anwar, 2008 |
| <b>NaOH</b>              | Sunflower     | 60                  | 2        | 6:1                  | 1.0                     | 97.1  | Rashid et al., 2008    |
| <b>KOH</b>               | Rapeseed      | 65                  | 2        | 6:1                  | 1.0                     | 96    | Rashid et al., 2008    |

As could be seen from the Table 1.3, refined oil in presence of homogeneous base catalyst yielded higher conversion level at relatively low reaction temperature and low methanol to oil molar ratio.

### 1.5.2 Homogeneous Acid Catalyst

In order to utilize high FFA containing vegetable oils as feedstock for biodiesel production, concentrated mineral acids such as H<sub>2</sub>SO<sub>4</sub>, HNO<sub>3</sub>, HCl, etc., were used as homogeneous acid catalysts for transesterification reaction (Narsimharao et al., 2007; Dholakiya, 2012; Su, 2013).

In homogeneous acid catalyzed transesterification reaction (shown in Fig. 1.5), first step includes the protonation of the carbonyl oxygen of the triglyceride molecule. The protonation of oxygen makes the carbonyl carbon susceptible to nucleophilic attack from alcohol and produces the tetrahedral intermediate. From this intermediate, diglyceride molecule is eliminated to yield fatty acid ester and acid catalyst ( $H^+$ ) is also regenerated. Presence of water in acid catalyzed esterification causes the hydrolysis of triglyceride to form free fatty acids. Also, water acts as a poison for homogeneous acid catalysts and hence, its concentration should be negligible during the reaction.

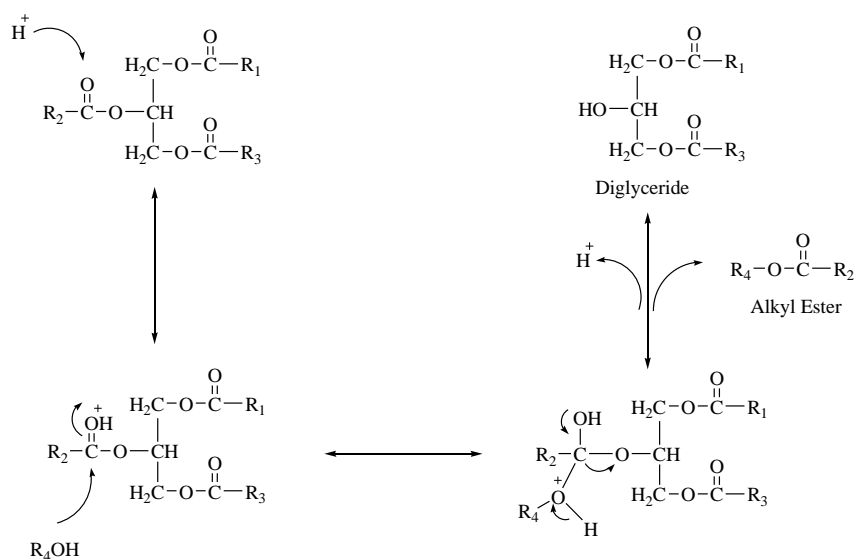


**Fig. 1.5. Mechanism of acid catalysed transesterification of vegetable oils (Mbaraka and shanks 2006).**

As discussed in case of base catalyzed mechanism alkoxide ion is involved in reaction which is a much stronger nucleophile than alcohol, involved in acid catalyzed reaction. This vital difference is ultimately responsible for the relatively higher reaction rate in case of base catalyzed reaction. Acids can catalyze simultaneous esterification of FFA and transesterification of triglycerides. However, they are mainly used in two step transesterification of high FFA containing vegetable oils. In first step, the esterification of FFA with acid catalysts is performed to reduce the FFA levels to lower than 1% and in the second step, ester rich oil is transesterified in presence of alkali catalysts. Wang et al. (2006) performed the transesterification reaction in presence of sulfuric acid followed by two-step transesterification in presence of ferric sulfate (2-0 wt%) and

NaOH (2 wt%) as catalyst. In this method 97.22% FAMES yield was obtained which was much higher than the yield obtained (90%) in single step method. Fan et al., (2009) reported the methanolysis of canola oil by two-step transesterification reaction with  $\text{H}_2\text{SO}_4$  (5%) and KOH (1 wt%). Under optimum methanol to oil molar ratio of 40:1, a 96.3% FAMES yield was obtained in 1.5 h of reaction duration. Fig. 1.6 shows the simplified block diagram for homogeneous acid-catalyzed biodiesel production process.

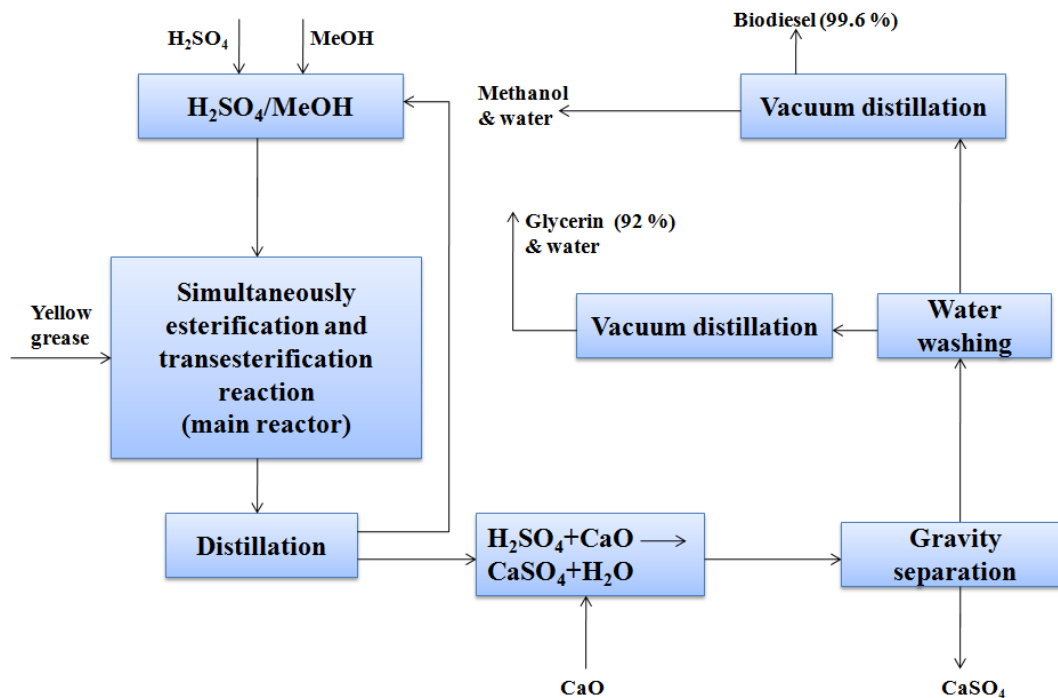


**Fig. 1.6. Process flow diagram for production of biodiesel via acid catalyzed transesterification of triglycerides (Helwani et al., 2009).**

Table 1.4 shows the homogeneous acidic catalysts used for biodiesel production. Owing to their lower reactivity in comparison to alkali catalysts, they usually required relatively higher alcohol to oil molar ratio and higher reaction temperature.

**Table 1.4. Activity of different homogeneous acid catalysts used for transesterification of vegetable oils.**

| Catalyst                       | Triglycerides | Reaction conditions |          |                      |                         | Yield | Ref.                      |
|--------------------------------|---------------|---------------------|----------|----------------------|-------------------------|-------|---------------------------|
|                                |               | Temp (°C)           | Time (h) | MeOH/oil Molar ratio | Catalytic Amount (wt %) |       |                           |
| H <sub>2</sub> SO <sub>4</sub> | Soybean       | 65                  | 50       | 30                   | 1                       | >99   | Narasimharao et al., 2007 |
| H <sub>2</sub> SO <sub>4</sub> | Soybean       | 120                 | 1        | 6                    | 3                       | >95   | Wahlen et al., 2008       |
| H <sub>2</sub> SO <sub>4</sub> | Waste cooking | 95                  | 10       | 20                   | 4                       | >90   | Wang et al., 2006         |
| MgSO <sub>4</sub>              | Cottonseed    | 65                  | 5.4      | 5.4                  | 1                       | 98    | Felizardo et al., 2006    |
| AlCl <sub>3</sub>              | Cooking oil   | 110                 | 18       | 24                   | 5                       | 98    | Soriano et al., 2005      |
| ZnCl <sub>2</sub>              | Cooking oil   | 110                 | 24       | 60                   | 5                       | 48    | Soriano et al., 2005      |
| HCl                            | Palm oil      | 90                  | NR       | 50                   | 0.5                     | 90    | Su, 2013                  |

Thus, cheaper homogeneous acid and alkali catalysts provide higher biodiesel yield under relatively mild reaction conditions, and in short reaction duration. However, after the reaction respective acid or base must be neutralized, and resulted salts should be washed away with water from the fatty acid esters. This process generates huge amount of industrial effluent to cause disposal problem. Finally, the produced biodiesel must be dried to remove the resultant moisture content. These problems associated with homogeneous catalysts could be circumvented by developing heterogeneous catalyst for the transesterification reaction.

## 1.6 Heterogeneous catalyst

Today biodiesel is mostly produced by homogeneous catalyst process which utilizes costly refined (FFA and moisture free) vegetable oil. Feedstock cost contributes significantly (75-90%) to overall biodiesel production cost and use of low quality feedstock such as waste cooking oil may reduce biodiesel production cost. In this context, application of a true heterogeneous catalyst could be advantageous as it would be insensitive towards high FFA and moisture concentration, produce uncontaminated biodiesel, and recovered and reused. Additionally, glycerol produced in heterogeneous catalysis process is of higher purity and biodiesel did not require the washing step to remove the metal contamination. Moreover, the catalysts surface can

be tuned to yield the desired acidic and/or basic properties. The major drawback of heterogeneous catalysts lies in their complicated preparation conditions and their slow reaction rate due to the phase difference (Mayani et al., 2012; Mayani et al., 2013).

The reaction mechanism for the solid base catalysts is similar to the mechanism of homogeneous base catalysts. In a typical mechanism, as shown in Fig. 1.7, initially  $O^{2-}$  (Lewis base/B) of metal oxide surface extracts  $H^+$  from methanol to form a surface methoxide anion ( $CH_3O^-$ ) which remain attach with the surface metal ion (Lewis acid/M). Methoxide ion is strongly basic and hence shows high catalytic activity towards transesterification. Later methoxide ion was attacked by carbonyl carbon of triglyceride molecule, which leads to the formation of an alkoxycarbonyl intermediate on the catalyst surface (Faungnawakij et al., 2012). In next step, the intermediate reacts either with  $H^+$  from the surface of the catalyst or with methanol to generate  $CH_3O^-$ . In the final step, the alkoxycarbonyl intermediate is break down into FAME and diglycerides molecule.

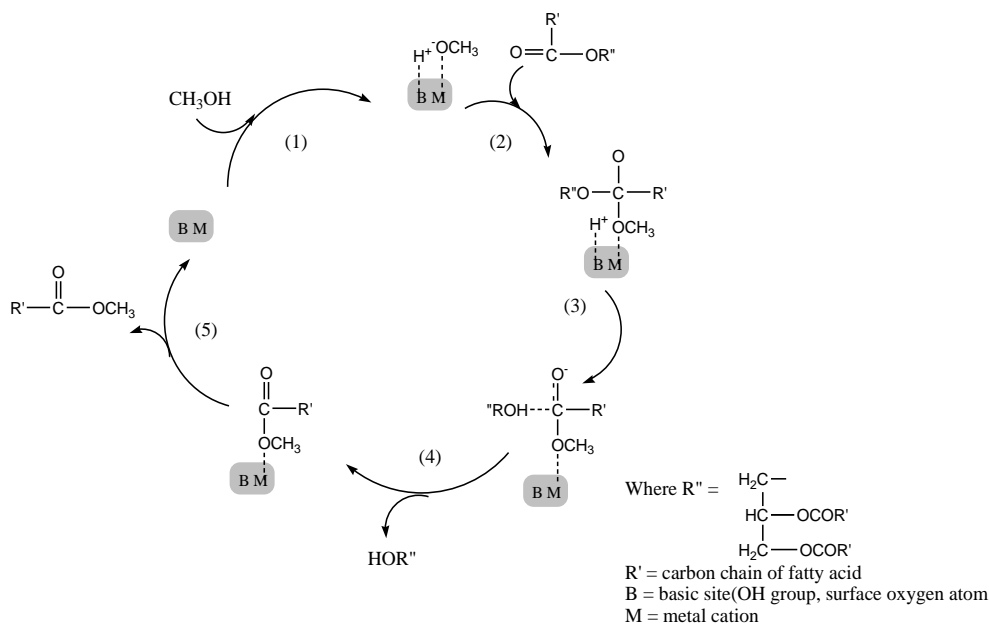


**Fig. 1.7. Mechanism for solid base catalyzed transesterification (Liu et al., 2014).**

### 1.6.1. Single metal oxides catalysts

Among single metal oxides alkali, alkaline earth and transition metal oxides are extensively used as solid catalysts for the transesterification reaction. Alkaline earth metal oxides (MgO, CaO, SrO and BaO) are promising catalysts because they are inexpensive and less soluble in alcohol than group I metal oxides. The basic sites of these metal oxides consist of metal cation (Lewis

acid) and oxygen anion (Lewis base). The basic strength of alkaline earth metal oxides increases in the order of  $\text{MgO} < \text{CaO} < \text{SrO} < \text{BaO}$ . This is due to the decrease of ionization energy on moving down the group which results in weakening of M–O bond and thus increasing basic strength of the oxides (Kiss et al., 2006; Zabeti et al., 2009). Among them CaO is most widely used because it is inexpensive, naturally occurring in the form of limestone and calcium hydroxide and is also non-toxic. The single metal oxide catalyst employed as a solid catalyst for transesterification reaction has been shown in Table 1.5. The pure metal oxides have relatively higher solubility in alcohol which resulted metal leaching into the biodiesel and glycerol. These catalysts also demand rigid reaction conditions such as high alcohol to oil molar ratio and high temperature for biodiesel production.

**Table 1.5. Single metal oxides catalysts for transesterification of triglycerides.**

| Catalysts        | Triglyceride | Reaction conditions     |                      |              |                             | Yield | Ref.                    |
|------------------|--------------|-------------------------|----------------------|--------------|-----------------------------|-------|-------------------------|
|                  |              | MeOH/oil<br>Molar ratio | Reaction time<br>(h) | Temp<br>(°C) | Catalyst<br>amount<br>(wt%) |       |                         |
| CaO              | Sunflower    | 13:1                    | 1.5                  | 60           | 2                           | 60    | Granados et al., 2007   |
| CaO              | Sunflower    | 6:1                     | 5.5                  | 80           | 1                           | 91    | Verziu et al., 2011     |
| CaO              | Soybean      | 12:1                    | 3                    | 65           | 8                           | 95    | Liu et al., 2008        |
| MgO              | Soybean      | 36:1                    | 0.16                 | 250          | 3                           | 99    | Wang and Yang, 2007     |
| SrO              | Soybean      | 12:1                    | 0.5                  | 65           | 3                           | 95    | Liu et al., 2007        |
| BaO              | Palm         | 9:1                     | 3                    | 65           | 3                           | 95.2  | Mootabdi et al., 2010   |
| ZrO <sub>2</sub> | Palm         | 16:1                    | 1                    | 200          | 3                           | 64.5  | Jitputti et al., 2006   |
| ZnO              | Palm         | 6:1                     | 1                    | 200          | 3                           | 86.1  | Jitputti et al., 2006   |
| SnO              | Soybean      | 18:1                    | 0.5                  | 65           | 10                          | 90    | Liu et al., 2008        |
| SiO <sub>2</sub> | Cooking      | 6:1                     | 5                    | 150          | 5                           | 60    | Alba-Rubio et al., 2010 |

### 1.6.2 Mixed Metal oxides catalysts

The single metal oxides was found to be soluble in reaction mixture and catalyzes the reaction at a slow reaction rate which increases production time, energy consumption and thus overall

cost of biodiesel production. To improve the catalyst activity mixed metal oxides, or supported metal oxides were prepared and used as a catalyst for the transesterification reaction.

The chemical behavior as well as activity of mixed-metal oxides may be different from single oxide as the cations in a mixed-metal oxide can work in a cooperative manner and hence catalyze different steps of a chemical process (Chumbale et al., 2001). Furthermore, the combination of two or more metals in an oxide matrix can produce materials with novel structural or electronic properties which, may result in superior catalytic activity and/or selectivity. At a structural level, formation of mixed metal oxides generates the stress into the lattice as well as defects which may also results in high chemical activity. Additionally, metal-metal or metal-oxygen-metal interactions in mixed-metal oxides could generate the electronic properties significantly different from a pure metal oxide (Rodriguez and Stacchiola, 2010; Chumbale et al., 2005).

On the commercial scale, mixed metal (Zn-Al)-oxide was used as heterogeneous catalyst for biodiesel production in Esterfif™ process (Fig. 1.8). In this process reaction was performed at higher pressure (3-5 Mpa) and temperature (483-523 K) to yield FAMES and glycerol (98% purity) which satisfies the European specifications. Thus this process didn't require catalyst neutralization after the reaction followed by water washing step to purify the biodiesel. However, this process is sensitive to the FFA (> 0.5 wt%) and water (> 1000 ppm) content, and also requires relatively high reaction temperature and pressure (Bournay et al., 2008).

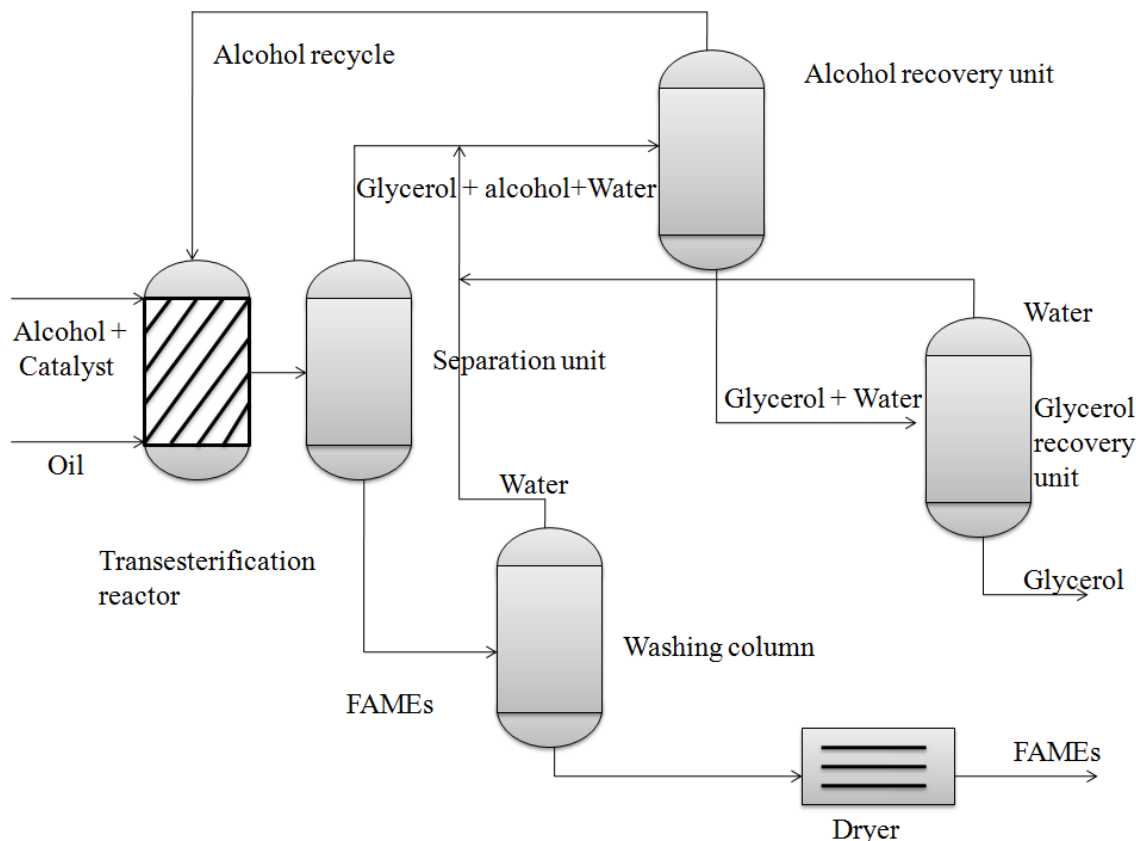


**Fig. 1.8. Conventional flow sheet for biodiesel production from biomass feedstock based on Esterfif™ process (Helwani et al., 2009).**

### 1.6.2.1 Basic mixed metal oxide catalysts

Various types of basic solid catalysts are reported in literature for transesterification of triglycerides *viz.*, supported metal oxides, hydrotalcites (Silva et al., 2010; Kannan, 2006) and mesoporous based catalysts (De Lima et al., 2014).

The catalyst preparation technique has played important role in catalysts stability and activity. The catalyst prepared by wet impregnation technique was found to show good activity but catalyst stability remains an issue due to the leaching of active catalytic species. In order to improve the catalyst stability high temperature calcination could be advantageous, although catalyst activity was found to be reduced due to the sintering of the catalyst particles at high temperature (Xie and Li, 2006). Kumar and Ali, (2013) have reported Zn/CaO catalyst prepared by impregnation method followed by calcination at 550 °C. The catalyst has shown reasonably good activity (> 98% FAMES) in 45 minutes and reusability during seven catalytic cycles. Yang and Xie (2007) have reported ZnO loaded with  $\text{Sr}(\text{NO}_3)_2$  or  $\text{Ba}(\text{NO}_3)_2$  for the transesterification

reaction of soybean oil with methanol. The strontium nitrate on ZnO was calcined at 600 °C for 5 h and used as solid catalyst to yield 94.7% conversion with 12:1 methanol to oil molar ratio in 5 h and at 65 °C. Application of THF as co-solvent, was found to increase the conversion upto 96.8%, but it will also increase the biodiesel production cost and add additional step of co-solvent removal. Kawashima et al., (2009) have reported various mixed metal oxide catalysts viz., CaMnO<sub>3</sub>, Ca<sub>2</sub>Fe<sub>2</sub>O<sub>5</sub>, Ca-CeO<sub>3</sub>, and CaZrO<sub>3</sub> for methanolysis and reported methyl ester yield ranging between 79-92% at 60 °C with 6:1; methanol to oil molar ratio in 10 h.

In order to prepare the catalysts of high surface area a combination of impregnation and sol gel methods were also employed. In this technique a support material with high surface area, such as mesoporous silica (MCM-41, SBA-15, etc.,) were prepared by sol gel method. Later, active catalytic species such as alkaline earth metal ions or organic amines were impregnated on the catalyst surface by chemical method (Singh and Patel; 2014; Zhuo et al., 2013).

De Lima et al., (2014) reported the aminopropyltriethoxy silane impregnated MCM-41 as solid base catalyst for transesterification of soybean oil at 70 °C to achieve a maximum conversion of 99% with 9:1 methanol to oil molar ratio. The catalyst was successfully reused five times, and after fifth cycle the activity was found to be lost completely may be due to the neutralization of the basic sites by the FFAs present in the soybean oil. Santiago-Torres et al., (2014) reported the sodium impregnated zirconia as basic catalyst for methanolysis of soybean oil. The catalyst was reused five times but it require high methanol to oil molar ratio (30:1) for the completion of the reaction. Few more basic mixed metal oxides reported in literature for transesterification along with reaction conditions are compared in Table 1.6.

**Table 1.6. Literature reported basic mixed metal oxide catalysts for transesterification of triglycerides by impregnation and sol gel method.**

| Catalyst/method  | Triglycerides    | Reaction conditions |                      |                        |          |             | Yield % | Ref.                            |
|--|------------------|---------------------|----------------------|------------------------|----------|-------------|---------|---------------------------------|
|  |                  | Temp (°C)           | MeOH/oil Molar ratio | Catalyst amount (wt %) | Time (h) | Reusability |         |                                 |
| <b><i>IMPREGNATION</i></b>                                     |                  |                     |                      |                        |          |             |         |                                 |
| <b>KI/Al<sub>2</sub>O<sub>3</sub></b>                          | Soybean          | 65                  | 15:1                 | 2                      | 6        | NR          | 87.4    | Xie and Li, 2006                |
| <b>Eu<sub>2</sub>O<sub>3</sub>/Al<sub>2</sub>O<sub>3</sub></b> | Soybean          | 70                  | 15:1                 | 5                      | 8        | NR          | 63.2    | Li et al., 2007                 |
| <b>CaO/La<sub>2</sub>O<sub>3</sub></b>                         | Soybean          | 61                  | 15                   | 4                      | 1        | 5           | 95.3    | Yan et al., 2010                |
| <b>CaO–CeO<sub>2</sub></b>                                     | Palm             | 85                  | 20                   | 5                      | 2        | 4           | 90      | Thitsartarn et al., 2011        |
| <b>Mg/ZrO<sub>2</sub></b>                                      | Algal oil        | 65                  | 2:1                  | 10                     | 4        | NR          | 28      | Li et al., 2011                 |
| <b>K/CaO</b>   | Waste cottonseed | 65                  | 12:1                 | 5                      | 1.25     | 3           | 98      | Kumar and Ali, 2012             |
| <b>Sr/MgO</b>  | Soybean          | 65                  | 12:1                 | 5                      | 0.5      | NR          | 93      | Tantirungrot echai et al., 2013 |
| <b>Li/CaO</b>  | Waste cottonseed | 65                  | 10:1                 | 5                      | 4        | 4           | 94      | Boro et al., 2014               |
| <b>K/Na<sub>2</sub>Ti<sub>3</sub>O<sub>7</sub> nanotubes</b>   | Soybean          | 80                  | 9:1                  | 5                      | 1        | NR          | 96      | Hernández-Hipólito et al., 2014 |
| <b>Na<sub>2</sub>ZrO<sub>3</sub></b>                           | Soybean          | 65                  | 30:1                 | 3                      | 3        | 5           | 98.3    | Santiago-Torres et al., 2014    |
| <b><i>IMPREGNATION + SOL GEL</i></b>                           |                  |                     |                      |                        |          |             |         |                                 |
| <b>Na/SiO<sub>2</sub></b>                                      | Jatropha         | 65                  | 15:1                 | 6                      | 0.75     | 5           | 99      | Akbar et al., 2009              |
| <b>TiO<sub>2</sub>/MgO</b>                                     | Waste cooking    | 65                  | 50:1                 | 12                     | 6        | 4           | 91.2    | Wen et al., 2010                |
| <b>Li/ZrO<sub>2</sub></b>                                      | Soybean          | 65                  | 13:1                 | 3                      | 3        | NR          | 98.2    | Ding et al., 2011               |
| <b>SrO/MgO</b>   | Soybean          | 67                  | 9:1                  | 5                      | 0.5      | NR          | > 92    | Dias et al., 2012               |
| <b>3-amino-propyl-triethoxy-silane/MCM-41</b>                  | Soybean          | 70                  | 9:1                  | 5                      | 3        | 5           | 99      | De Lima et al., 2014            |

Co-precipitation is simultaneous precipitation of more than one compound from a solution in presence of a precipitating agent. The co-precipitation method is more advantageous than

impregnation as it has better control over catalyst particles morphology. The catalysts prepared by co-precipitation method have shown the promising yield of fatty acid alkyl esters because of high concentration of active catalytic sites (Endalew et al., 2011). Wan et al., (2014) have reported the preparation of  $\text{MnCO}_3/\text{ZnO}$  catalyst by co-precipitation method and its application for the transesterification of soybean with methanol. Results showed FAMES yield of 94.2% in 1 h with 4 wt% of catalyst, methanol/oil molar ratio of 18:1 and reaction temperature of 175 °C. The catalyst was successfully reused in 17 catalytic cycles without major loss in activity. Fan et al., (2012) have reported the preparation of  $\text{KF}/\text{CaO-MgO}$  catalyst by co-precipitation method followed by calcination at 600 °C. The catalyst was employed for the transesterification of soybean oil to obtain 97.9% methyl ester yield in 2.5 h of reaction duration. Literature reported few basic mixed metal oxides prepared by co-precipitation method are given in Table 1.7.

**Table 1.7. Literature reported basic mixed metal oxide catalysts for transesterification of triglycerides by co-precipitation method.**

| Catalyst   | Triglycerides     | Reaction conditions |                      |                        |          |             | Yield % | Ref.                            |
|--|-------------------|---------------------|----------------------|------------------------|----------|-------------|---------|---------------------------------|
|  |                   | Temp (°C)           | MeOH/oil Molar ratio | Catalyst amount (wt %) | Time (h) | Reusability |         |                                 |
| $\text{KF}/\text{CaO-Fe}_3\text{O}_4$                      | Stillingia        | 65                  | 12                   | 1                      | 3        | NR          | 97      | Hu et al., 2011                 |
| $\text{KF}/\text{CaO-MgO}$                                 | Soybean           | 65                  | 9:1                  | 2                      | 2.5      | 4           | 97.9    | Fan et al., 2012                |
| $\text{MgAl-La}$   | Moringa Olei fera | 110                 | 30:1                 | 10                     | 6        | NR          | 96.1    | Trakarnpruk and Chuayplod, 2012 |
| $\text{Sr/Zr}$   | Soybean           | 60                  | 12:1                 | 3                      | 3        | NR          | 98      | Lima et al., 2013               |
| $\text{MnCO}_3/\text{ZnO}$                                 | Soybean           | 175                 | 18:1                 | 4                      | 1        | 17          | 94.2    | Wan et al., 2014                |
| $\text{CaO-La}_2\text{O}_3$                                | Jatropha          | 65                  | 24:1                 | 4                      | 4        | NR          | > 85    | Taufiq-Yapa et al., 2014        |
| $\text{CaFe}_2\text{O}_4\text{-Ca}_2\text{Fe}_2\text{O}_5$ | Jatropha          | 100                 | 15                   | 4                      | 0.5      | NR          | 85.4    | Xue et al., 2014                |

### 1.6.1.2 Acidic mixed metal oxide catalysts

The heterogeneous acid catalyzed transesterification reaction is more advantageous over liquid acid catalyst as solid acid catalysts are reusable, easily separable from the reaction mixture, and non corrosive. However, use of solid acid catalyst for biodiesel production has not been widely explored due to its slow reaction rate and leaching of active species from support. A variety of solid acid catalysts such as silica-alumina, sulphated zirconia, sulphated polystyrene ion exchange resins, zeolites, heteropoly acids, polyoxometalates acids and mesoporous oxides containing sulphonic acid moieties has been frequently used in literature for transesterification reactions (Sharma, 1995; Chakrabarti and Sharma, 1993; Bekkum, 1991; Kulkarni et al., 2006; Corma, 2003; Valkenberg and Hölderich, 2002).

There are various methods reported in the literature for the preparation of acidic mixed metal oxides *viz.*, precipitation, co-precipitation, impregnation, sol gel, and hydrothermal sulfonation. The sol-gel process is a wet chemical technique which utilizes metal oxides and metal chlorides as precursors to produce integrated network of metal oxides/hydroxides. Domingues et al., (2013) have reported vanadium phosphorus oxides (V/P = 1 atomic ratio) by sol–gel method and applied them as heterogeneous catalyst for the transesterification of rapeseed oil to obtain > 80% FAMEs yield at 125 °C in 6 h of reaction duration.

The hydrothermal sulfonation method was found to give better yield for transesterification reaction as compare to other reported methods. In hydrothermal sulfonation, the sulphonic acid group is incorporated over a support by treating the support and solvent (sulphonic acid) in an autoclave at temperature well above the boiling point of solvent (Xu et al., 2014). Dawodu et al., (2014) have reported the preparation of sulfonated carbon nanotubes by hydrothermal method for the transesterification of non-edible seed oil (*Calophyllum inophyllum*), having 15 wt% FFA content to obtain 99% conversion in 5 h of reaction duration. The catalyst was successfully recycled five times without any significant loss in activity. As given in Table 1.8, literatures reported acidic mixed metal oxide catalysts required high temperature, a high alcohol to oil molar ratio and longer reaction duration to obtain the higher FAME yield.

Table 1.8. Literature reported acidic mixed metal oxide catalysts for transesterification of triglycerides.

| Catalyst  | Triglycerides          | Reaction conditions |                      |                        |          |             | Yield % | Ref.                          |
|---|------------------------|---------------------|----------------------|------------------------|----------|-------------|---------|-------------------------------|
|   |                        | Temp (°C)           | MeOH/oil Molar ratio | Catalyst amount (wt %) | Time (h) | Reusability |         |                               |
| <b><u>PRECIPITATION</u></b>   |                        |                     |                      |                        |          |             |         |                               |
| Sulfated SnO <sub>2</sub>   | Soybean                | 200                 | 40:1                 | 0.75                   | 1        | NR          | 90.3    | Furuta et al., 2004           |
| H <sub>3</sub> PW <sub>12</sub> O <sub>40</sub> /ZrO <sub>2</sub>               | Canola                 | 200                 | 6:1                  | 3                      | 10       | NR          | 77      | Kulkarni et al., 2006         |
| H <sub>3</sub> PW <sub>12</sub> O <sub>40</sub> .6H <sub>2</sub> O              | Waste frying oil       | 65                  | 70:1                 | 1                      | 14       | NR          | 87      | Cao et al., 2008              |
| Cs <sub>2.5</sub> H <sub>0.5</sub> PW <sub>12</sub> O <sub>40</sub>             | Horn oil               | 60                  | 12:1                 | 1                      | 0.16     | 9           | 96.2    | Zhang et al., 2010            |
| ZnFe <sub>2</sub> O <sub>4</sub>  | Jatropha               | 65                  | 9:1                  | 1                      | 10       | NR          | > 99    | Sankaranarayanan et al., 2012 |
| <b><u>SOL GEL</u></b>   |                        |                     |                      |                        |          |             |         |                               |
| H <sub>3</sub> PW <sub>12</sub> O <sub>40</sub> /Ta <sub>2</sub> O <sub>5</sub> | Soybean oil            | 65                  | 90:1                 | 1                      | 6        | NR          | 51.4    | Xu et al., 2008               |
| ZS/SPVA   | Waste cooking oil      | 200                 | 6:1                  | 4                      | 2.5      | 5           | 94.5    | Shi et al., 2010              |
| Vanadyl phosphate   | rapeseed               | 125                 | 15:1                 | 5                      | 6        | NR          | > 80    | Domingues et al., 2013        |
| p-toluenesulfonic acid/MCM-41   | Soybean                | 80                  | 24:1                 | 2.7                    | 3        | NR          | 84.1    | Xu et al., 2014               |
| <b><u>IMPREGNATION</u></b>  |                        |                     |                      |                        |          |             |         |                               |
| Al <sub>2</sub> O <sub>3</sub> /ZrO <sub>2</sub> /WO <sub>3</sub>               | Soybean oil            | 250                 | 40:1                 | 4                      | 20       | 2           | 90      | Furuta et al., 2006           |
| ZrHPW <sub>12</sub> O <sub>40</sub> /nanotube                                   | Waste cooking          | 65                  | -                    | 5                      | 8        | NR          | 97      | Katada et al., 2009           |
| WO <sub>3</sub> /ZrO <sub>2</sub>   | Waste cooking          | 150                 | 9:1                  | 0.4                    | 2        | NR          | 96      | Park et al., 2010             |
| ZnO-TiO <sub>2</sub> -Nd <sub>2</sub> O <sub>3</sub> /ZrO <sub>2</sub>          | Soybean                | 190                 | 13.3:1               | 5                      | 1.2      | NR          | 84.9    | Kim et al., 2012              |
| <b><u>CO-PRECIPIATION</u></b>   |                        |                     |                      |                        |          |             |         |                               |
| SZ/Al <sub>2</sub> O <sub>3</sub>   | Palm                   | 180                 | 8:1                  | 6                      | 3        | NR          | 82.8    | Kansedo et al., 2009          |
| Cs/TPA  | Rice bran              | 65                  | 14:1                 | 5                      | 3        | 5           | 92      | Srilatha et al., 2012         |
| <b><u>HYDROTHERMAL SULFONATION</u></b>  |                        |                     |                      |                        |          |             |         |                               |
| Sulphated carbon nanohorns  | Vegetable oil          | 64                  | 33:1                 | 5                      | 5        | NR          | > 90    | Poonjarernsilp et al., 2014   |
| Sulphonated carbontubes   | C. inophyllum seed oil | 150                 | 30:1                 | 5                      | 5        | NR          | 99      | Dawodu et al., 2014           |
| Sulphonated carbonspheres   | Karanja                | 160                 | 45:1                 | 5                      | 4        | NR          | > 99    | Devi et al., 2014             |

Mesoporous silica/alumina materials due to the inert nature, high surface area and being having tuneable surface also gained attention as a support for the preparation of efficient solid acid catalysts for the transesterification reaction. Singh and Patel, (2014) has reported 12-tungstophosphoric acid (TPA) supported MCM-48 for transesterification of waste cooking and jatropha oil with methanol. Under optimized reaction conditions, > 93% FAMEs yield was obtained in 16 h of reaction time with 8:1 methanol to oil molar ratio. Zhuo et al., (2013) have reported sulfonic acid functionalized mesoporous SBA-15 catalyst for methanolysis of soybean oil. Under optimized reaction conditions of 5 wt% of catalyst, 16:1 alcohol to oil molar ratio, 95% biodiesel yield was obtained in 30 minutes at 190 °C reaction temperature. The catalyst has shown reasonably good reusability as it was recycled in five catalytic runs.

Shi et al., (2010) has reported sulphated zirconia supported silica for transesterification of waste cooking oil. A maximum conversion of > 98% was achieved at 200 °C reaction temperature in 2.5 h and the catalyst was reused in five runs without any significant loss in activity. The main drawback of the prepared catalyst was the leaching of sulphate ions into the product.

As evident from the literature review, solid catalyst has the potential to overcome the problems associated with the conventionally used homogeneous catalysts for biodiesel production. However, most of the literature reported heterogeneous catalysts for transesterification reactions were studied at laboratory scale only. Few other important problems associated with the application of heterogeneous catalyst and their possible solutions are provided in Table 1.9.

**Table 1.9. Problems and possible solutions related with the application of solid catalysts for biodiesel production**

| S. No. | Problem                            | Possible cause   | Possible solutions   |
|--------|------------------------------------|--|--|
| 1.     | Deactivation of solid catalysts    | Strong interaction of impurities/substrate/product with the catalyst active sites.                 | Washing with suitable solvent or re-calcination at high temperature.   |
| 2.     | Mass transfer                      | Formation of three phases <i>viz.</i> , oil, alcohol and catalyst                                  | Preparation of catalysts of high surface area and use of co-solvent (THF, n-hexane, DMSO) to make single phase of oil and alcohol. |
| 3.     | Low reactivity                     | Phase difference of catalysts and reagent  | Use of catalyst support with high surface area and pore size and high density of active sites at the catalyst surface.             |
| 4.     | Leaching and product contamination | More solubility of the active sites in alcohol or glycerol   | Improved catalyst preparation method to result stronger interactions between catalyst support and active sites                     |
| 5.     | High reaction temperature          | Catalytic sites covered by adsorbed substrate or product molecules<br>Relatively weak active sites | Preparation of catalyst with strong acidic/basic sites   |

## 1.7 Conclusions

1. Biodiesel is a non-toxic, biodegradable fuel that reduces the greenhouse gas emissions. It is an alternative to petroleum diesel fuel. At the moment, preference is given to biodiesel production by the transesterification of vegetable oils with methanol of petrochemical origin.
2. Use of high FFA containing cheap feedstock to produce biodiesel seems to be more economically viable. Homogeneous acid catalysts could be used for such feedstocks but they require high temperature, high methanol to oil molar ratio, acid resistance costly reactors, and acid neutralization after the completion of the reaction.
3. The heterogeneous catalysts could be advantageous for the transesterification as they are reusable, do not generate huge amount of effluents and do not require FAME and glycerol purification after the reaction.
4. Mixed metal oxides for the transesterification could be used as heterogeneous catalysts for the transesterification of high FFA and moisture containing vegetable oils.

### 1.8 Objectives

- i. To synthesize a series of alkali metal supported mixed metal oxides (e.g. NiO, CaO, MgO etc) and transition metal (e.g. Mo, W etc.) supported silica in nano particle form by following the different preparation techniques viz., co-precipitation, sol gel, wet impregnation method etc. and characterization of the prepared mixed metal oxides by various techniques
- ii. Application of the prepared mixed oxides as solid catalysts for the transesterification of the triglycerides having high free fatty acid contents viz., jatropha and karanja oil to produce biodiesel and optimizing the suitable reaction conditions.
- iii. To study the physiochemical properties of the prepared biodiesel samples.
- iv. To explore the scale up of the transesterification reaction with selected catalysts.

### References

- Abou-Shanab, R. A. I.; Hwang, J. H.; Cho, Y.; Min, B. and Jeon, B. H.; Characterization of microalgal species isolated from fresh water bodies as a potential source for biodiesel production. *Appl Energ.*; **2011**, 88, 3300-3306.
- Ahmad, M.; Rashid, S.; Ajab, A. K.; Zafar, M.; Sultana, S. and Gulzar, S.; Optimization of base catalyzed transesterification of peanut oil biodiesel. *Afr. J. Biotechnol.*; **2009**, 8, 441-446.
- Akbar, E.; Binitha, N.; Yaakob, Z.; Kamarudin, S. K.; Salimon, J.; Preparation of Na doped SiO<sub>2</sub> solid catalysts by the sol-gel method for the production of biodiesel from jatropha oil. *Green Chem.*, 2009, 11, 1862-1866.
- Atapour, M. and Kariminia, H. R.; Characterization and transesterification of Iranian bitter almond oil for biodiesel production. *Appl. Energ.*; **2011**, 88, 2377-2381.
- Alba-Rubio, A.C.; Vila, F.; Alonso, D.M.; Ojeda, M.; Mariscal, M. and Granados, M.L.; *Appl. Catal. B: Environ.*; **2010**, 95, 279-287.
- Bamikole, A.; Johann, G.; Hansie, K.; Biomethanol production from gasification of non-woody plant in South Africa: Optimum scale and economic performance. *Energ. Policy.*; **2010**, 38, 312-322.
- Bournay, L.; Casanave, D.; Delfort, B.; Hillion, G.; Chodorge, J.A.; New heterogeneous process for biodiesel production: a way to improve the quality and the value of the crude glycerin produced by biodiesel plants. *Catal. Today*; **2005**, 106, 190-192.
- Bao-jin, X. B-J.; Luo, J.; Zhang, F.; Fang, Z.; Biodiesel production from soybean and Jatropha oils by magnetic CaFe<sub>2</sub>O<sub>4</sub>-Ca<sub>2</sub>Fe<sub>2</sub>O<sub>5</sub>-based catalyst. *Energ.*; **2014** (In press).

Boro, J.; Konwar, L. J.; Deka, D.; Transesterification of non edible feedstock with lithium incorporated egg shell derived CaO for biodiesel production. *Fuel Process. Technol.*; **2014**, 122, 72–78.

Brunet, R.; Reyes-Labarta, J. A.; Gosálbez, G. G.; Jiménez, L.; Boer, D.; Combined simulation–optimization methodology for the design of environmental conscious absorption systems. *Comp. Chem. Eng.*, **2012**, 46, 205-16.

Chisti, Y.; Yan J.; Energy from algae: current status and future trends: Algal biofuels – a status report. *Appl. Energ.*; **2011**, 88, 3277-3279.

Chia, H. S.; Recoverable and reusable hydrochloric acid used as a homogeneous catalyst for biodiesel production. *Appl. Energ.*; **2013**, 104, 503-509.

Chai, F.; Cao, F.; Zhai, F.; Chen, Y.; Wang, X.; Su, Z.; Transesterification of Vegetable Oil to Biodiesel using a Heteropolyacid Solid. *Adv. Synth. Catal.*; **2007**, 349, 1057-1065.

Cao, F.; Chen, Y.; Zhai, F.; Li, J.; Wang, J.; Wang, X.; Wang, S.; Zhu, W.; Biodiesel production from high acid value waste frying oil catalyzed by super acid heteropolyacid. *Biotechnol. Bioenerg.*; **2008**, 101, 93-100.

Chakrabarti, A.; Sharma, M. M.; Cationic ion exchange resins as catalyst: a review. *React. Funct. Polym.*; **1993**, 20, 1-45.

Chumbhale, V. R.; Awasarkar, P. A.; Oxidative dehydrogenation of ethylene glycol into glyoxal over phosphorus-doped ferric molybdate catalyst. *Appl. Catal. A: Gen.*, **2001**, 205, 109–115.

Chumbhale, V. R.; Paradhy, S. A.; Anilkumar, M.; Kadam, S. T.; Bokade, V. V.; Vapour Phase Oxidation of Acetophenone to Benzoic Acid Over Binary Oxides of V and Mo. *Chem. Eng. Res. Design.*, **2005**, 83, 75–80.

Corma, A.; State of the art and future challenges of zeolites as catalysts. *J. Catal.*; **2003**, 216, 298-312.

Demirbas, A. Political, economic and environmental impacts of biodiesels: review. *Appl. Energ.*; **2009**, 86, 108-117.

Demirbas, A.; Competitive liquid biofuels from biomass. *Appl. Energ.*; **2011**, 88, 17-28.

Dholakiya, B. Z.; Super Phosphoric Acid Catalyzed Biodiesel Production from Low Cost Feed Stock. *Arch. Appl. Sci. Res.*; **2012**, 4,551-561.

Devi, B. L. A. P.; Reddy, T. V. K.; Lakshmi, K. V.; Prasad, R. B. N.; A green recyclable SO<sub>3</sub>H-carbon catalyst derived from glycerol for the production of biodiesel from FFA-containing karanja (*Pongamia glabra*) oil in a single step. *Bioresour. Technol.*; **2014**, 153, 370-373.

Dawodu, F. A.; Ayodele, O.; Xin, J.; Zhang, S.; Yan, D.; Effective conversion of non-edible oil with high free fatty acid into biodiesel by sulphonated carbon catalyst. *Appl. Energ.*; **2014**, 114, 819-826.

Domingues, C.; Correia, M. J. N.; Carvalho, R.; Henriques, C.; Bordado, J.; Dias, A. P. S.; Vanadium phosphate catalysts for biodiesel production from acid industrial by-products. *J. Biotechnol.*; **2013**, 164, 433-440.

De Lima, A. L.; Mbengueb, A.; Gil R. A. D. S.; Ronconib, C. M.; Mota, C. J. A.; Synthesis of amine-functionalized mesoporous silica basic catalysts for biodiesel production. *Catal. Today*; **2014**, 226, 210-216.

Dias, A. P. S.; Bernardo, J.; Felizardo, P.; Correia, M. J. N.; Biodiesel production by soybean oil methanolysis over SrO/MgO catalysts The relevance of the catalyst granulometry. *Fuel Process. Technol.*; **2012**, 102, 146-155.

Ding, Y.; Sun, H.; Duan, Z.; Chen, P.; Lou, H.; Zheng, X.; Mesoporous Li/ZrO<sub>2</sub> as a solid base catalyst for biodiesel production from transesterification of soybean oil with methanol. *Catal. Commun.*, **2011**, 12, 606–610.

Freedman, B.; Butterfield, R.O.; Pryde, E. H.; Transesterification kinetics of soybean oil. *J. Am. Oil. Chem. Soc.*; **1986**, 63, 1375-1380.

Fan, X.; Burton, R.; Austic, G.; Preparation and characterization of biodiesel produced from recycled canola oil. *Open Fuel. Energ. Sci. J.*; **2009**, 2, 113-118.

Felizardo, P.; Correia, M. J. N.; Raposo, I.; Mendes, J. F.; Berkemeier, R.; Bordado, J. M.; Production of biodiesel from waste frying oils. *Waste Manag.*; **2006**, 26, 487-494.

Faungnawakij, K.; Yoosuk, B.; Namuangruk, S.; Krasae, P.; Viriya-empikul, N.; Puttasawat B.; Sr-Mg Mixed Oxides as Biodiesel Production Catalysts. *Chem. Cat. Chem.*; **2012**, 4, 209-216.

Furuta, S.; Matsushashi, H.; Arata, K.; Biodiesel fuel production with solid superacid catalysis in fixed bed reactor under atmospheric pressure. *Catal. Commun.*; **2004**, 5, 721-723.

Furuta, S.; Matsushashi, H.; Arata, K.; Biodiesel fuel production with solid amorphous zirconia catalysis in fixed bed reactor. *Biomass Bioenerg.*; **2006**, 30, 870-873.

Fan, M.; Zhang, P.; Ma, Q.; Enhancement of biodiesel synthesis from soybean oil by potassium fluoride modification of a calcium magnesium oxides catalyst. *Bioresour. Technol.*; **2012**, 104, 447-450.

Goering, C. E.; Schwab, A. W.; Daugherty, M. J.; Pryde, E. H.; Heakin, A. J.; Fuel properties of Elven vegetable oils. *Trans ASAE.*; **1982**, 85, 1472-1483.

Granados, M. L.; Poves, M. D. Z.; Alonso, D. M.; Mariscal, R.; Galisteo, F.C.; Moreno-Tost, R.; Santamaria, J. and Fierro, J.L.G.; Biodiesel from sunflower oil by using activated calcium oxide. *Appl. Catal. B: Environ.*; **2007**; 73, 317-326.

Hu, S.; Guan, Y.; Wang, Y.; Han, H.; Nano-magnetic catalyst KF/CaO-Fe<sub>3</sub>O<sub>4</sub> for biodiesel production. *Appl. Energ.*; **2011**, 88, 2685-2690.

Hernández-Hipólitoa, P.; Juárez-Floresa, N.; Martínez-Klimovab, E.; Gómez-Cortés, A.; Bokhimic, X.; Escobar-Alarcónd, L.; Klimovaa, T. E.; Novel heterogeneous basic catalysts for biodiesel production: Sodium titanate nanotubes doped with potassium. *Catal. Today*; **2014** (In press).

Hernandez, M. R.; Reyes-Labarta, J. A.; Valde's F. J.; New Heterogeneous Catalytic Transesterification of Vegetable and Used Frying Oil. *Ind. Eng. Chem. Res.*; **2010**, 49, 9068-9076.

Joshi, R.M.; Pegg, M.; Flow properties of biodiesel fuel blends at low temperatures. *Fuel*; **2007**, 86, 143-151.

Ji, J.; Wang, J.; Li, Y.; Yu, Y.; Xu, Z.; Preparation of biodiesel with the help of ultrasonic and hydrodynamic cavitation. *Ultrasonics*; **2006**, 44, 411-414.

Kannan, S.; Catalytic applications of hydrotalcite-like materials and their derived forms. *Catal. Surv. Asia*; **2006**, 10, 117-137.

Karatay, S. E.; Dönmez, G.; Microbial oil production from thermophile cyanobacteria for biodiesel production. *Appl. Energ.*; **2011**, 88, 3632-3635.

Kumar, A.; Sharma, S.; Potential non-edible oil resources as biodiesel feedstock: an Indian perspective. *Renew Sustain Energ. Rev.*; **2011**, 15, 1791-1800.

Kim, M.; Maggio, C. D.; Salley, S. O.; Ng, K. Y. S.; A new generation of zirconia supported metal oxide catalysts for converting low grade renewable feedstocks to biodiesel. *Bioresour. Technol.*, **2012**, 118, 37-42.

Kiss, A. A.; Dimian, A. C.; Rothenberg, G.; Solid acid catalysts for biodiesel production-towards sustainable energy. *Adv. Synth. Catal.*; **2006**, 348,75-81.

Kulkarni, M. G.; Gopinath, R.; Meher, L. C.; Dalai, A. K.; Solid acid catalyzed biodiesel production by simultaneous esterification and transesterification. *Green Chem.*; **2006**, 8, 1056-1062.

Kim, H-J.; Kanga, B-S.; Kima, M-J.; Park, Y. M.; Kimb, D-K.; Lee, J-S.; Lee, K-Y.; Transesterification of vegetable oil to biodiesel using heterogeneous base catalyst. *Catal. Today*; **2004**, 93-95, 315-320.

Katada, N.; Hatanaka, T.; Ota, M.; Yamada, K.; Okumura, K.; Niwa, M.; Biodiesel production using heteropoly acid-derived solid acid catalyst  $H_4PNbW_{11}O_{40}/WO_3-Nb_2O_5$ . *Appl. Catal. A: Gen.*; **2009**, 363, 164-168.

Kumar, D.; Ali, A.; Nanocrystalline K-CaO for the Transesterification of a Variety of Feedstocks: Structure, Kinetics and Catalytic Properties. *Biomass Bioenerg.*; **2012**, 46, 459-468.

Kawashima, A.; Matsubara, K.; Honda, K.; Development of heterogeneous base catalysts for biodiesel production. *Bioresour. Technol.*; **2008**, 99, 3439-3443.

Kansedo, J.; lee, K. T.; Bhatia, S.; *Cerbera odollam* (sea mango) oil as a promising non-edible feedstock for biodiesel production. *Fuel*; **2009**, 88, 1148-1150.

Leduc, S.; Natarajan, K.; Dotzauer, E.; McCallum, I.; Obersteiner, M.; Optimizing biodiesel production in India. *Appl. Energ.*; **2009**, 86, 125-131.

Leung, D. Y. C.; Guo Y.; Transesterification of neat and used frying oil: optimization for biodiesel production. *Fuel Process. Technol.*; **2006**, 87, 883-8890.

Lima, J. R. O.; Ghani, Y. A.; da Silva, R. B.; Batista, F. M. C.; Binib, R. A.; Varanda, L. C.; Oliveira, J. E.; Strontium zirconate heterogeneous catalyst for biodiesel production: Synthesis, characterization and catalytic activity evaluation. *Appl. Catal. A: Gen.*; **2012**, 445-446, 76-82.

Liu, Q.; Wang, B.; Wang, C.; Tian, Z.; Qu, W.; Ma, H.; Xu, R.; Basicities and transesterification activities of Zn–Al hydrotalcites-derived solid bases. *Green Chem.*; **2014**, (In press).

Liu, X.; He, H.; Wang, Y.; Zhu, S.; Transesterification of soybean oil to biodiesel using SrO a solid base catalyst. *Catal. Commun.*; **2007**, 8, 1107-1111.

Li, Y.; Lian, S.; Tong, D.; Song, R.; Yang, W.; Fan, Y.; Qing, R. and Hua, C.; One-step production of biodiesel from *Nannochloropsis sp.* on solid base Mg-Zr catalyst. *Appl. Energ.*; **2011**, 88, 3313-3317.

Montefrio, M. J.; Xinwen, T.; Obbard, J. P.; Recovery and pre-treatment of fats, oil and grease from grease interceptors for biodiesel production. *Appl. Energ.*; **2010**, 87, 3155-3161.

Meher, L. C.; Sagar, D. V.; Naik, S. N.; Technical aspects of biodiesel production by transesterification - a review. *Renew. Sustain. Energ. Rev.*; **2006**, 10, 248-268.

Moser, B. R.; Vaughn, S. F.; Coriander seed oil methyl esters as biodiesel fuel: Unique fatty acid composition and excellent oxidative stability. *Biomass Bioenerg.*; **2010**, 34, 550-558.

Moser, B. R.; Biodiesel production, properties, and feedstocks. *In Vitro Cell. Dev. Biol. Plant*; **2009**, 45, 229-266.

Mamoru, I.; Chen, B. X.; Masashi, E.; Takashi, K.; Surekha, S.; Production of biodiesel fuel from triglycerides and alcohol using immobilized lipase. *J. Mol. Catal. B: Enzym.*; **2001**, 16, 53-8.

Mayani, S. V.; Mayani, V. J.; Kim, S. W.; Synthesis of molybdovanadophosphoric acid supported hybrid materials and their heterogeneous catalytic activity. *Mater. Lett.*; **2013**, 111, 112–115.

Mayani, S. V.; Mayani, V. J.; Park, S. K.; Kim, S. W.; Synthesis and characterization of metal incorporated composite carbon materials from pyrolysis fuel oil. *Mater. Lett.*; **2012**, 82, 120–123.

Meher, L. C.; Kulkarni, M. G. ; Dalai, A. K.; Naik, S. N.; Transesterification of karanja (*Pongamia pinnata*) oil by solid basic catalysts. *Eur. J. Lipid Sci. Technol.*; **2006**, 108, 389-397.

Ma, F.; Clements, L. D.; Hanna, M. A.; Biodiesel fuel from animal fat. Ancillary studies on transesterification of beef tallow. *Ind. Eng. Chem. Res.*; **1998**, 37, 3768-3771.

Mootabdi, H.; Salamatinia, B.; Bhatia, S.; Abdullah, A. Z.; Ultrasonic assisted biodiesel production process from palm oil using alkaline earth metal oxides as the heterogeneous catalysts. *Fuel*; **2010**, 89, 1818-1825.

Martins G. C.; Teixeira, S.; Ledo M. L.; Schuchardt, U.; Transesterification of soybean oil catalyzed by sulfated zirconia. *Bioresourc. Technol.*; **2008**, 99, 6608-6613.

Niza, N. M.; Tan, K. T.; Lee, K. T.; Ahmad, Z.; Biodiesel production by non-catalytic supercritical methyl acetate: thermal stability study. *Appl. Energ.*; **2013**, 101, 198-202.

Narsimharao, K.; Lee, A.; Wilson, K.; Catalysis in production of biodiesel: A review. *J. Biobased. Mater. Bioenerg.*; **2007**, 1, 19-30.

Orthoefer, F.T. Rice bran oil. In: 6<sup>th</sup> ed. Shahidi F., editor. *Bailey's industrial oil & fat products*, Volume 2. New Jersey: John Wiley & Sons, Inc.; **2005**.

Orcaire, O.; Buisson, P.; Pierre, A.C.; Application of silica aerogel encapsulated lipase in the synthesis of biodiesel by transesterification reactions. *J. Mol. Catal. B: Enzym.*; **2006**, 42, 106-113.

Park, Y. M., Chung, S., Eom, H. J., Lee, J., Lee, K. Tungsten oxide zirconia as solid superacid catalyst for esterification of waste acid oil. *Bioresour. Technol.*, **2010**, 101, 6589-6593.

Poonjarernsilp, C.; Sano, N.; Tamon, H.; Hydrothermally sulfonated single-walled carbon nanohorns for use as solid catalysts in biodiesel production by esterification of palmitic acid. *Appl. Catal. B: Environ.*; **2014**, 147, 726-732.

Rasoul-Amini, S.; Montazeri-Najafabady, N.; Mobasher, M. A.; Hoseini-Alhashemi, S.; Ghasemi, Y.; *Chlorella sp.*: a new strain with highly saturated fatty acids for biodiesel production in bubble-column photobioreactor. *Appl. Energ.*; **2011**, 88, 3354-3356.

Rashid, U.; Anwar, F.; Production of biodiesel through optimized alkaline-catalyzed transesterification of rapeseed oil. *Fuel*; **2008**, 87, 265-273.

Rashid, U.; Anwar, F.; Moser, B. R. and Ashraf, S.; Production of sunflower oil methyl esters by optimized alkali catalyzed methanolysis. *Biomass bioenerg.*; **2008**, 32, 1202-1205.

Rashid, U.; Anwar, F.; Production of Biodiesel through Base-Catalyzed Transesterification of Safflower Oil Using an Optimized Protocol. *Energ. Fuel*; **2008**, 22, 1306-1312.

Rashtizadeh, E.; Farzaneh, F.; Talebpour, Z.; Synthesis and characterization of Sr<sub>3</sub>Al<sub>2</sub>O<sub>6</sub> nanocomposite as catalyst for biodiesel production. *Bioresour. Technol.*; **2014**, 154, 32-37.

Rodriguez, J. A.; Stacchiola, D.; Catalysis and the nature of mixed-metal oxides at the nanometer level: special properties of  $\text{MO}_x/\text{TiO}_2(110)$  {M= V, W, Ce} surfaces. *Phys. Chem. Chem. Phys.*; **2010**, 12, 9557-9565.

Saka, S.; Kusdiana, D.; Biodiesel fuel from rapeseed oil as prepared in supercritical methanol. *Fuel*; **2001**, 80, 225-231.

Sankaranarayanan, T. M.; Shanthi, V.; Thirunavukkarasu, K.; Pandurangan, A.; Sivasanker, S.; Catalytic properties of spinel-type mixed oxides in transesterification of vegetable oils. *J. Mol. Catal. A: Chem.*, **2013**, 379, 234-242.

Santiago-Torres, N.; Romero-Ibarra, I. C.; Pfeiffer, H.; Sodium zirconate ( $\text{Na}_2\text{ZrO}_3$ ) as a catalyst in a soybean oil transesterification reaction for biodiesel production. *Fuel Process. Technol.*, **2014**, 120, 34-39.

Schuchardt, U.; Serchelia, R.; Vargas, R. M.; Transesterification of vegetable oils: a review. *J. Braz. Chem. Soc.*; **1998**, 9, 199-210.

Schwab, A.W.; Bagby, M.O.; Freedman, B.; Preparation and properties of diesel fuels from vegetable oils. *Fuel*; **1987**, 66, 1372-1378.

Sharma, M. M.; Some novel aspects of cationic ion-exchange resins as catalysts: a review. *React. Funct. Polym.*; **1995**, 26, 3-23.

Shi, W.; He, B.; Ding, J.; Li, J.; Yan, F.; Liang, X.; Preparation and characterization of the organic-inorganic hybrid membrane for biodiesel production. *Bioresour. Technol.*; **2010**, 101, 1501-1505.

Singh, S.; Patel, A.; 12-Tungstophosphoric acid supported on mesoporous molecular material: synthesis, characterization and performance in biodiesel production. *J. Cleaner Prod.*, **2014** (In press).

Singh, A.; He, B.; Thompson, J.; Gerpen, J. V.; Process of optimization of biodiesel production using alkaline catalysts. *Appl. Eng. Agric.*; **2006**, *22*, 597-600.

Silva, C. C. C. M.; Ribeiro, N. F. P.; Souza, M. M. V. M.; Biodiesel production from soybean oil and methanol using hydrotalcites as catalyst. *Fuel Process. Technol.*; **2010**, *91*, 205-210.

Soriano, N. U.; Migo, V. P.; Sato, K.; Matsumura, M.; Crystallization behavior of neat biodiesel and biodiesel treated with ozonized vegetable oil. *Eur. J. Lipid Sci. Technol.*; **2005**, *107*, 689-696.

Srilatha, K.; Sree, R.; Devi, B. L. A. P.; Prasad, P. S. S.S.; Prasad, R. B. N.; Lingaiah, N.; Preparation of biodiesel from rice bran fatty acids catalyzed by heterogeneous cesium-exchanged 12-tungstophosphoric acids. *Bioresour. Technol.*, **2012**, *116*, 53-57.

Sun, H.; Ding, Y.; Duan, J.; Zhang, Q.; Wang, Z.; Lou, H.; Zheng, X., Transesterification of sunflower oil to biodiesel on ZrO<sub>2</sub> supported La<sub>2</sub>O<sub>3</sub> catalyst. *Bioresour. Technol.*, **2010**, *101*, 953-958.

Suwannakarn, K.; Lotero, E.; Goodwin, Jr. J. G.; Simultaneous free fatty acid esterification and triglyceride transesterification using a solid acid catalyst with in situ removal of water and unreacted methanol. *Ind. Eng. Chem. Res.*; **2009**, *48*, 2810-2818.

Stavarache, C.; Vinatoru, M.; Nishimura, R.; Maed, Y.; Fatty acids methyl esters from vegetable oil by means of ultrasonic energy. *Ultrason. Sonochem.*; **2005**, *12*, 367-3672.

Talebian-Kiakalaieh, A.; Amin, N. A. S.; Mazaheri, H.; A review on novel processes of biodiesel production from waste cooking oil. *Appl. Energ.*; **2013**, *104*, 683-710.

Tantirungrotechai, J.; Thepwatee, S.; Yoosuk, B.; Biodiesel synthesis over Sr/MgO solid base catalyst. *Fuel*; **2013**, *106*, 279-284.

Taufiq-Yapa, Y. H.; Teoa, S. H.; Rashid, U.; Islam, A.; Hussien, M. Z.; Leed, K. T.; Transesterification of *Jatropha curcas* crude oil to biodiesel on calcium lanthanum mixed oxide catalyst: Effect of stoichiometric composition. *Energ. Conserv. Manag.*, **2014** (In press).

Thitsartarna, W.; Kawi, S.; An active and stable CaO-CeO<sub>2</sub> catalyst for transesterification of oil to biodiesel. *Green Chem.*; **2011**, 13, 3423-3430.

Trakarnpruk, W.; Chuayplod, P.; Biodiesel from Moringa Oleifera Oil Using K-Promoted Layered Double Hydroxide Derived Mgallao Catalysts. *Int. J. Energ. Power*, **2012**, 1, 58-63.

Varghaa, V.; Truterb, P.; Biodegradable polymers by reactive blending transesterification of thermoplastic starch with poly(vinyl acetate) and poly(vinyl acetate-co-butyl acrylate. *Eur. Polymer J.*; **2005**, 41, 715-726.

Verziu, M.; Coman, S. M.; Richards, R.; Parvulescu, V. I.; Transesterification of vegetable oils over CaO catalysts. *Catal. Today*; **2011**, 167, 64-70.

Valkenberg, M. H.; Hölderich, W. F.; Preparation and use of hybrid organic-inorganic catalysts. *Catal. Rev. Sci. Eng.*; **2002**, 44, 321-374.

Wahlen, B. D.; Barney, B. M.; Seefeldt, L. C.; Synthesis of biodiesel from mixed feedstocks and longer chain alcohols using an acid-catalyzed method. *Energ. Fuel*; **2008**, 22, 4223-4228.

Wu, X.; Leung, D. Y. C.; Optimization of biodiesel production from camelina oil using orthogonal experiment. *Appl. Energ.*; **2011**, 88, 3615-3624.

Wen, Z.; Yu, X.; Tu, S. T.; Yan, J.; Dahlquist, E.; Synthesis of biodiesel from vegetable oil with methanol catalyzed by Li-doped magnesium oxide catalysts. *Appl. Energ.*; **2010**, 87, 743-748.

Warabi, Y.; Kusdiana, D.; Saka, S.; Reactivity of triglycerides and fatty acids of rapeseed oil in supercritical alcohols. *Bioresour. Technol.*; **2004**, 91, 283-287.

Wang, Y.; Ou, S.; Liu, P.; Xue, F.; Tang, S.; Comparison of two different processes to synthesize biodiesel by waste cooking oil. *Mol. Catal. A. Chem.*; **2006**, 252, 107-112.

Wang, L. and Yang, J.; Transesterification of soybean oil with nano-MgO or not in supercritical and subcritical methanol. *Fuel*; **2007**, 86, 328-33.

Wana, L.; Liua, H.; Skalab, D.; Biodiesel production from soybean oil in subcritical methanol using  $\text{MnCO}_3/\text{ZnO}$  as catalyst. *Appl. Catal. B: Environ.*; **2014**, 152-153, 352-359.

Wen, Z.; Yu, X.; Tu, S-T.; Yan, J.; Dahlquist, E.; Biodiesel production from waste cooking oil catalyzed by  $\text{TiO}_2\text{-MgO}$  mixed oxides. *Bioresour. Technol.*, **2010**, 101, 9570-9576.

Xie, W.; Li, H.; Alumina-supported potassium iodide as a heterogeneous catalyst for biodiesel production from soybean oil. *J. Mol. Catal. A: Chem.*; **2006**, 255, 1-9.

Xie, W. L.; Huang, X. M.; Synthesis of biodiesel from soybean oil using heterogeneous  $\text{KF/ZnO}$  catalyst. *Catal. Lett.*; **2006**, 107, 53-59.

Xu, L.; Guanzhong, L.; Yanglong, G.; Yun, G.; Yanqin, W.; Zhigang, Z.; Xiaohui, L.; Yunsong, W.; A novel solid superbase of  $\text{Eu}_2\text{O}_3/\text{Al}_2\text{O}_3$  and its catalytic performance for the transesterification of soybean oil to biodiesel. *Catal. Commun.*; **2007**, 8, 1969-1972.

Xu, L.; Yang, X.; Yu, X.; Guo, Y.; Maynurdader; Preparation of mesoporous polyoxometalate-tantalum pentoxide composite catalyst for efficient esterification of fatty acid. *Catal. Commun.*; **2008**, 9, 1607-1611.

Xu, W.; Gao, L.; Wang, S.; Xiao, G.; Biodiesel production in a membrane reactor using MCM-41 supported solid acid catalyst. *Bioresour. Technol.*; **2014**, 159, 286-291.

Yan, J.; Lin, T.; Biofuels in Asia. *Appl. Energ.*; **2009**, 86, S1-S10.

Yang, Z.; Xie, W.; Soybean oil transesterification over zinc oxide modified with alkali earth metals. *Fuel Process. Technol.*; **2007**, 88, 631-638.

Yan, S.; Kim, M.; Mohan, S.; Salley, S. O.; Simon, N. K. Y.; Effects of preparative parameters on the structure and performance of Ca–La metal oxide catalysts for oil transesterification, *Appl. Catal. A: Chem.*; **2010**, 373, 104-111.

Zabeti, M.; Daud, W. M. A. W.; Aroua, M. K.; Activity of solid catalysts for biodiesel production: a review. *Fuel Process. Technol.*; **2009**, 90, 770-777.

Zhang, S.; Zu, Y-G.; Fu, Y-J.; Luo, M.; Zhang, D. Y.; Efferth, T.; Rapid microwave-assisted transesterification of yellow horn oil to biodiesel using a heteropolyacid solid catalyst. *Bioresour. Technol.*, **2010**, 101, 931–936.

Zhuo, D.; Lane, J.; Culy, D.; Schultz, M.; Pullar, A.; Waxman, M.; Sulfonic acid functionalized mesoporous SBA-15 catalysts for biodiesel production. *Appl. Catal. B: Environ.*, **2013**, 129, 342-350.

---

**Materials and Methods**

---

|            | <b>Contents</b>                                 | <b>Page number</b> |
|------------|---|--------------------|
| <b>2.1</b> | <b>Chemicals</b>                                | 40                 |
| <b>2.2</b> | <b>Chemical analysis of vegetable oils</b>      | 40                 |
| <b>2.3</b> | <b>Fatty acid composition of vegetable oils</b> | 41                 |
| <b>2.4</b> | <b>Thin layer Chromatography (TLC)</b>          | 41                 |
| <b>2.5</b> | <b>Instruments</b>                              | 42                 |
|            | <b>References</b>                               | 46                 |

---

### **Abstract**

This chapter includes the list of chemicals and materials, and detailed description of methods and analytical techniques which are frequently employed in present thesis.

**Materials and Methods**

---

|            | <b>Contents</b>                                 | <b>Page number</b> |
|------------|---|--------------------|
| <b>2.1</b> | <b>Chemicals</b>                                | 40                 |
| <b>2.2</b> | <b>Chemical analysis of vegetable oils</b>      | 40                 |
| <b>2.3</b> | <b>Fatty acid composition of vegetable oils</b> | 41                 |
| <b>2.4</b> | <b>Thin layer Chromatography (TLC)</b>          | 41                 |
| <b>2.5</b> | <b>Instruments</b>                              | 42                 |
|            | <b>References</b>                               | 46                 |

---

### **Abstract**

This chapter includes the list of chemicals and materials, and detailed description of methods and analytical techniques which are frequently employed in present thesis.

---

**Potassium Fluoride Impregnated CaO/NiO: An Efficient Heterogeneous Catalyst for Transesterification of Waste cottonseed oil**

---

|            | <b>Contents</b>  | <b>Page</b> |
|------------|--|-------------|
| <b>3.1</b> | <b>Introduction</b>  | 47          |
| <b>3.2</b> | <b>Experimental section</b>  | 48          |
|            | 3.2.1 Catalyst preparation   | 48          |
|            | 3.2.2 Transesterification of waste cottonseed oil                                      | 48          |
|            | 3.2.3 Reaction kinetics  | 48          |
| <b>3.3</b> | <b>Results and discussion</b>  | 49          |
|            | 3.3.1 Catalyst characterization  | 49          |
|            | 3.3.1.1 SEM and TEM analysis   | 49          |
|            | 3.3.1.2 BET surface area and Basic strength  | 50          |
|            | 3.3.1.3 Powder X-ray diffraction study   | 51          |
|            | 3.3.2 FAMES characterization by <sup>1</sup> H NMR                                     | 52          |
| <b>3.4</b> | <b>Catalytic activity of KF/CaO/NiO</b>  | 54          |
|            | 3.4.1 Effect of Impregnated KF Concentration and catalyst concentration on FAMES yield | 55          |
|            | 3.4.2 Effect of Reaction Temperature and molar ratio on FAMES yield                    | 56          |
| <b>3.5</b> | <b>Effect of FFA on catalyst activity</b>  | 57          |
| <b>3.6</b> | <b>Reusability of the catalyst</b>   | 58          |
| <b>3.7</b> | <b>Kinetic study</b>   | 60          |
| <b>3.8</b> | <b>Physicochemical properties of the FAMES</b>   | 61          |
| <b>3.9</b> | <b>Conclusions</b>   | 62          |
|            | <b>References</b>  | 63          |

---

### **Abstract**

Potassium fluoride impregnated CaO/NiO has been prepared by wet impregnation method in nano particle form as supported by powder X-ray diffraction, scanning electron microscopy and transmission electron microscopy studies. Brunauer-Emmett-Teller surface area and basic sites measurement studies have been performed to establish the effect of potassium fluoride impregnation on catalyst surface morphology and basic strength. CaO/NiO impregnated with 20 wt% potassium fluoride was used as solid catalyst for the transesterification of waste cottonseed oil having up to 5.8 wt% free fatty acid content. The variables used for the transesterification were, amount of KF impregnated on CaO/NiO, catalyst concentration, reaction temperature and methanol to oil molar ratio. Reaction parameters have been optimized to achieve the least reaction period for the completion of the reaction. Complete transesterification (> 98 % FAMEs yield) of waste cotton seed oil with methanol (1:15 molar ratio) required 4 h in the presence of 5 wt% catalyst (with respect to oil) at 65 °C. Reusability study suggests that catalyst could be recycled in four successive runs without significant loss in activity. A pseudo first order kinetic equation was applied to evaluate the kinetic parameters and under optimized conditions first order rate constant and activation energy was found to be  $0.023 \text{ min}^{-1}$  (65 °C) and  $41.2 \text{ kJ mol}^{-1}$ , respectively. Few physicochemical properties of the prepared biodiesel sample have also been studied and compared with standard values.

### 3.1 Introduction

Homogeneous alkali catalyst is sensitive to the moisture and free fatty acids (FFA) and consequently required FFA and moisture free costlier refined oil for the transesterification reaction (Reddy et al., 2006). In India due to the shortage of edible oils, application of non edible and waste cooking oils is encouraged for biodiesel production in order to avoid food *versus* fuel situation. However, such oils usually possess high FFA (1-10%) and moisture (0.5-5%) content (Knothe, 2001), and hence, homogeneous base catalysts could not be directly employed for their transesterification. In order to circumvent the problem associated with homogeneous catalyst, there has been an increased research activity directed toward the development of reusable heterogeneous catalysts.

Mixed metal oxides usually possess higher catalytic activity, in comparison to the pure oxides and have several synthetic applications *viz.*, oxidation, dehydration, dehydrogenation and isomerization (Wachs, 2006; Hodnett, 2010; Centi, 2001). The active centres in mixed oxides could be either oxygen atoms or the dopant itself. In literature large number of mixed oxides has been reported for the transesterification reactions such as MgO-ZrO<sub>2</sub> (Omar et al., 2011; Sree et al., 2009), MgO-La<sub>2</sub>O<sub>3</sub> (Desmartin-Chomel et al., 2010; Babu et al., 2008; Ivanova et al., 2005), KNO<sub>3</sub>/Al<sub>2</sub>O<sub>3</sub> (Xie et al., 2006), KOH/MgO (Ilgen and Akin, 2009), Li/ZnO (Xie et al., 2007), KF/ZnO (Xie and Huang, 2006), KF/Ca-Mg-Al (Gao et al., 2010) and CaO supported on porous carbon (Zu et al., 2010) and KF/CaO-Fe<sub>3</sub>O<sub>4</sub> (Hu et al., 2011).

Gao et al. (2010), have reported KF/Mg-Al hydrotalcite as solid catalyst for the transesterification of palm oil with 85% FAMES yield under optimized reaction conditions. Wen et al. (2010) have reported the application of KF/CaO as reusable nano catalyst for the transesterification of Chinese tallow seed oil to obtain 96% FAMES yield. They proposed that interaction of KF with CaO leads to the formation of KCaF<sub>3</sub> which is responsible for the increase in basic (active) sites as well as activity of the KF/CaO catalyst. Sun et al. (2008) reported the preparation of KF impregnated Eu<sub>2</sub>O<sub>3</sub> for the transesterification of rapeseed oil, but a maximum FAMES yield of 92.5% was achieved at 65 °C reaction temperature. Thus in most of the literature reported KF based catalysts the FAMES yield is less than the acceptable value of 96.5%.

In order to achieve the complete conversion of waste cotton seed oil into FAMES (> 98%), in present study a support of Ca and Ni mixed oxides (CaO/NiO) has been prepared and

impregnated with 5-25 wt% KF to improve its activity. The prepared catalyst has been employed as solid catalyst for the transesterification of the waste cotton seed oil with methanol. The reaction parameters for the optimum catalytic activity have been optimized by varying the reaction temperature, catalyst concentration, and methanol to oil molar ratio. Under optimized reaction conditions, effect of FFA on catalytic activity and kinetics of the reaction has also been evaluated.

### **3.2 Experimental section**

#### **3.2.1 Catalyst preparation**

For KF impregnation, a support of CaO/NiO was prepared by doping 5 wt% CaO in NiO by wet chemical method. In a typical preparation, 10 g of nickel oxide was suspended in 40 mL of deionized water, and to this 10 mL calcium nitrate solution was added. The resulted slurry was stirred for 5 h, dried at 120 °C for 24 h and finally calcined at 500 °C to yield CaO/NiO.

Prepared CaO/NiO (10 g) was suspended in deionized water (40 mL) and to this KF solution of desired concentration was added. The resulted suspension was stirred for 4 h, dried at 120 °C for 24 h and finally calcined at 700 °C. The catalysts prepared in such a manner were designated as  $x$ -KF/CaO/NiO-700, where  $x$  represents the wt% of impregnated KF in CaO/NiO.

The prepared catalysts were characterized by XRD, BET surface area measurement, Hammett indicator test, SEM and TEM techniques.

#### **3.2.2 Transesterification of waste cottonseed oil**

Transesterification reactions were carried out in a 250 ml two-necked round-bottom flask equipped with a reflux condenser, a thermometer, and a heating mantle with magnetic stirrer. In a typical run, the flask charged with 10 g WCO, desired amount of methanol, and catalyst, were heated at specific temperature. In order to monitor the progress of the reaction, aliquots were collected from the reaction mixture after every 30 min and subjected to the proton NMR analysis.

#### **3.2.3 Reaction Kinetics**

Transesterification is generally assumed to be a pseudo-first order reaction as alcohol in these reactions is usually employed in excess to the required stoichiometric molar ratio of 3:1 (alcohol

to oil). The conversion of WCO at different reaction duration was obtained and fitted in equation 1 to calculate the apparent first order rate constants. To calculate the activation energy, the reactions were performed at 35, 45, 55 and 65 °C and respective reaction rate constants were fitted in Arrhenius equation 2.

$$-\ln(1-X_{me}) = kt \quad (1)$$

$$\ln k = -E_a/RT + \ln A \quad (2)$$

where,  $k$  is the apparent first order rate constant ( $\text{min}^{-1}$ ),  $X_{me}$  is the conversion of oil into FAMES at time  $t$ ,  $E_a$  is the activation energy ( $\text{kJ mol}^{-1}$ ),  $A$  is the pre-exponential factor ( $\text{min}^{-1}$ ),  $R$  is the gas constant ( $8.314 \times 10^{-3} \text{ kJ K}^{-1} \text{ mol}^{-1}$ ) and  $T$  is the reaction temperature ( $^{\circ}\text{K}$ ).

TOF of the catalyst is calculated from equation 3.

$$\text{TOF} = \text{moles of FAMES produced}/t.f_m \quad (3)$$

where,  $t$  is time (min) and  $f_m$  is the basic sites (in mmol) present in catalyst obtained from acid base titration.

### 3.3 Results and discussion

#### 3.3.1 Catalyst characterization

##### 3.3.1.1 SEM and TEM analysis

To determine the surface morphology and structure, the prepared catalyst (20-KF/CaO/NiO-700) was characterized by SEM and TEM techniques. The SEM study of 20-KF/CaO/NiO-700, support the formation of clusters of the catalyst particles of about 1.8  $\mu\text{m}$  size (Fig. 3.1a). The cluster formation could be due to the agglomeration of the particles during their preparation. A further investigation of the catalyst by TEM study reveals that these clusters are made up of rhombus shaped particles with an average size of about 150 nm as shown in Fig. 3.1b.

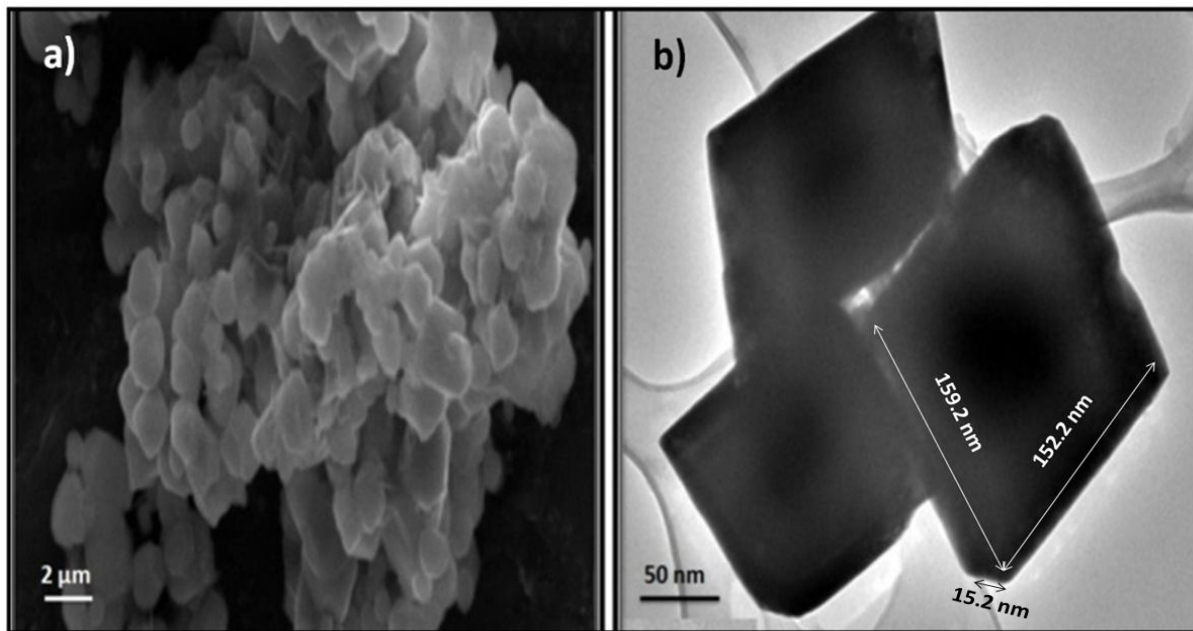


**Fig.3.1. a) SEM image of 20-KF/CaO/NiO-700 and b) TEM image of 20-KF/CaO/NiO-700.**

### 3.3.1.2 BET surface area and Basic strength

The basic strength of CaO/NiO was found in the range of 10.1-11.1 as measured by Hammett indicators. In order to enhance the basic strength further, it was impregnated with 5-25 wt% KF. A successive increase in KF concentration in CaO/NiO was found to increase the basic strength and a maximum value of 15.0-18.4 was obtained upon 20 wt% KF impregnation. A further increase ( $> 20$  wt%) in KF concentration was not found to alter the basic strength, and hence 20 wt% KF loading was selected as the optimum loading for the catalyst preparation.

The increase in KF concentration in CaO/NiO was also found to increase the total basic sites which in turn enhance the activity (TOF) of KF/CaO/NiO catalyst as shown in Table 3.1.

**Table 3.1. Comparisons of the specific surface area, basic strength, basicity, rate of reaction and TOF of 5-25 wt% KF impregnated CaO/NiO-700.**

| Catalyst          | Specific Surface Area (m <sup>2</sup> /g) | Basic Strength (H <sub>+</sub> ) | Basicity (mmol g <sup>-1</sup> ) | r (x 10 <sup>-4</sup> ) mol min <sup>-1</sup> g <sup>-1</sup> of catalyst | TOF (x 10 <sup>-2</sup> ) (min <sup>-1</sup> ) |
|-------------------|---|----------------------------------|----------------------------------|---|--|
| CaO/NiO           | 3.22                                      | 9.8 < H <sub>+</sub> < 10.1      | 4.7                              | 1.74  | 3.71   |
| 5-KF/CaO/NiO-700  | 2.57                                      | 10.1 < H <sub>+</sub> < 11.1     | 5.10                             | 2.08  | 4.16   |
| 10-KF/CaO/NiO-700 | 2.21                                      | 11.1 < H <sub>+</sub> < 15.0     | 5.31                             | 2.32  | 4.37   |
| 15-KF/CaO/NiO-700 | 1.76                                      | 11.1 < H <sub>+</sub> < 15.0     | 5.52                             | 2.61  | 4.70   |
| 20-KF/CaO/NiO-700 | 0.87                                      | 15.0 < H <sub>+</sub> < 18.4     | 6.11                             | 2.92  | 4.83   |
| 25-KF/CaO/NiO-700 | 0.89                                      | 15.0 < H <sub>+</sub> < 18.4     | 7.33                             | 2.98  | 3.91   |

\*Reaction conditions: Catalyst amount = 5 wt% of oil, MeOH:oil molar ratio = 15:1, Reaction temperature = 65°C.

The specific surface area of CaO/NiO decreases gradually on increasing the KF loading due to the pore plugging of the support material upon KF impregnation. The lesser surface area of CaO/NiO as well as KF impregnated CaO/NiO also indicates their nonporous nature. Thus, activity of the catalyst was found to be function of their basic strength rather than surface area. Similar observation was reported in literature for heterogeneous catalyst (Deng and Patil, 2009; Sankaranarayanan et al., 2012).

### 3.3.1.3 Powder X-ray diffraction study

The powder XRD study of CaO/NiO and 5-25 wt% KF impregnated CaO/NiO have been performed and comparison of respective diffraction patterns are given in Fig. 2. Pure NiO was found to exist in cubic phase (JCPDS-01-1239). A solid solution was formed upon 5 wt% CaO impregnation in NiO as no characteristic peak corresponding to CaO structure was observed in the XRD pattern of CaO/NiO.

Addition of 5 wt% KF in CaO/NiO followed by calcination at 700 °C leads to the formation of CaF<sub>2</sub> in cubic phase (2θ ~ 29.5°, 47.3°, JCPDS-01-1274) and KCaF<sub>3</sub> in orthorhombic phase (2θ ~ 28.9°, 41.3°, 51.4°, JCPDS-21-1341) as supported by the respective XRD patterns in

Fig. 3.2. A further increase in KF concentration ( $\geq 10$  wt%), leads to the formation of  $\text{KCaF}_3$  phase and diffraction patterns corresponding to the  $\text{CaF}_2$  phase was no longer found. Thus, higher basic strength as well as activity of  $\text{KF}/\text{CaO}/\text{NiO}$  catalyst (with 20 wt% KF), as shown in Table 2, is due to the formation of  $\text{KCaF}_3$ .

The crystallite size of 20-KF/ $\text{CaO}/\text{NiO}$ -700 catalyst was determined by the Debye-Scherrer method (Quadri et al., 1999) corresponding to (200) plane using powder XRD data and found to be about 41.7 nm. Thus, XRD as well as TEM study support the formation of 20-KF/ $\text{CaO}/\text{NiO}$ -700 catalyst in the form of nano-particles.

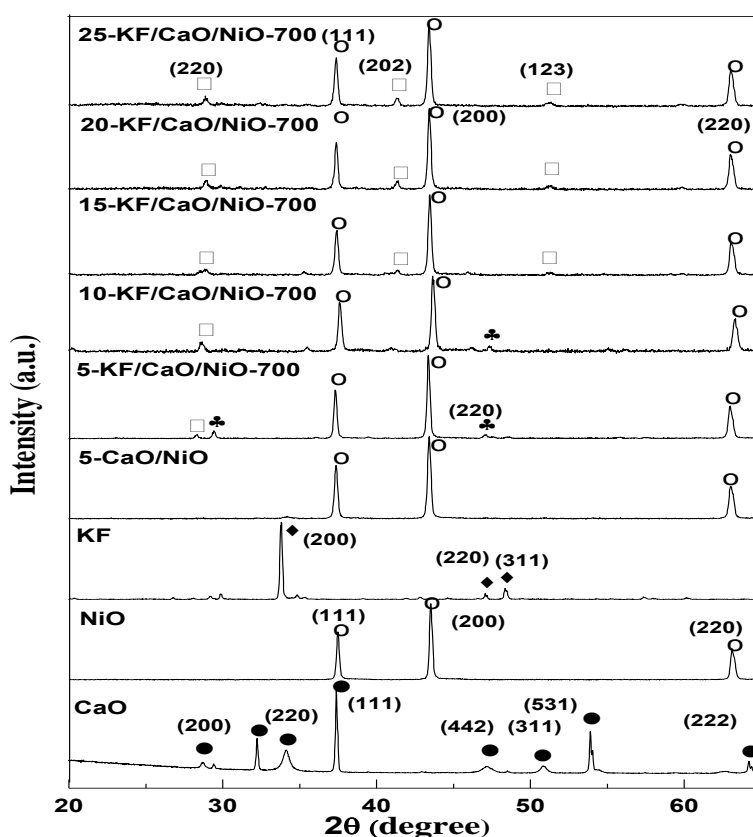


Fig. 3.2. Comparative powder XRD patterns of  $\text{CaO}$ ,  $\text{NiO}$ ,  $\text{KF}$ , 5- $\text{CaO}/\text{NiO}$  and 5-25 wt%  $\text{KF}$  impregnated  $\text{CaO}/\text{NiO}$ -700 [ $\text{CaO}$  (●),  $\text{NiO}$  (○),  $\text{KF}$  (◆),  $\text{CaF}_2$  (♣),  $\text{KCaF}_3$  (□)].

### 3.3.2 FAMES characterization by $^1\text{H}$ NMR

The efficiency of the prepared catalyst has been evaluated for the transesterification of a variety of feedstocks, *viz.*, WCO, FO, SO and KO. However, WCO was selected as feedstock for

optimizing the reaction parameters to achieve the complete conversion (> 98 % FAEEs yield) in minimum possible time. The FAMES were characterized and quantified by proton NMR technique, as this technique is not only quick, simple, and non destructive but also not required any derivatization of the products.

The  $^1\text{H}$  NMR spectrum of WCO shows a multiplet at 4.15-4.34 ppm due to the presence of glyceridic protons. The peaks appearing at 0.8-2.8 ppm in the proton NMR spectra of biodiesel as well as WCO (Fig. 3.3) are due to the presence of saturated hydrocarbon protons of fatty acids. The unsaturated protons of fatty acid carbon chain in WCO as well as FAMES appear at 5.25 ppm. In proton NMR spectrum of FAMES, a new peak appears at 3.6 ppm due to  $-\text{OCH}_3$  protons, and peaks corresponding to the glyceridic protons were no longer found, to support the formation of fatty acid methyl ester upon methanolysis of oil. FAMES produced during the methanolysis of WCO were quantified (Knothe, 2001) by following equation (1):

$$\% C_{\text{ME}} = 100 [2I_a / 3I_b] \quad (1)$$

where,  $I_a$  and  $I_b$  are the integration of peaks corresponding to  $-\text{OCH}_3$  protons (3.6 ppm), and  $\alpha$ -methylene protons (2.3 ppm), respectively in the  $^1\text{H}$  NMR of FAMES.

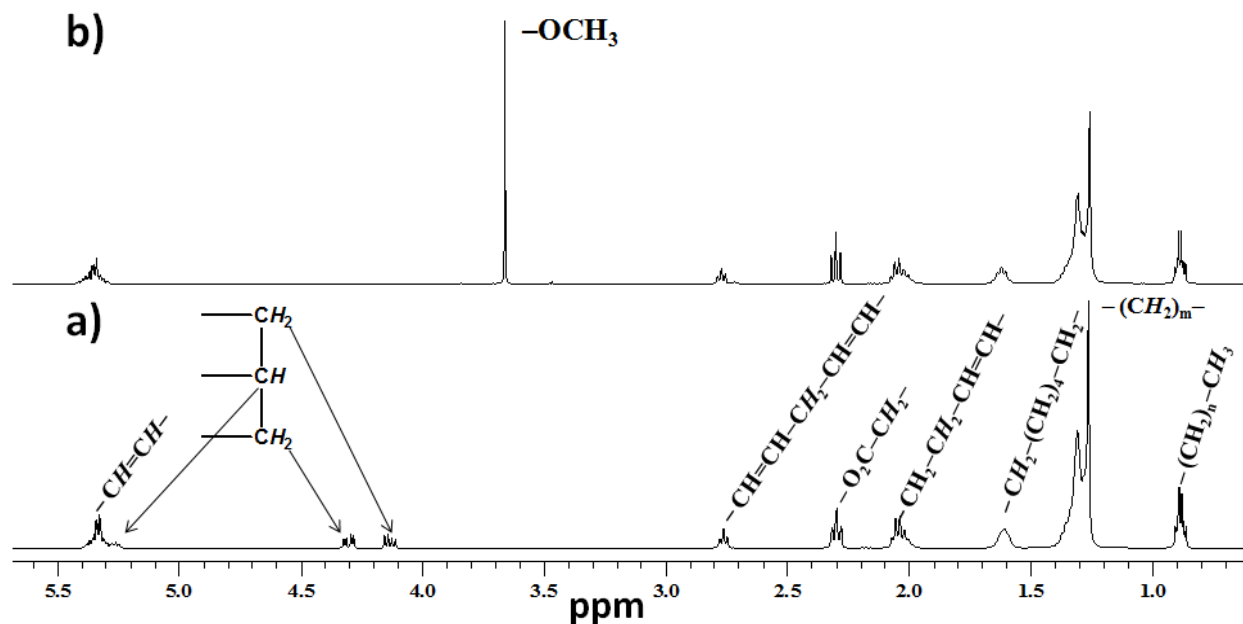
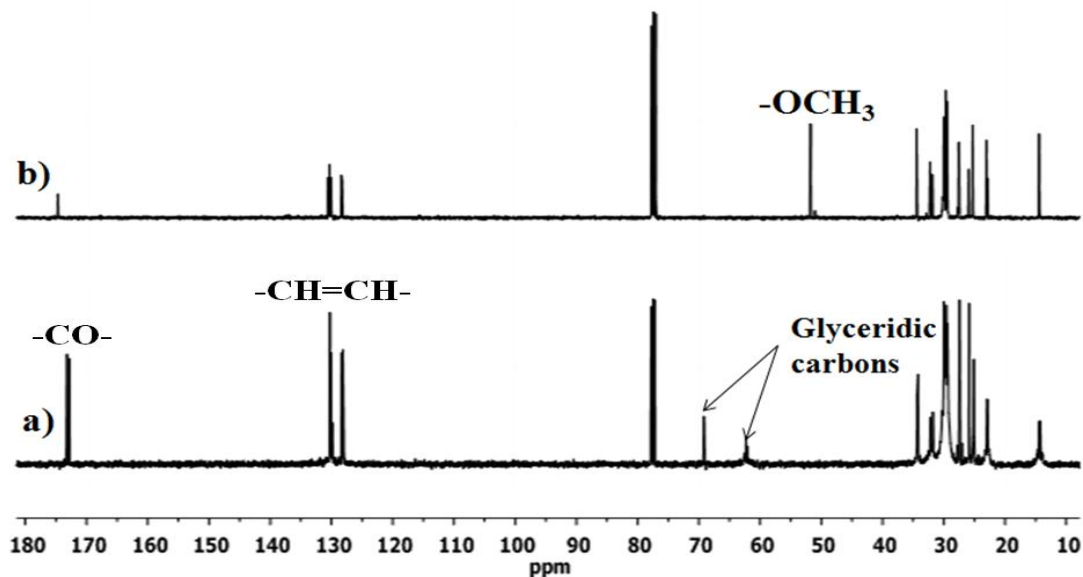


Fig 3.3. Comparison of the  $^1\text{H}$  NMR spectra of a) waste cottonseed oil and b) FAMES

In  $^{13}\text{C}$ -NMR spectrum of WCO, peaks due to glyceridic carbon appear at 61.2 and 69.1 ppm, as shown in Figure 3.4a. The formation of FAMEs was supported by the appearance of a peak at 51.2 due to  $-\text{OCH}_3$  group. The signals due to carbonyl, unsaturated and saturated carbons appeared at 172-174, 127-130, and 13-34 ppm, respectively in WCO as well as in FAMEs. The peaks corresponding to the glyceridic carbons were no longer found in the  $^{13}\text{C}$ NMR spectrum of FAMEs, to support the conversion of WCO into respective alkyl esters.



**Fig.3.4.** Comparison of  $^{13}\text{C}$ -NMR spectra of a) waste cottonseed oil and b) FAMEs

### 3.4 Catalytic activity of KF/CaO/NiO

The efficiency of the catalyst, KF/CaO/NiO, has been tested for the methanolysis of WCO. The reaction parameters for have been optimized to achieve the complete transesterification (> 98%) of oil with methanol in minimum possible time. The transesterification reactions have been performed by varying one parameter at a time out of the followings: (i) impregnated KF concentration, (ii) catalyst concentration, (iii) reaction temperature, and (iv) methanol to oil molar ratio.

Besides, reusability of the catalyst and effect of FFA on catalytic activity has also been studied.

### 3.4.1 Effect of impregnated KF concentration and catalyst concentration on FAMEs yield

To determine the optimum amount of impregnated KF in CaO/NiO, a series of catalysts were prepared by varying KF concentration 5-25 wt%. Transesterification reactions were performed at 65 °C, employing a 15:1 methanol to oil molar ratio and 5 wt% (oil/catalyst) catalysts. The time required for the complete transesterification of WCO was found to reduce from 8 to 4 h as the KF concentration in CaO/NiO support was increased from 5 to 20 wt%. The increase in reaction rate on increasing KF concentration in CaO/NiO is due to the increase in catalyst basic sites as given in Table 3.1. A further increase in KF concentration (from 20 to 25 wt %) was not found to reduce the time required for the complete transesterification as shown in Fig.3.5a. Hence, 20-KF/CaO/NiO-700 catalyst was employed to optimize other parameters to achieve the minimum time for the complete transesterification of WCO.

The amount of catalyst employed in a chemical process significantly affects the production cost of desired products. In general, a higher concentration of catalyst increases the rate of reaction because of more number of active sites available on catalyst surface. However, in order to make the process economically viable and greener, it is preferable to use the minimum amount of catalyst. To determine the optimum catalyst concentration, transesterification reactions were performed at 65 °C, employing a 15:1 methanol to oil molar ratio in the presence of 20-KF/CaO/NiO-700 catalyst by varying its concentration from 1 to 6 wt% (catalyst/oil). Time required for the complete conversion of WCO into FAMEs was found to be reduced from 10 to 4 h, on increasing the catalyst concentration from 1 to 5 wt%. Further increase in catalyst concentration (5 to 6 wt%) doesn't reduce the reaction time significantly as shown in Fig. 3.5b. Hence, transesterification reactions were further studied with 5 wt% catalyst concentration (oil/catalyst) for optimizing the other parameters.

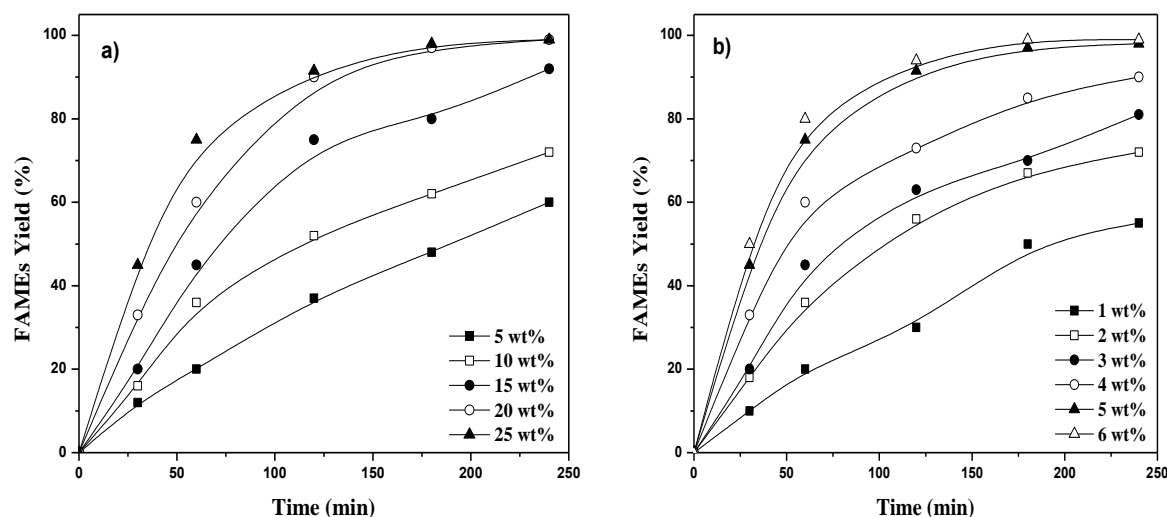


**Fig. 3.5.** Effect of a) KF concentration in CaO/NiO and b) catalyst concentration on transesterification of WCO.

### 3.4.2 Effect of reaction temperature and methanol/oil molar ratio on FAMES yield

Transesterification reactions are usually carried out at the boiling point of alcohol to achieve the completion of the reaction in minimum time. In order to determine the optimum activity of the prepared catalyst, reactions were performed in temperature range of 35-75 °C. Although, 20-KF/CaO/NiO-700 was able to complete the transesterification of WCO even at room temperature (35 °C), but required longer reaction duration (48 h). However, time required for the complete transesterification decreases from 48 to 4 h on increasing the temperature from 35 to 65 °C. Further increase in reaction temperature doesn't reduce the reaction time significantly as shown in Fig. 3.6a, and hence, transesterification reaction has been performed at 65 °C.

Theoretical minimum methanol to oil molar ratio should be 3:1 for the complete conversion of triglycerides into FAMES. However, transesterification, being a reversible reaction, is usually performed with excess amount of methanol to shifts the equilibrium in forward direction and to achieve the maximum methyl ester yield. Further, in case of heterogeneous catalysts, usually excess of alcohol is required (Yan et al., 2008) not only to shift the equilibrium towards the forward direction but also to wash away the product molecules for the catalyst surface to regenerate the active sites. Nevertheless, use of excess methanol may not only increase the biodiesel production cost but also harmful for human being due to its inherent toxicity.

To determine the optimum methanol/oil molar ratio the reactions were performed with 3:1 to 18:1 molar ratios at 65 °C using 5 wt% of 20-KF/CaO/NiO-700 catalyst. The rate of transesterification reaction increases as methanol to oil ratio was increased from 3:1 to 15:1. The reaction was found to complete in 4 h with 15:1 molar ratio of methanol to oil. Further increase in methanol to oil molar ratio was not found to reduce the reaction time significantly as shown in Fig. 3.6b, and hence, a 15:1 methanol to oil molar ratio has been employed for the optimum catalytic activity.

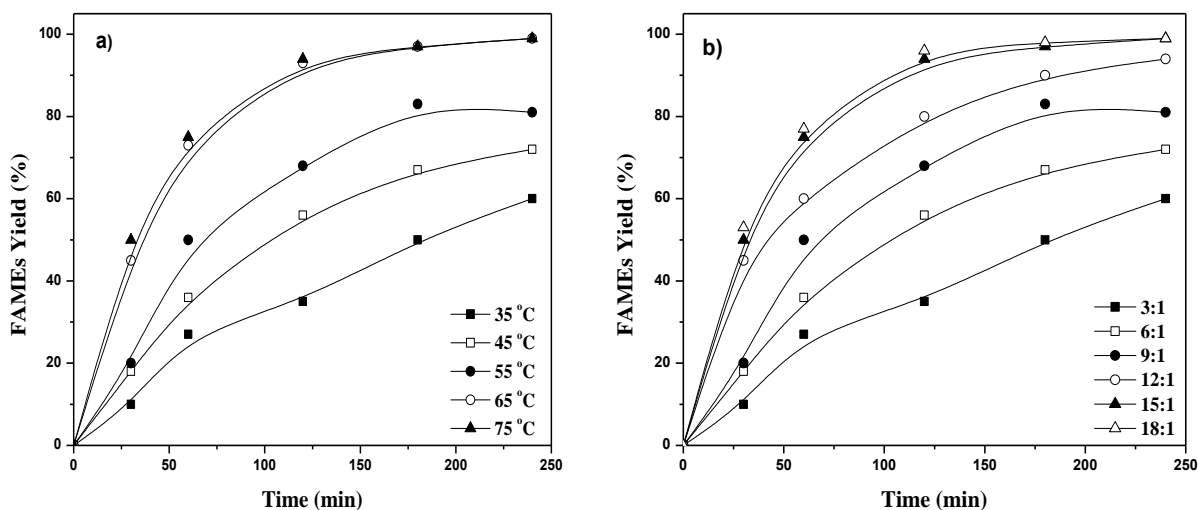


**Fig. 3.6.** Effect of a) reaction temperature and b) MeOH/oil molar ratio on transesterification of WCO.

Thus, a 5wt% of 20-KF/CaO/NiO-700 catalyst with respect to oil, 15:1 methanol to oil molar ratio and reaction temperature of 65 °C, were the optimized reaction conditions to achieve the complete transesterification (> 98 % FAMES yield) of WCO in minimum reaction duration (4 h).

### 3.5 Effect of FFA on catalyst activity

The presence of FFA in feedstock affects the catalytic activity of alkali catalyst adversely by neutralizing the basic sites. Methanolysis of WCO when performed by homogeneous catalysts (NaOH or KOH) soap formation took place instead of biodiesel production. However, 20-KF/CaO/NiO-700 catalyst leads to the completion of transesterification of WCO. In order to find out the maximum FFA tolerance of the catalyst, transesterification reactions of WCO

(having 2.8 wt% FFA) were performed in presence of palmitic acid (up to 5 wt%). Under optimized reaction conditions, the catalyst 20-KF/CaO/NiO-700 was found to resist the presence of up to 3 wt% added FFA and yielded complete transesterification of the WCO, as shown in Fig. 3.7. However, a further increase in the FFA (> 4 wt%) was found to deactivate the catalyst and only partial conversion of oil into FAME was achieved even after 14 h of reaction duration.

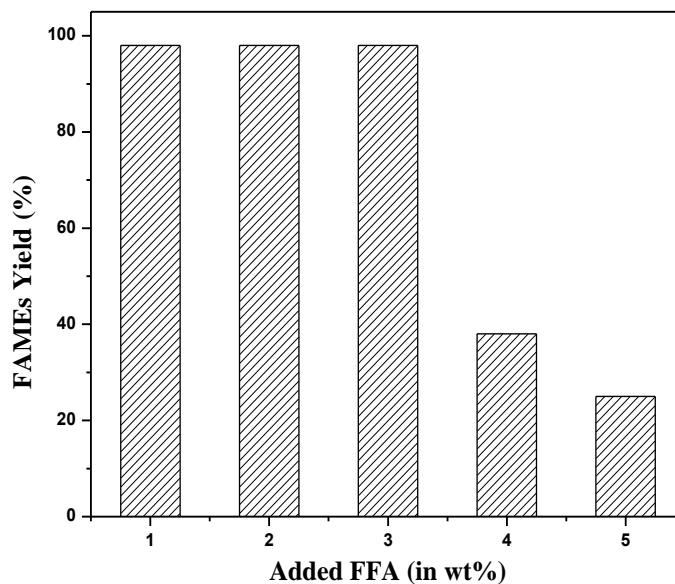


**Fig. 3.7.** Effect of added FFA (Palmitic acid) on the catalyst activity for the transesterification of WCO (Reaction conditions: MeOH/oil molar ratio = 15:1; Catalyst amount = 5 wt% of oil; Temperature = 65 °C).

### 3.6 Reusability of the catalyst

Reusability is an attractive feature of the heterogeneous catalysts as it could reduce the effective production cost of a molecule. To test the reusability of 20-KF/CaO/NiO-700, it was recovered from the reaction mixture by filtration, washed with hexane and dried at 120 °C. The catalyst thus recovered was used for five consecutive runs, under the same experimental condition and regeneration method. The catalyst was able to complete (> 98 %) the transesterification of oil in 4 successive cycles as shown in Fig. 3.8. However, in fifth catalytic run ~ 50 % conversion was achieved. The loss in catalytic activity may be due to partial leaching of the active species (KCaF<sub>3</sub>) during successive runs. Thus catalyst shows reasonably good recyclability towards the transesterification of the WCO.

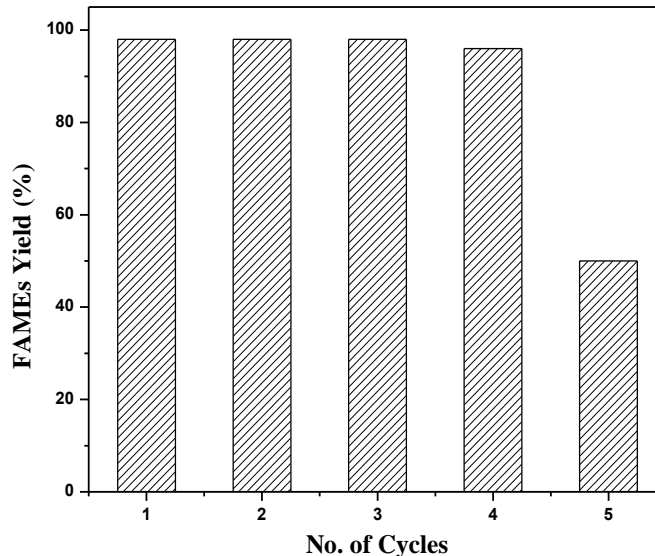


**Fig. 3.8. Effect of reusability on the FAMES yield for the transesterification of WCO (Reaction conditions: MeOH/oil molar ratio = 15:1; Catalyst amount = 5 wt% of oil; Temperature = 65 °C).**

A comparison of few literature reported KF supported solid catalysts with present catalyst is provided in Table 3.2.

**Table 3.2. Comparison of reaction conditions of literature reported heterogeneous catalysts used for methanolysis with present catalyst.**

| Catalyst                          | MeOH/<br>Oil<br>molar<br>ratio | Catalyst<br>amount<br>(wt%) | Temp.<br>(°C) | Time<br>(h) | Yield<br>(%) | Reusability<br>(cycles) | Ref.                 |
|-----------------------------------|--------------------------------|-----------------------------|---------------|-------------|--------------|-------------------------|----------------------|
| KF/Al <sub>2</sub> O <sub>3</sub> | 12:1                           | 4                           | 65            | 3           | 90           | NR                      | Bo et al.,<br>2007   |
| KF/Mg-Al                          | 9:1                            | 3                           | 65            | 5           | 92           | NR                      | Gao et al.,<br>2008  |
| KF/Ca-Mg-Al                       | 12:1                           | 5                           | 65            | 0.16        | > 90         | 2                       | Gao et al.,<br>2010  |
| KF/Mg-La                          | 12:1                           | 5                           | 65            | 1           | > 95         | 2                       | Song et al.,<br>2011 |
| KF/CaO/NiO                        | 15:1                           | 5                           | 65            | 4           | > 98         | 4                       | Present study        |

It is evident from the comparison, the reported catalysts were not able to yield the acceptable levels of > 96.5 % FAME yield, and moreover the reusability of the catalysts was found to be

poor. In present study, the prepared catalyst is not only yielding  $> 98\%$  FAME yield under relatively milder reaction conditions but also successfully recycled four times without any significant loss in activity.

### 3.7 Kinetic Study

To study the kinetics of transesterification reaction, the samples were withdrawn from the reaction mixture after every 30 minutes and subjected to proton NMR analysis. Fig. 3.9, represent a typical proton NMR spectra of the reaction mixture recorded at various time intervals. The FAME yield obtained at various time intervals was fitted in equation 1 and corresponding plot is shown in Fig. 3.10a. The activation energy ( $E_a$ ) and Arrhenius constant ( $A$ ) was calculated from plot between  $\ln k$  versus  $1/T$  (Fig. 3.10b).

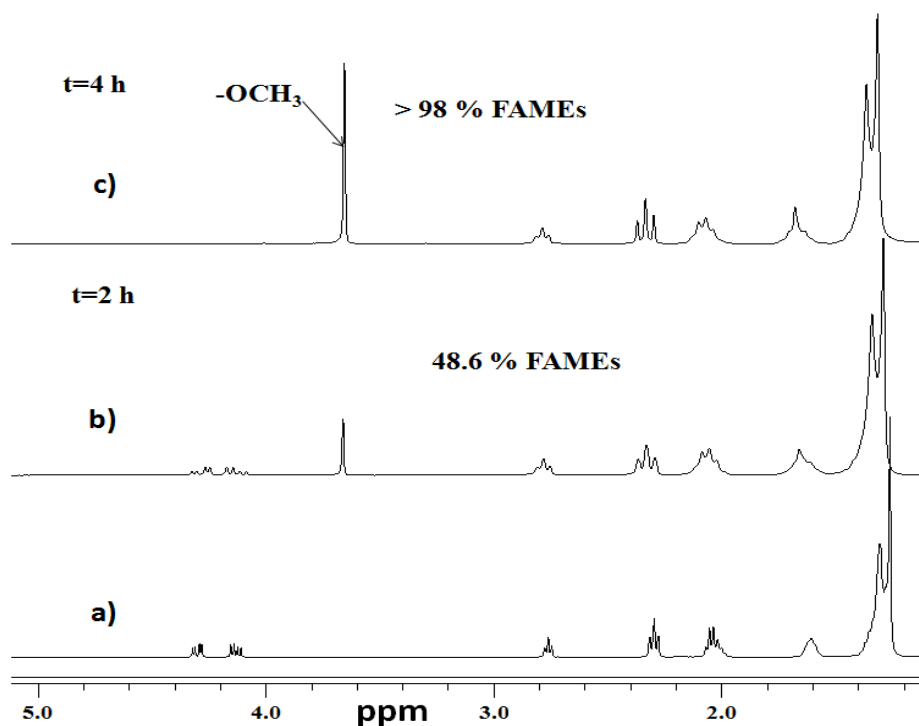


**Fig. 3.9.** Comparison for  $^1\text{H}$  NMR of a) waste cottonseed oil b) FAMEs with 48.6 % conversion c) FAMEs with  $> 98\%$  conversion.

The linear nature of these plots support that (pseudo) first order kinetic equation is followed by the 20-KF/CaO/NiO-700 catalyzed reaction (Freedman et al., 1986). The apparent first order rate constant from the plot at  $65\text{ }^\circ\text{C}$  was found to be  $0.023\text{ min}^{-1}$ . The Arrhenius model was employed

to estimate the activation energy ( $E_a$ ) and pre-exponential factor ( $A$ ) for methanolysis of WCO following the equation 2. The values of  $E_a$  and  $A$  was found to be  $41.2 \text{ kJ mol}^{-1}$  and  $3.9 \times 10^{10} \text{ min}^{-1}$ , respectively. The value of  $E_a$  was found within the range ( $33\text{-}84 \text{ kJ mol}^{-1}$ ) of reported values (Sun et al., 2008) for the methanolysis of vegetable oils.

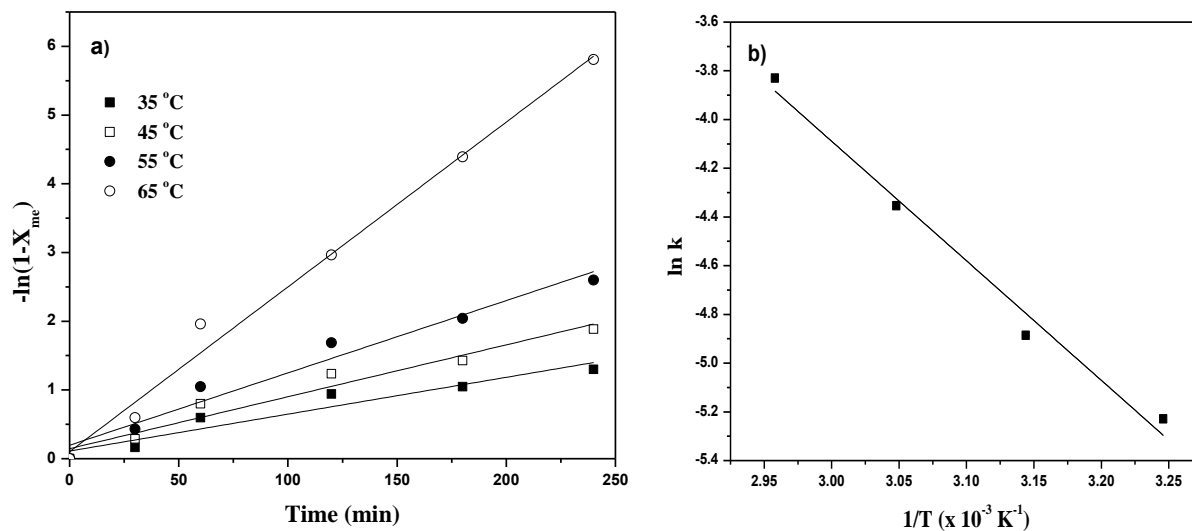


**Fig. 3.10.** a) Plot of a)  $-\ln(1-X_{me})$  versus reaction time ( $t$ ) at different temperatures (Reaction conditions: MeOH/oil molar ratio = 15:1; catalyst amount = 5 wt% of oil) and b) The Arrhenius plot for methanolysis of WCO in presence of 20-KF/CaO/NiO-700 ( $X_{me}$  = FAMES yield).

### 3.8 Physicochemical properties of the FAMES

Few important properties of FAMES produced from the methanolysis of WCO in presence of 20-KF/CaO/NiO-700 catalyst have been evaluated following the standard test methods as given in Table 3.2. The studied biodiesel properties such as flash point, pour point, kinematic viscosity, density and ash content were found with the EN limitations.

**Table 3.3. Physicochemical properties of the FAMEs prepared from WCO.**

| S.No. | Parameters                         | FAMEs  | EN14214   | Test method        |
|-------|------------------------------------|--------|-----------|--------------------|
| 1     | Ester content (%)                  | > 98 % | > 96.5    | <sup>1</sup> H-NMR |
| 2     | Flash point (°C)                   | 110    | 100–170   | ASTM D93           |
| 3     | Pour point (°C)                    | 1      | –5 to10   | ASTM D2500         |
| 4     | Kinematic viscosity at 40 °C (cSt) | 4.50   | 3.5–5.0   | ASTM D445          |
| 5     | Density at 31 °C (g/mL)            | 0.88   | 0.86–0.89 | EN ISO 3675        |
| 6     | Ash (%)                            | NIL    | 0.02      | ASTM D874          |

### 3.9 Conclusions

Present chapter demonstrates the preparation of a series of KF impregnated CaO/NiO and investigation of their catalytic activity towards the transesterification of WCO (having 2.8 wt % FFA content). CaO/NiO impregnated with 20 wt% KF was found to have the highest basic strength ( $15.0 < H_{-} < 18.4$ ) as supported by Hammett indicator tests and same catalyst required 4 h to yield the complete transesterification of WCO (> 98 % FAMEs yield) under optimized reaction conditions. The catalyst was found to complete the transesterification of WCO even in presence of 3 wt% additional FFA contents. Further, reusability study of the catalyst has demonstrated that it was able to catalyze four catalytic cycles without significant loss in activity. Thus, the prepared catalyst has the potential to convert the WCO, having up to 5.8 wt% FFAs contents, into biodiesel. The physicochemical properties of the WCO derived FAMEs have also been evaluated and observed values were found within the limits of EN 14214 specifications.

---

**References**

- Babu, N. S.; Sree, R.; Prasad, P. S. S.; Lingaiah, N.; Room-temperature transesterification of edible and non-edible oils using a heterogeneous strong basic Mg/La catalyst. *Energ. Fuel*; **2008**, *22*, 1965–1971.
- Bo, Xu.; Guomin, X.; Lingfeng, C.; Ruiping, W.; Lijing, G.; Transesterification of Palm Oil with Methanol to Biodiesel over a KF/Al<sub>2</sub>O<sub>3</sub> Heterogeneous Base Catalyst. *Energ. Fuel*; **2007**, *21*, 3109–3112.
- Desmartin-Chomel, A.; Hamad, B.; Palomeque, J.; Essayem, N.; Bergeret, G.; Figueras, F.; Basic properties of MgLaO mixed oxides as determined by microcalorimetry and kinetics. *Catal. Today*; **2010**, *152*, 110–114.
- Freedman, B.; Butterfield, R.O.; Pryde, E.H.; Transesterification kinetics of soybean oil, *J. Am. Oil. Chem. Soc.*; **1986**, *63*, 1375–1380.
- Gao, L. J.; Xu, B.; Xiao, G.; Lv, J.; Transesterification of Palm Oil with Methanol to Biodiesel over a KF/Hydrotalcite Solid Catalyst. *Energ. Fuel*; **2008**, *22*, 3531–3535.
- Gao, L. J.; Teng, G. Y.; Lv, J. H.; Xiao, G. M.; Biodiesel Synthesis Catalyzed by the. KF/Ca-Mg-Al Hydrotalcite Base Catalyst. *Energ. Fuel*; **2010**, *24*, 646–651.
- Hu, S.; Guan, Y.; Wang, Y.; Han, H.; Nano-magnetic catalyst KF/CaO–Fe<sub>3</sub>O<sub>4</sub> for biodiesel production. *Appl. Energ.*; **2011**, *88*, 2685–2690.
- Ilgen, O.; Akin, A. N.; Transesterification of Canola Oil to Biodiesel Using MgO Loaded with KOH as a Heterogeneous Catalyst. *Energ. Fuel*; **2009**, *23*, 1786–1789.
- Ivanova, A.; Moroz, B.; Moroz, E.; Larichev, Y.; Paukshtis, E.; Bukhtiyarov, V. J.; New binary systems Mg–M–O (M=Y, La, Ce): Synthesis and physico-chemical characterization. *Solid State Chem.*; **2005**, *178*, 3265–3274.

Patil, P. D.; Deng, S.; Transesterification of *Camelina sativa* oil using heterogeneous metal oxide catalysts. *Energ. Fuel*; **2009**, *23*, 4619-4624.

Qadri, S. B.; Skelton, E. F.; Hsu, D.; Dinsmore, A. D.; Yang, J.; Gray, H. F.; Ratna, B. R.; Size-induced transition-temperature reduction in nanoparticles of ZnS. *Phys. Rev. B.*; **1999**, *60*, 9191-9193.

Reddy, C. R. V.; Oshel, R.; Verkade, J. G.; Room-temperature conversion of soybean oil and poultry fat to biodiesel catalyzed by nanocrystalline calcium oxides. *Energ. Fuel*; **2006**, *20*, 1310-1314.

Sankaranarayanan, S.; Antonyraj, C. A.; Kannan, S.; Transesterification of edible, non-edible and used cooking oils for biodiesel production using calcined layered double hydroxides as reusable base catalysts. *Bioresour. Technol.*; **2012**, *109*, 57-62.

Singh, A. K.; Fernando, S. D.; Preparation and reaction kinetics studies of Na-based mixed metal oxide for transesterification, *Energ. Fuel*; **2009**, *23*, 5160-5164.

Song, R.; Tong, D.; Tang, J.; Hu, C.; Effect of Composition on the Structure and Catalytic Properties of KF/MgLa Solid Base Catalysts for Biodiesel Synthesis via Transesterification of Cottonseed Oil. *Energ. Fuel*; **2011**, *25*, 2679-2686.

Sun, H.; Hu, K.; Lou, H.; Zheng, X.; Biodiesel Production from Transesterification of Rapeseed Oil Using KF/Eu<sub>2</sub>O<sub>3</sub> as a Catalyst. *Energ. Fuel*; **2008**, *22*, 2756-2760.

Sree, R.; Babu, N.S.; Prasad, P. S. S.; Lingaiah, N.; Transesterification of edible and non-edible oils over basic solid Mg/Zr catalysts. *Fuel Process. Technol.*; **2009**, *90*, 152-157.

Wan Omar, W. N. N.; Amin, N. A. S.; Biodiesel production from waste cooking oil over alkaline modified zirconia catalyst. *Fuel Process Technol.*; **2011**, *92*, 2397-2405.

Xie, W. L.; Peng, H.; Chen, L. G.; Transesterification of soybean oil catalyzed by potassium loaded on alumina as a solid-base catalyst. *Appl. Catal. A: Chem.*; **2006**, 300, 67–74.

Xie, W. L.; Yang, Z. Q.; Chun, H.; Catalytic Properties of Lithium-Doped ZnO Catalysts Used for Biodiesel Preparations. *Ind. Eng. Chem. Res.*; **2007**, 46, 7942–7949.

Xie, W. L.; Huang, X. M.; Synthesis of biodiesel from soybean oil using heterogeneous KF/ZnO catalyst. *Catal. Lett.*, **2006**, 107, 53–59.

Yan, S.; Lu, H.; Liang, B.; Supported CaO catalysts used in the transesterification of rapeseed oil for the purpose of biodiesel production. *Energ. Fuel*; **2008**, 22, 646–651.

Zu, Y.; Liu, G.; Wang, Z.; Shi, J.; Zhang, M.; Zhang, W.; Jia, M.; CaO Supported on Porous Carbon as Highly Efficient Heterogeneous Catalysts for Transesterification of Triacetin with Methanol. *Energ. Fuel*; **2010**, 24, 3810–3816.

---

**Ethanolysis of Waste cottonseed oil over Lithium Impregnated Calcium oxide:  
Kinetics and Reusability Studies**

---

|            | <b>Contents</b>  | <b>Page</b> |
|------------|--|-------------|
| <b>4.1</b> | <b>Introduction</b>  | 66          |
| <b>4.2</b> | <b>Experimental section</b>  | 66          |
|            | 4.2.1 Catalyst preparation   | 66          |
|            | 4.2.2 Transesterification of waste cottonseed oil                                | 66          |
| <b>4.3</b> | <b>Results and discussion</b>  | 67          |
|            | 4.3.1 Catalyst characterization  | 67          |
|            | 4.3.1.1 BET surface area and basic strength                                      | 67          |
|            | 4.3.1.2 Powder X-ray diffraction   | 67          |
|            | 4.3.1.3 SEM and TEM analysis   | 68          |
|            | 4.3.2 FAMES and FAEEs characterization by <sup>1</sup> HNMR                      | 69          |
| <b>4.4</b> | <b>Catalytic activity</b>  | 72          |
|            | 4.4.1 Effect of Impregnated lithium ion concentration and catalyst concentration | 72          |
|            | 4.4.2 Effect of reaction temperature   | 73          |
|            | 4.4.3 Effect of ethanol/oil molar ratio  | 74          |
| <b>4.5</b> | <b>Effect of FFA on catalytic activity</b>                                       | 75          |
| <b>4.6</b> | <b>Catalyst Reusability and Homogeneous contribution</b>                         | 76          |
| <b>4.7</b> | <b>Kinetic study</b>   | 79          |
| <b>4.7</b> | <b>Physicochemical properties of FAEEs</b>                                       | 80          |
| <b>4.8</b> | <b>Conclusions</b>   | 81          |
|            | <b>References</b>  | 82          |

---

### **Abstract**

This chapter demonstrates the preparation of Li/CaO catalyst by impregnating 0.5-5.0 wt% Li in CaO by wet chemical method. Prepared Li/CaO catalysts have been characterized by powder X-ray diffraction, scanning electron and transmission electron microscopy and Brunauer-Emmett-Teller (BET) surface area studies, in order to establish the structure and surface morphology of the catalyst. Hammett indicator test study was performed to determine the basic strength of the Li/CaO catalysts. Li/CaO catalyst was also found to be effective for the ethanolysis and methanolysis of vegetable oils having up to 3.4 wt% free fatty acids. Under optimal reaction conditions *viz.*, ethanol/oil molar ratio of 12:1, catalyst to oil weight fraction of 5 % and 65 °C reaction temperature, 98 % fatty acid ethyl ester yield was obtained in 2.5 h of reaction duration. Under the optimized reaction conditions, the pseudo first order constant and Arrhenius activation energy was found to be  $0.03 \text{ min}^{-1}$  (65 °C) and  $70.0 \text{ kJ mol}^{-1}$ , respectively. The use of 3-Li/CaO catalyst is advantageous considering that it not only utilizes waste cotton seed oil as feedstock, but also renewable and nontoxic alcohol, ethanol, for the biodiesel production.

### 4.1 Introduction

The literature reports regarding the ethanolysis of triglycerides to produce fatty acid ethyl esters (FAEEs) are fewer in comparison to methanolysis (Hajek et al., 2012; Yan et al., 2009; Ali et al., 2011). The catalysts reported for the ethanolysis of triglycerides includes mixed metal oxides (Benjapornkulaphong et al., 2009), ion exchange resins (Abreu et al., 2005), sulfonated carbohydrates and heteropolyacids (Charusiri et al., 2006; Suppes et al., 2004). Due to the phase difference, and lower reactivity of ethanol these catalysts often required high reaction temperature (up to 200 °C) and pressure (up to 25 atm), higher catalyst amount (20 mol % to oil) and higher ethanol to oil molar ratio (> 30:1) to achieve satisfactory (> 96.5 %) FAEEs yield (Ngamcharussrivichai et al., 2008).

In order to utilize the waste cooking oil for biodiesel production, present work demonstrates the preparation of Li impregnated CaO by wet chemical method and its application for the ethanolysis of the waste cotton seed oil. The parameters for ethanolysis have been optimized to obtain the complete transesterification of oil in minimum possible time to reduce the energy demand for FAEEs production. The reusability of the catalysts and kinetics of the reaction were also studied under optimized reaction conditions.

### 4.2 Experimental section

#### 4.2.1. Catalyst Preparation

A series of lithium ion impregnated CaO (Li/CaO) catalysts was prepared by wet chemical method. In a typical preparation 10 g of calcium oxide was mixed with 40 mL of deionized water to form a slurry and to this 10 mL aqueous solution of  $\text{Li}_2\text{CO}_3$  of desired concentration was added to obtain 0.5–5 wt% Li in CaO. The resulted slurry was stirred for 2 h at room temperature (30 °C), and finally dried at 120 °C in oven for 24 h. The prepared catalysts were designated as  $x\text{-Li/CaO}$ , where  $x$  being the wt% of lithium.

#### 4.2.2 Transesterification of Waste cottonseed oil

All transesterification reactions were carried out in 250 ml, three necked round bottom flask equipped with a water cooled reflux condenser, thermometer, oil bath and a magnetic stirrer. In a typical run, the flask was charged with 10 g vegetable oil, desired amount of ethanol and catalyst and heated at required temperature (35-75 °C). To monitor the progress of the reaction, aliquots

were collected from the reaction mixture after every 15 min with the help of glass capillary and subjected to the  $^1\text{H}$  NMR study.

### 4.3. Results and discussion

#### 4.3.1 Catalyst Characterization

##### 4.3.1.1 BET surface area and Basic strength

In present chapter, CaO being non toxic and inexpensive has been preferred as support over other corresponding alkaline earth metal oxides. Additionally, the basic strength of CaO could be tuned by impregnating it with alkali metal ions. The basic strength of commercial CaO was found to be in the range of 9.8-10 which was found to increase up to 15-18.4 upon 3 wt % Li impregnation as given in Table 4.1. The increase in basic strength could be attributed to the formation of strong basic site in CaO upon Li impregnation.

The surface area was found to reduce from 8.1 to 1.3  $\text{m}^2 \text{g}^{-1}$ , may be due to the pore plugging of CaO, upon lithium impregnation. The crystallite size of the 3-Li/CaO catalyst was determined by the Debye-Scherrer method (Qadri et al., 1999) using the peak width of the reflection plane at  $34.41^\circ$  and found to be  $\sim 60$  nm.

**Table 4.1. Comparison of BET surface area and basic strength of CaO with 3-Li/CaO catalyst.**

| S. No. | Catalyst type | BET surface area<br>( $\text{m}^2 \text{g}^{-1}$ ) | Basic strength<br>( $\text{H}_+$ ) | Crystallite size<br>(nm) |
|--------|---------------|--|------------------------------------|--------------------------|
| 1.     | CaO           | 8.1  | 9.8< $\text{H}_+$ <10.1            | 80                       |
| 2.     | 3-Li/CaO      | 1.3  | 15< $\text{H}_+$ <18.4             | 60                       |

##### 4.3.1.2 Powder X-ray diffraction

The powder X-ray diffraction patterns of CaO, and  $\text{Li}^+$  impregnated (0.5-5 wt%) CaO have been compared in Fig. 4.1. The XRD patterns of the commercial CaO shows reflections corresponding to the CaO in cubic phase (JCPDS-84-1276), and  $\text{Ca}(\text{OH})_2$  (as impurity) in hexagonal phase (JCPDS-82-1690). The XRD pattern of the Li/CaO shows peaks at  $2\theta = 20.94^\circ$ ,  $37.25^\circ$ ,  $48.99^\circ$ ,  $53.70^\circ$ ,  $64.40^\circ$  and  $72.2^\circ$ , due to the conversion of CaO into  $\text{Ca}(\text{OH})_2$  hexagonal phase during wet impregnation of lithium. The absence of XRD patterns corresponding to lithium carbonate in

Li/CaO confirms the high degree of dispersion of lithium in calcium oxide. The minor peaks of orthorhombic and hexagonal calcium carbonate were also observed at  $2\theta = 21.46^\circ$ ,  $36.3^\circ$ ,  $43.3^\circ$ ,  $48.8^\circ$  (JCPDS-01-0628) and  $32.2^\circ$  (JCPDS-01-1033), respectively.

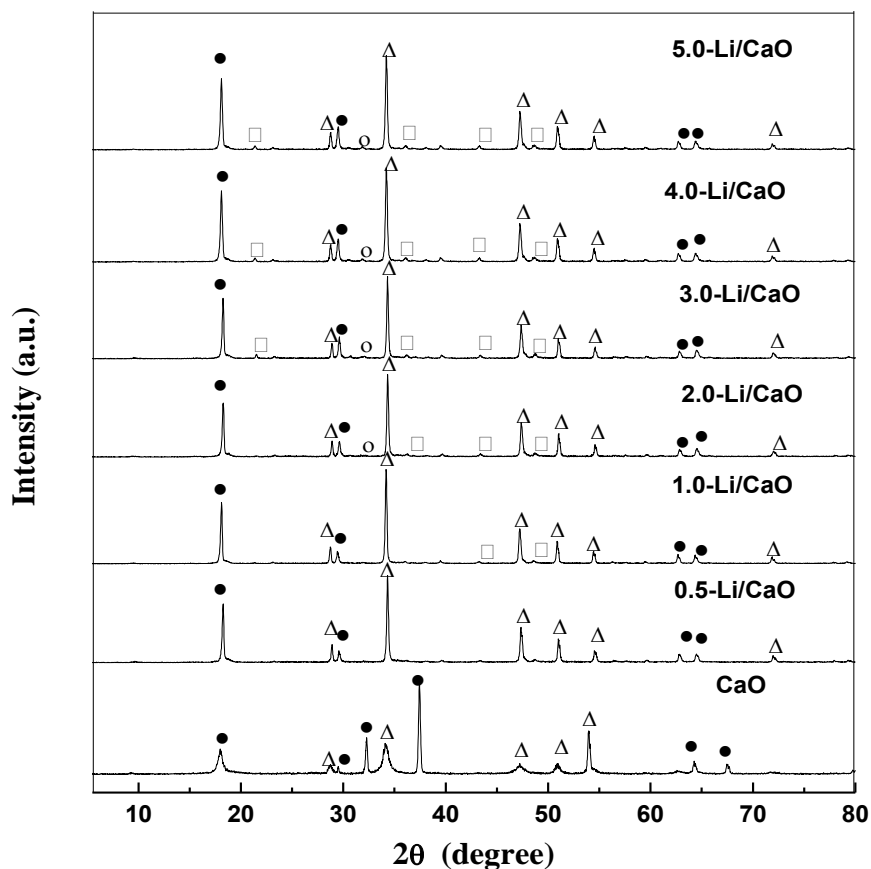


**Fig. 4.1.** Comparison of powder XRD patterns of commercially available CaO and 0.5-5 wt% Li impregnated CaO (● = cubic calcium oxide; Δ = hexagonal calcium hydroxide; □ = orthorhombic calcium carbonate; and ○ = hexagonal calcium carbonate)

#### 4.3.1.3 SEM and TEM analysis

The SEM study gives the morphological characteristics of 3-Li/CaO, which supports the formation of clusters of oval and irregular shaped particles as shown in Fig. 4.2a. The cluster formation is due to the agglomeration of the catalyst particles during their preparation by wet chemical method. The average size of the catalyst particles by SEM studies was found to be  $\sim 1\mu\text{m}$ . The crystalline size and shape of the agglomerated particles was further analyzed by the

TEM analysis. The TEM image (Fig. 4.2b) confirms that catalyst particles are either in spherical or oval shape. The average size of these particles by TEM study was found to be ~ 13 nm.

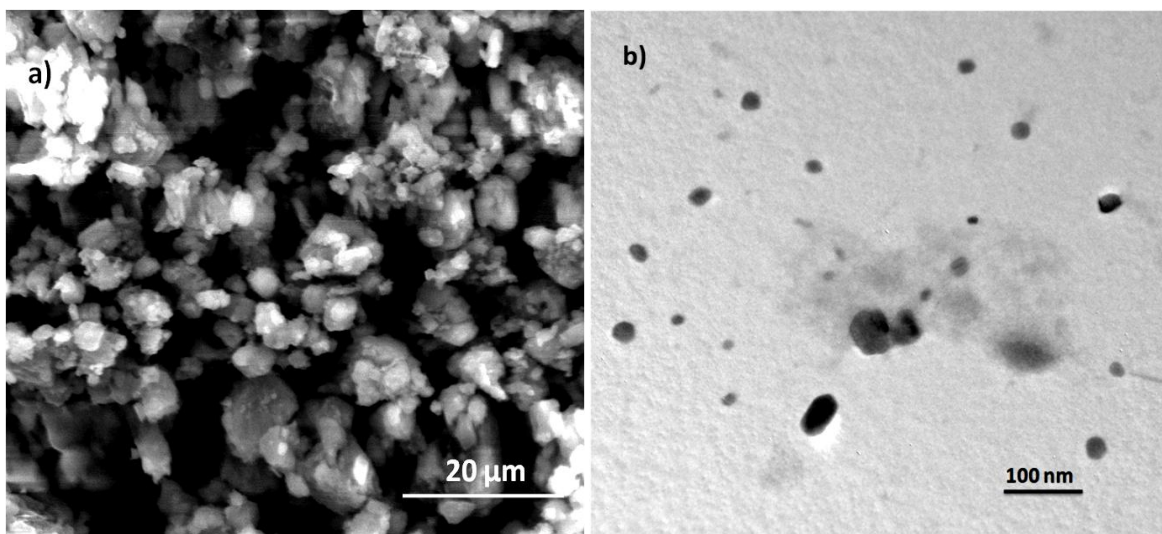


**Fig. 4.2. a) SEM and b) TEM images of 3-Li /CaO catalyst.**

#### 4.3.2 FAMES and FAEEs characterization by $^1\text{H}$ NMR

The  $^1\text{H}$  NMR spectrum of waste cottonseed oil shows a multiplet at 4.15-4.34 ppm due to the presence of glyceridic protons. The peaks appearing at 0.8-2.8 ppm in the proton NMR spectra of biodiesel as well as WCO (Fig. 4.3a) are due to the presence of saturated hydrocarbon protons of fatty acids. The unsaturated protons of fatty acid carbon chain in WCO as well as FAMES/FAEEs appear at 5.25 ppm. In proton NMR spectrum of FAMES (Fig. 4.3b) a new peak appears at 3.6 ppm due to  $-\text{OCH}_3$  protons, and peaks corresponding to the glyceridic protons were no longer found, to support the formation of fatty acid methyl ester upon methanolysis of oil. FAMES produced during the methanolysis of WCO were quantified (Knothe, 2001) by following equation (1):

$$\% C_{\text{ME}} = 100 [2I_a / 3I_b] \quad (1)$$

where,  $I_a$  and  $I_b$  are the integration of the methoxy (3.6 ppm) and  $\alpha$ -methylene protons (2.3 ppm), respectively in  $^1\text{H}$  NMR spectrum of FAMES.

In proton NMR spectrum of FAEEs (Fig. 3c) appearance of a quartet at 4.09-4.16 ppm due to the methylenic protons ( $-\text{OCH}_2-$ ) of ester group, supports the formation of fatty acid ethyl esters.

FAEEs produced during the ethanolysis of triglycerides were calculated (Ghesti et al., 2007) by following equation (2):

$$\% C_{EE} = 100 \times [4(I_{c+d} - I_c) / \{4(I_{c+d} - I_c) + 6(2I_c)\}] \quad (2)$$

where  $I_{c+d}$  = integration of glyceryl methylenic +  $-\text{OCH}_2$  of ethoxy hydrogens superimposed (4.10-4.20 ppm) and  $I_c$  = integration of glyceryl methylenic hydrogens (4.25-4.35 ppm) in  $^1\text{H}$  NMR spectrum of FAEEs.

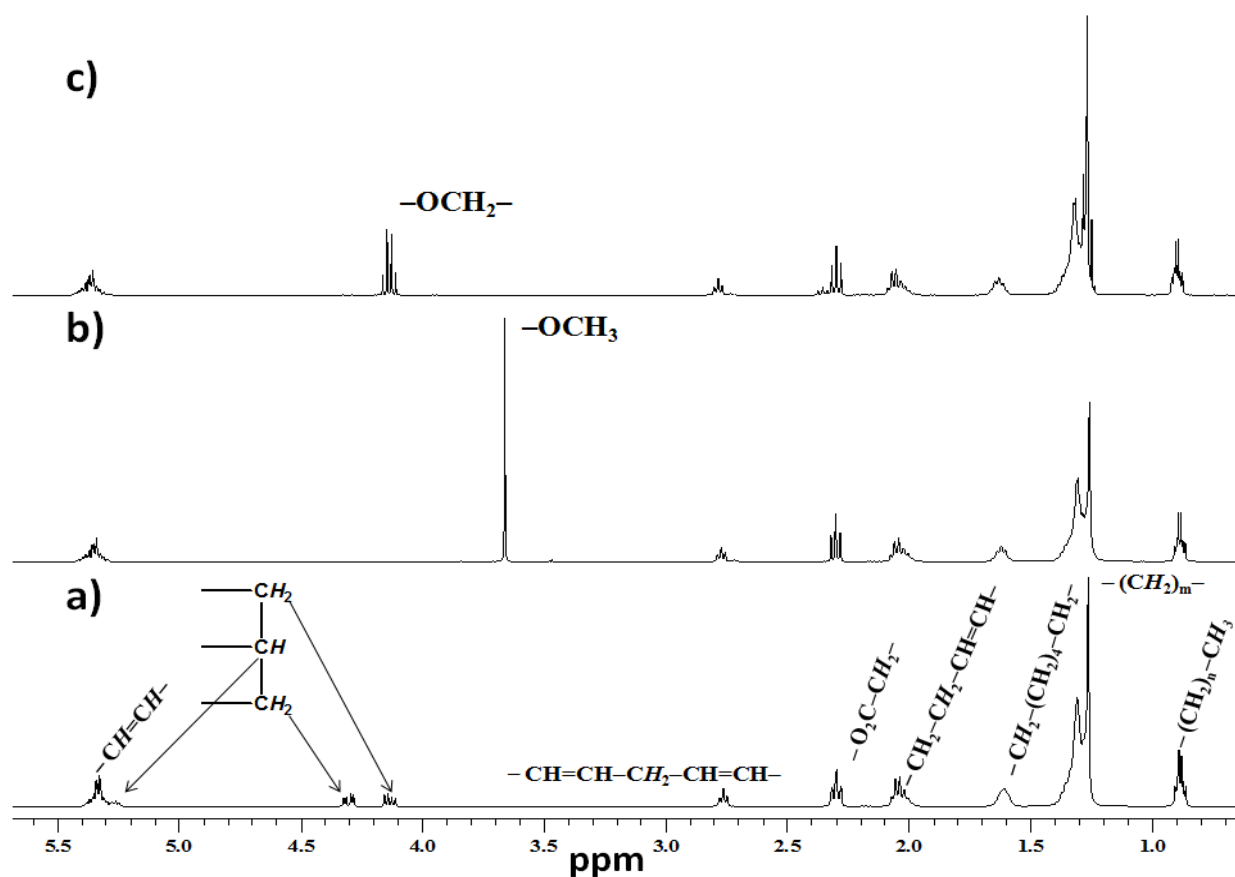


**Fig 4.3. Comparison of the  $^1\text{H}$  NMR spectra of a) waste cottonseed oil b) FAMES and c) FAEEs.**

In  $^{13}\text{C}$ -NMR spectrum of WCO, peaks due to glyceridic carbon appear at 61.2 and 69.1 ppm, as shown in Fig. 4.4a. The formation of FAMES, and FAEEs was supported by the appearance of a peak at 51.2 and 61.1 ppm, respectively due to  $-\text{OCH}_3$  and  $-\text{OCH}_2\text{CH}_3$  groups, respectively. The signals due to carbonyl, unsaturated and saturated carbons appeared at 172-174, 127-130, and 13-34 ppm, respectively in WCO as well as FAEEs and FAMES. The peaks corresponding to the

glyceridic carbons were no longer found in the  $^{13}\text{C}$ NMR spectrum of FAMEs as well as FAEEs, to support the conversion of WCO into respective alkyl esters.

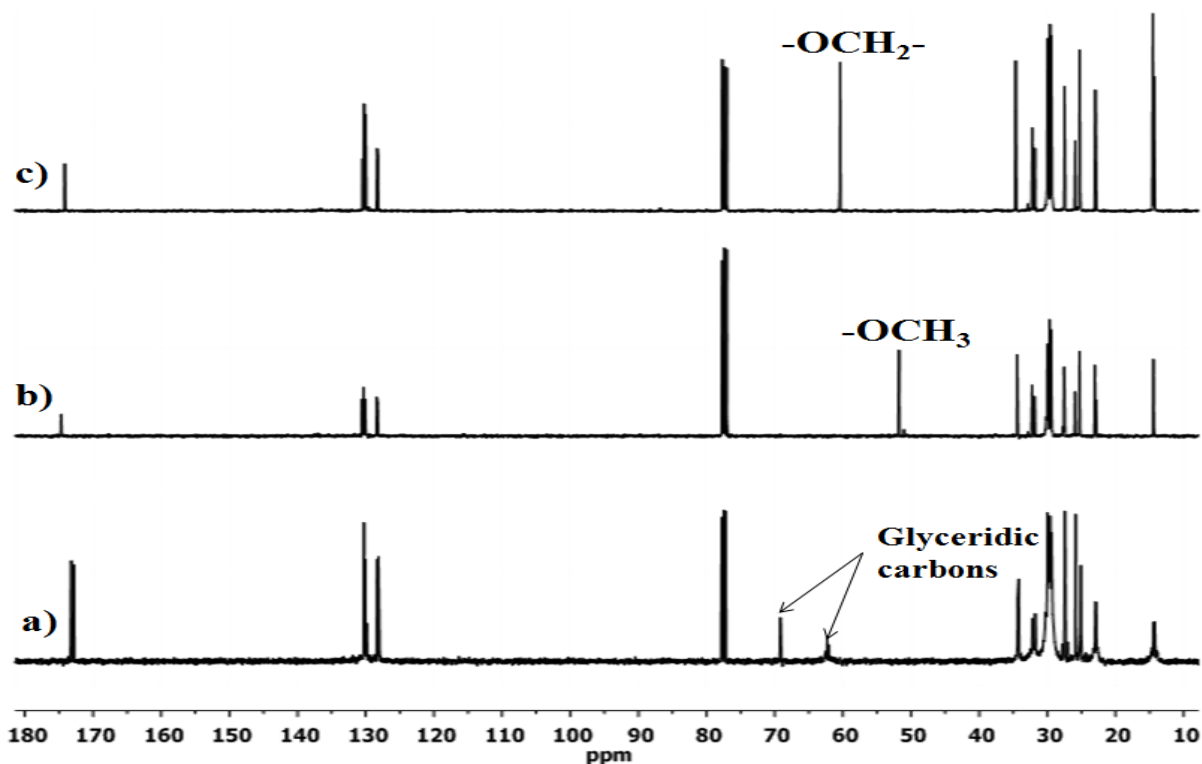


**Fig. 4.4.** Comparison of  $^{13}\text{C}$ -NMR spectra of a) waste cottonseed oil b) FAMEs and (c) FAEEs.

The quantification of the completely transesterified product and ester profile of prepared FAEEs was also determined by GC-MS technique and the relative percentage of each fatty acid ester is given in Table 4.2.

**Table 4.2.** Composition of waste cotton seed oil derived FAEEs by GC-MS technique.

| S. No. | Compound <sup>a</sup>   | wt %  |
|--------|-------------------------|-------|
| 1.     | Ethyl palmitate (C16:0) | 34.13 |
| 2.     | Ethyl stearate (C18:0)  | 3.99  |
| 3.     | Ethyl oleate (C18:1)    | 21.68 |
| 4.     | Ethyl linoleate (C18:2) | 40.20 |

<sup>a</sup>In  $C_n : x, n$  indicates the number of carbons and  $x$  number of  $-\text{C}=\text{C}-$  bonds in the FAEEs.

## 4.4 Catalytic activity

Transesterification reactions of ethanol with WCO (12:1 molar ratio) were performed in the presence of prepared catalysts in order to optimize the reaction conditions to achieve the complete conversion of oil into corresponding fatty acid ethyl esters in minimum possible time. During the course of study, the following parameters have been varied (i) impregnated lithium ion concentration in CaO support, (ii) catalyst amount, (iii) reaction temperature, and (iv) ethanol/oil molar ratio.

### 4.4.1 Effect of impregnated lithium ion concentration and catalyst concentration

To determine the optimum lithium concentration for better catalytic activity, a series of Li/CaO was prepared by varying the lithium amount 0.5-5 wt%. Transesterification of WCO was performed with ethanol (1:12 molar ratio) at 65 °C in the presence of 5 wt% Li/CaO (oil/catalyst). The reaction time required for the complete transesterification (> 98% FAEEs yield) was found to decrease from 5 h to 2.5 h as the Li amount in CaO was increased from 0.5 to 3 wt% as shown in Fig. 4.5a. Hence, Li/CaO catalyst having 3 wt% Li has been selected for optimizing other reaction parameters.

In order to find the optimum catalyst concentration, a series of transesterification reactions of WCO with ethanol (1:12 molar ratio) at 65 °C were performed in the presence of 3-Li/CaO catalyst by varying its concentration in the range of 1-8 wt% (catalyst/oil). The reaction rate was found to increase as the catalyst amount was increased from 1-5 wt%, and complete conversion of WCO to FAEEs was achieved in 2.5 h in presence of 5 wt% catalyst. A further increase in catalyst concentration (> 5 wt%) doesn't reduce the reaction time significantly as shown in Fig. 4.5b, and hence, the transesterification reactions of WCO were studied in presence of 5 wt% catalyst concentration.

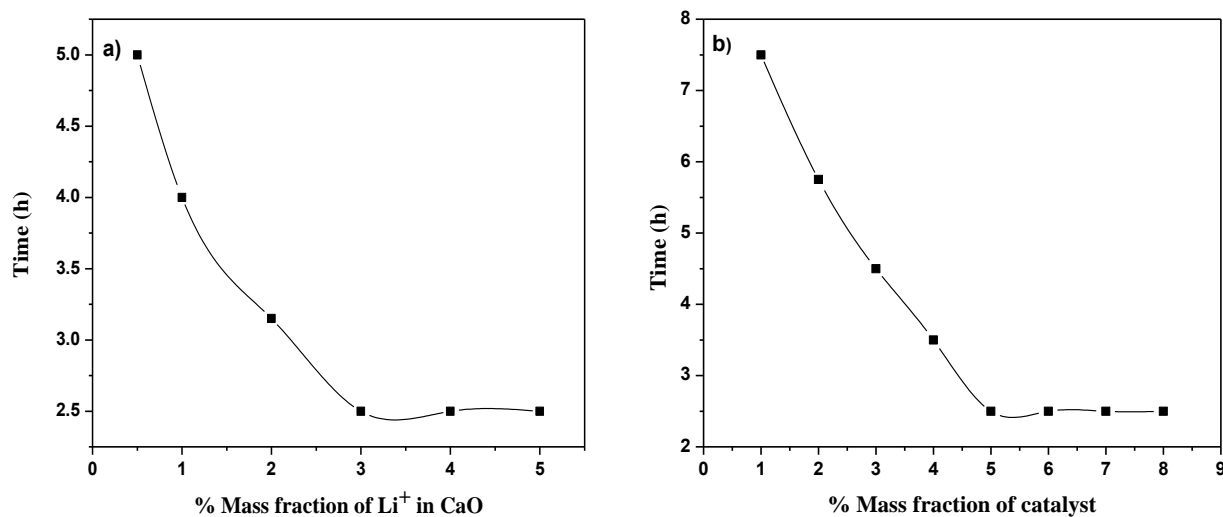


**Fig. 4.5. Effect of a) lithium ion concentration and b) catalyst concentration on transesterification of WCO.**

#### 4.4.2 Effect of reaction temperature

To determine the optimum reaction temperature for the transesterification of WCO, a series of reactions have been performed using 12:1 molar ratio of ethanol to oil in the presence of 5 wt% 3-Li/CaO catalyst, and varying the reaction temperature 35 to 75 °C. The rate of ethanolysis of WO was found to increase with increase in temperature and complete conversion of WCO to FAEEs required 2.5 h at 65 °C. A further increase in the reaction temperature does not reduce the reaction time significantly as shown in Fig. 4.6, and hence all transesterification reactions were performed at 65 °C.

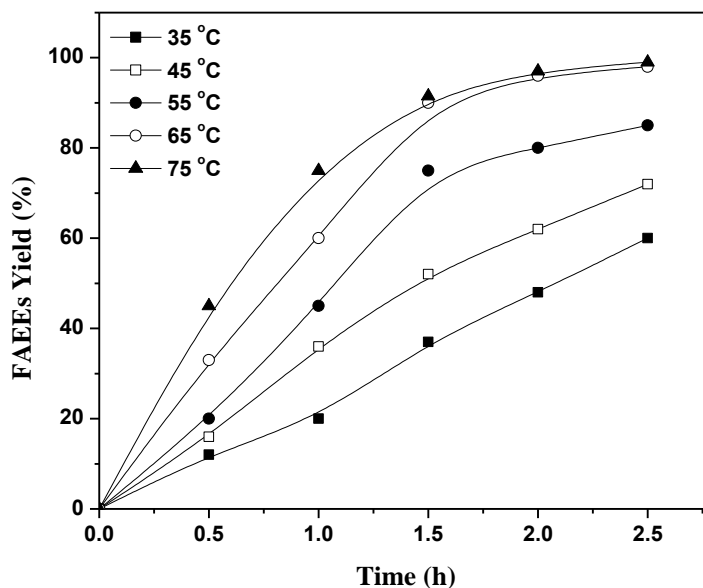


**Fig. 4.6. Effect of reaction temperature on transesterification of WCO (Reaction conditions: EtOH/oil = 12:1; Catalyst amount = 5 wt%).**

#### 4.4.3 Effect of ethanol/oil molar ratio

The effect of ethanol/oil molar ratio on transesterification reaction is one of the important parameter which affects the ester yield as well as cost of the biodiesel production. Theoretical minimum alcohol to oil molar ratio should be 3:1 for the complete conversion of vegetable oil to corresponding mono alkyl esters. However, transesterification being a reversible reaction, usually such reactions were performed with excess of alcohol to shifts the equilibrium in forward direction and to achieve the maximum ester yield. Heterogeneous catalysts, due to phase difference, usually catalyze the transesterification reaction at slower rate and required more time for the completion of reaction. The efficacy of the solid catalysts has been reported to improve when higher alcohol to oil molar ratios was used (Xie et al., 2006).

To determine the optimum ethanol/oil molar ratios for the better catalytic activity, a series of reactions were performed in presence of 5 wt% 3-Li/CaO catalyst at 65 °C employing 3:1 to 18:1 ethanol to oil molar ratio. The rate of transesterification reaction increases as ethanol/oil molar ratio was increased from 3:1 to 12:1 and reaction were found to be completed in 2.5 h when 12:1 ratio was employed. A further increase in ethanol/oil ratio was not found to increase the percentage conversion to the significant extent as shown in Fig. 4.7.

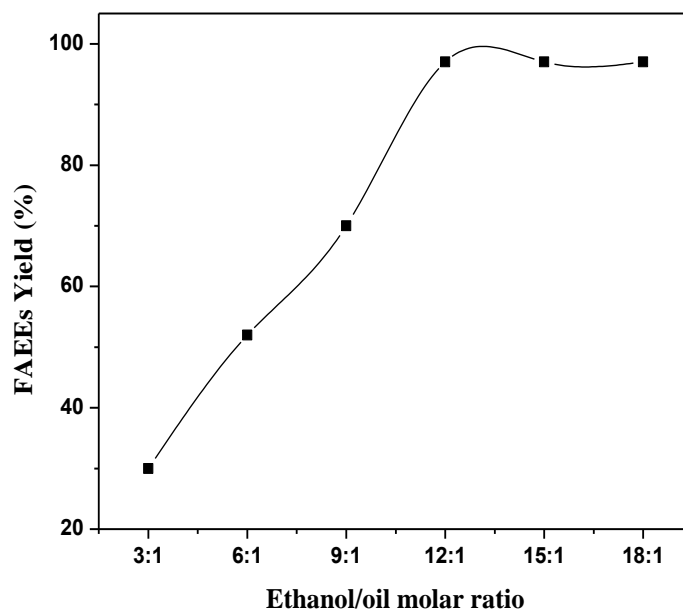


**Fig. 4.7. Effect of ethanol/oil molar ratio on transesterification of WCO (Reaction conditions: Catalyst amount = 5 wt%; Temperature = 65 °C and reaction time = 2.5 h).**

Hence, on the basis of above mentioned experiments, a 12:1 ethanol to oil molar ratio, 5 wt% of 3-Li/CaO catalyst, and at 65 °C reaction temperature, were established as optimum reaction conditions to achieve the maximum fatty acid ethyl ester yield (98%) in 2.5 h of reaction duration.

#### 4.5 Effect of FFA on catalyst activity

In order to test the efficacy of 3-Li/CaO catalyst towards the transesterification of few commonly available vegetable oils (having various amount of FFA) in the vicinity, it has also been employed for the ethanolysis and methanolysis of WCO, FCO, KO and SO. All reactions were performed in presence of 5 wt% of catalyst at 65 °C using ethanol or methanol with oil in 12:1 molar ratio. The time required for conversion of various feedstocks to fatty acid methyl/ethyl esters is shown in Fig. 4.8. The catalyst required longer reaction duration for the ethanolysis than the corresponding methanolysis reaction and the activity of catalyst was found to be adversely affected with the increase in FFA in feedstock.

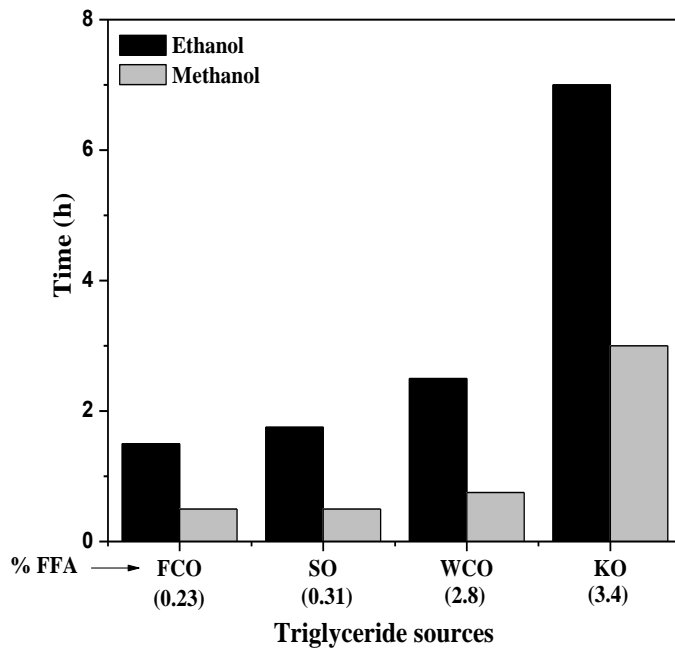


**Fig. 4.8. Effect of FFA on 3-Li/CaO catalyzed ethanolysis and methanolysis of various triglycerides.**

As evident from Fig. 4.8, under optimized reaction conditions 3-Li/CaO catalyst required more time for the ethanolysis than methanolysis for the all vegetable oils. The difference in activity may be due to the fact that methanol is more reactive than ethanol due to high mobility of methoxy group than ethoxy group (Kim et al., 2010). A longer reaction duration would also increase the energy consumption during the reaction which in turn may increase the FAEEs production cost. Although FAEEs produced during the reaction expected to be a more eco-friendly fuel than FAMEs, however, lesser reactivity of ethanol is a major hurdle for the commercialization of this reaction (Kim et al., 2010; Saleh, 2011).

#### 4.6 Catalyst reusability and homogeneous contribution

To test the reusability of 3-Li/CaO catalyst, the ethanolysis of WCO has been performed under the optimized reaction condition. Catalyst was recovered from the reaction mixture through filtration after the first catalytic run. Recovered catalyst was washed with hexane in order to remove the adsorbed organic molecules from its surface and finally dried at 120 °C. The catalyst thus recovered and regenerated was used for three more successive runs under the same

experimental condition and regeneration methods, respectively. Reused catalyst was able to yield 98, 90 and 84 % conversion of WCO into FAEEs in first, second, and third catalytic run, respectively as shown in Fig. 4.9. Thus regenerated catalyst could catalyze the transesterification of WCO, but with the partial loss of activity in every successive run.

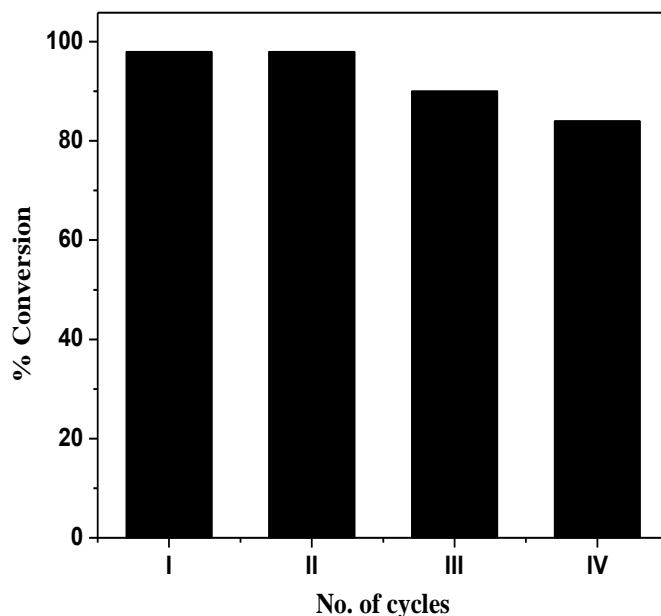


**Fig. 4.9. Reusability studies of 3-Li/CaO catalyst towards the ethanolsis of waste cottonseed oil.**

This gradual loss in catalytic activity, after every successive cycle, could be due to the partial leaching of the active species ( $\text{Li}^+$ ) from the catalyst support. The leached  $\text{Li}^+$  from the catalyst could catalyze the transesterification reaction similar to the homogeneous catalyst. Hence, it is noteworthy to quantify the homogeneous contribution in catalytic activity. In order to quantify the homogeneous contribution, 3-Li/CaO (500 mg), was refluxed with ethanol (4.8 g) for 2.5 h at 65 °C. After the stipulated time the catalyst was filtered out, and ethanol thus obtained has been employed for the transesterification of WCO (EtOH/oil = 12:1, m/m) at 65 °C for 2.5 h. Under these experimental conditions negligible conversion (~ 5%) of the WCO into FAEEs was achieved. Thus it is safe to assume that there is no significant homogeneous contribution involved in catalytic activity.

To establish the reason behind the loss in catalytic activity, the BET surface, basic strength, crystallite size and XRD patterns of the fresh and reused catalyst were compared. It is evident from Table 4.3 that surface area as well as basic strength of Li/CaO catalyst decreases upon reuse. On the other hand the crystallite size of the reused catalyst was found to be smaller than the fresh catalyst.

**Table 4.3. Comparison of BET surface area, basic strength and crystallite size of fresh and reused 3–Li/CaO catalyst.**

| S. No. | 3–Li/CaO | BET surface area<br>( $\text{m}^2 \text{g}^{-1}$ ) | Basic strength<br>( $H_{\text{L}}$ ) | Crystallite size<br>(nm) |
|--------|----------|--|--------------------------------------|--------------------------|
| 1.     | Fresh    | 1.3  | $15 < H_{\text{L}} < 18.4$           | 60                       |
| 2.     | Reused   | 0.88   | $11.1 < H_{\text{L}} < 15.0$         | 52                       |

The comparison of the XRD patterns (Fig. 4.10) of fresh and reused catalyst signifies that some structural changes in reused catalyst. Appearance of peaks at  $2\theta = 32.3^\circ$  and  $67.6^\circ$  in the diffraction patterns of reused catalyst supported the formation of hexagonal calcium carbonate as one of the major phase. The formation of calcium carbonate may be due to the reaction of calcium hydroxide with atmospheric  $\text{CO}_2$  during repeated use of catalyst and drying at  $120^\circ\text{C}$ . Thus, decrease in basic strength and structural changes may be responsible for the reduction in Li/CaO catalytic activity upon its repeated use.

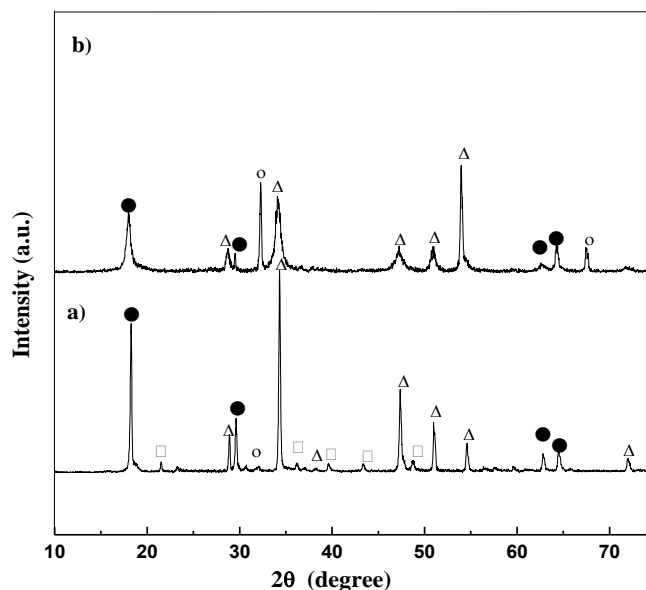


**Fig. 4.10.** Comparison of powder XRD patterns of a) Fresh 3-Li/CaO and b) Reused 3-Li/CaO catalysts. (● = cubic calcium oxide; Δ = hexagonal calcium hydroxide; □ = orthorhombic calcium carbonate; and o = hexagonal calcium carbonate).

#### 4.7 Kinetic study

In order to study the kinetics of the ethanolysis of WCO in presence of 3-Li/CaO catalyst, reaction has been performed under optimized reaction conditions, but varying the temperature 35-65 °C.

Plots between  $-\ln(1-X_{ee})$  and 't' for reactions performed in the temperature range of 35-65 °C, are given Fig. 4.11. Linear nature of these plots support that 3-Li/CaO catalyzed ethanolysis of WCO has followed the pseudo first order kinetic equation.

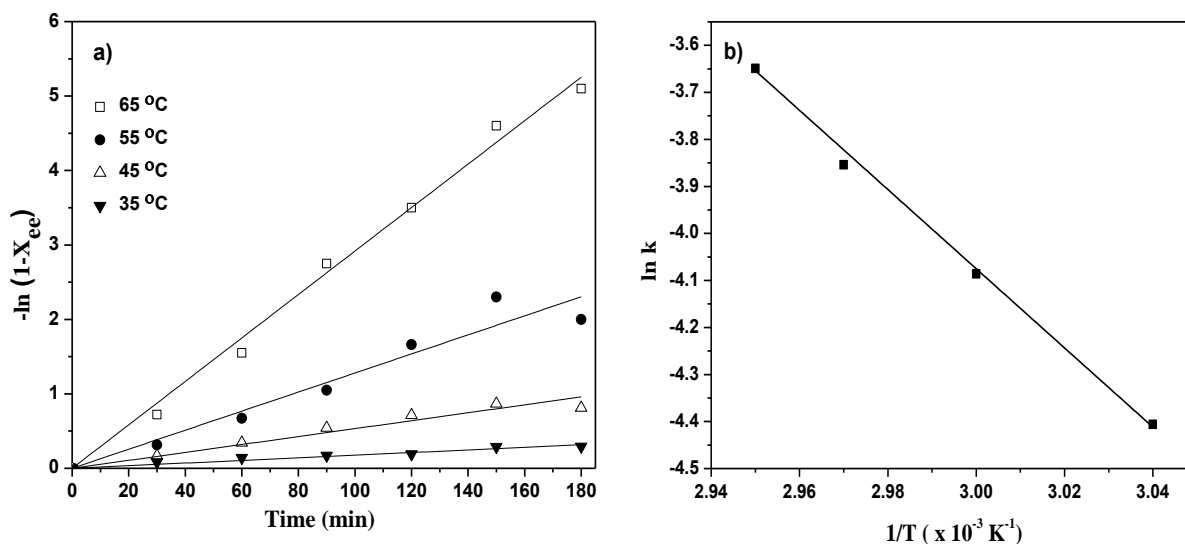


**Fig. 4.11.** Plots of a)  $-\ln(1-X_{ee})$  versus reaction time ‘t’ at different temperatures (Reaction conditions: EtOH/oil molar ratio = 12:1; catalyst amount = 5 wt%) and b) Arrhenius plot for the ethanolysis of waste cottonseed oil ( $X_{ee}$  = FAEEs yield).

The values of  $E_a$  and  $A$  from this plot were found to be  $70.0 \text{ kJ mol}^{-1}$  and  $1.6 \times 10^9 \text{ min}^{-1}$ , respectively. The calculated activation energy was found pretty close to the reported value of  $70.6 \text{ kJ mol}^{-1}$  for the ethanolysis of castor oil in presence of homogeneous catalyst (Silva et al., 2009).

#### 4.8 Physicochemical properties of FAEEs

The standards for the FAEEs has not been defined separately and hence, physicochemical properties (Table 4.4) of the FAEEs produced in 3–Li/CaO catalyzed ethanolysis of WCO have been compared with the EN standards given for FAMES. The observed values of the studied properties of prepared FAEEs were found within the limits of the EN 14214 specifications except the kinematic viscosity. The kinematic viscosity at  $40 \text{ }^\circ\text{C}$  of WCO derived FAEEs was found to be marginally higher (5.47 cSt) than the maximum accepted value of 5.0 cSt.

**Table 4.4. Physicochemical properties of waste cottonseed oil derived FAEEs.**

| Physicochemical properties               | WO derived FAEEs | EN 14214 specifications | Test Methods      |
|--|------------------|-------------------------|-------------------|
| Ester content (%)                        | 98 %             | 96.5                    | <sup>1</sup> HNMR |
| Flash point (°C)                         | 120              | ≥100                    | ASTM D 93         |
| Pour point (°C)                          | 0                | NR                      | ASTM D 2500       |
| Kinematic viscosity at 40 °C (cSt)       | 5.47             | 3.5–5.0                 | ASTM D 445        |
| Calorific value (MJ kg <sup>-1</sup> )   | 39.44            | NR                      | ASTM D 7870       |
| Ash (%)                                  | NIL              | 0.02                    | ASTM D 874        |
| Density at 31°C (g mL <sup>-1</sup> )    | 0.88             | 0.86–0.90               | EN ISO 3675       |
| Acid KOH value (mg KOH g <sup>-1</sup> ) | 0.35             | 0.5                     | ASTM D 974        |

*NR = Not reported*

## 4.9 Conclusions

The catalyst, 3-Li/CaO, was found efficient for the ethanolysis of vegetable oils having up to 3.4 wt% FFAs. The catalytic activity was found to be a function of ethanol to oil molar ratio, catalyst amount, reaction temperature and FFA present in the feedstock. Under optimized reaction condition, catalyst was found to follow pseudo first order kinetic model and values of the first order rate constant and activation energy was found to be 0.03 min<sup>-1</sup> (at 65 °C) and 70.0 kJ mol<sup>-1</sup> (at 35-65 °C), respectively. The lixiviation study suggested negligible homogeneous contribution in catalyst activity. The catalyst was also recovered and reused in four catalytic runs but with partial loss in activity during successive catalytic cycles. Few physicochemical properties of the waste cotton seed oil derived FAEEs were also evaluated and observed values (except kinematic viscosity) were found within the limits of EN 14214 specifications.

---

## References

Abreu, F. R.; Alves, M. B.; Macedo, C. C. S.; Zara, L. F.; Suarez, P. A. Z.; New multi-phase catalytic systems based on tin compounds active for vegetable oil transesterification reaction. *J. Mol. Catal. A: Chem.*; **2005**, *227*, 263–267.

Ali, A.; Kaur, M.; Mehra, U.; Use of immobilized *Pseudomonas sp.* as whole cell catalyst for the transesterification of used cotton seed oil. *J. Oleo Sci.*; **2011**, *60*, 7-10.

Balat, M.; and Balat, H.; Progress in biodiesel processing. *Appl. Energ.*; **2010**, *87*, 1815–1835.

Benjapornkulaphong, S.; Ngamcharussrivichai, C.; Bunyakiat, K.; Al<sub>2</sub>O<sub>3</sub>-supported alkali and alkali earth metal oxides for transesterification of palm kernel oil and coconut oil. *Chem. Eng. J.*; **2009**, *145*, 468–474.

Charusiri, W.; Yongchareon, W.; Vitidsant, T.; Conversion of waste vegetable oils to liquid fuels and chemicals over HZSM-5, sulfated zirconia and hybrid catalysts. *Korean J. Chem. Eng.*; **2006**, *23*, 349–355.

Encinar, J. M.; González, J. F.; Rodríguez-Reinares, A.; Ethanolysis of used frying oil: Biodiesel preparation and characterization. *Fuel Process. Technol.*; **2007**, *88*, 513–522.

Ghesti, G. F.; de Macedo, J. L.; Resck, I. S.; Dias, J. A.; Dias, S. C. L.; FT-Raman spectroscopy quantification of biodiesel in a progressive soybean oil transesterification reaction and its correlation with <sup>1</sup>H NMR spectroscopy methods. *Energ. Fuel*; **2007**, *21*, 2475–2480.

Hajek, M.; Skopal, F.; Cernoch, M.; Effect of phase separation temperature on ester yields from ethanolysis of rapeseed oil in the presence of NaOH and KOH as catalysts. *Bioresour. Technol.*; **2012**, *110*, 288–291.

Kim, M.; Di Maggio, C.; Yan, S.; Salley, S. O.; Ng, K. Y. S.; The synergistic effect of alcohol

mixtures on transesterification of soybean oil using homogeneous and heterogeneous catalysts. *Appl. Catal. A: Gen.*; **2010**, 378, 134–143.

Knothe, G.; Determining the blend level of mixtures of biodiesel with conventional diesel fuel by fiber optic NIR spectroscopy and  $^1\text{H}$  NMR spectroscopy. *J. Am. Oil Chem. Soc.*; **2011**, 78, 1025–1028.

Ngamcharussrivichai, C.; Totarat, P.; Bunyakiat, K.; Ca and Zn mixed oxide as a heterogeneous base catalyst for transesterification of palm kernel oil. *Appl. Catal. A: Gen.*; **2008**, 341, 77–85.

Qadri, S. B.; Skelton, E. F.; Hsu, D.; Dinsmore, A. D.; Yang, J.; Gray, H. F.; Ratna, B. R.; Size-induced transition-temperature reduction in nanoparticles of ZnS. *Phys. Rev. B*; **1999**, 60, 9191–9193.

Rashid, U.; Anwar, F.; Moser, B. R.; Ashraf, S.; Production of sunflower oil methyl esters by optimized alkali-catalyzed methanolysis. *Biomass Bioenerg.*; **2008**, 32, 1202–1205.

Saleh, H. E.; The preparation and shock tube investigation of comparative ignition delays using blends of diesel fuel with bio-diesel of cottonseed oil. *Fuel*; **2011**, 90, 421–429.

Sankarnarayanan, S.; Antonyraj, C. A.; Kannan, S.; Transesterification of edible, non-edible and used cooking oils for biodiesel production using calcined layered double hydroxides as reusable base catalysts. *Bioresour. Technol.*; **2012**, 109, 57–62.

Saravanan, N.; Puhan, S.; Nagarajan, G.; Vedaraman, N.; An experimental comparison of transesterification process with different alcohols using acid catalysts. *Biomass Bioenerg.*; **2010**, 34, 999–1005.

Silva, N. L.; Batistella, C. B.; Filho, R. M.; Maciel, M. R. W.; Biodiesel Production from Castor Oil: Optimization of Alkaline Ethanolysis. *Energ. Fuel*; **2009**, 23, 5636–5642.

Sun, P.; Sun, J.; Yao, J.; Zhang, L.; Xu, N.; Continuous production of biodiesel from high acid value oils in microstructured reactor by acid-catalyzed reactions. *Chem. Eng. J.*; **2010**, 162, 364–370.

Suppes, G. J.; Dasari, M. A.; Duskocil, E. J.; Mankidy, P. J.; Goff, M. J.; Transesterification of soybean oil with zeolite and metal catalysts. *Appl. Catal. A: Gen.*; **2004**, 257, 213–223.

Xie, W.; Peng, H.; Chen, L.; Calcined Mg–Al hydrotalcites as solid base catalysts for ethanolysis of soybean oil. *J. Mol. Catal. A: Chem.*; **2006**, 246, 24–32.

Yan, S.; Kim, M.; Salley, S. O.; Ng Simon, K. Y.; Oil transesterification over calcium oxides modified with lanthanum. *Appl. Catal. A: Gen.*; **2009**, 360, 163–170.

---

**An Efficient and Reusable Li/NiO Heterogeneous Catalyst for Ethanolysis of Waste Cottonseed oil**

---

|            | <b>Contents</b>   | <b>Page</b> |
|------------|---|-------------|
| <b>5.1</b> | <b>Introduction</b>   | 85          |
| <b>5.2</b> | <b>Experimental section</b>   | 85          |
|            | 5.2.1 Catalyst preparation  | 85          |
|            | 5.2.2 Transesterification reaction                                  | 86          |
| <b>5.3</b> | <b>Results and discussion</b>                                       | 86          |
|            | 5.3.1 Catalyst characterization                                     | 86          |
|            | 5.3.1.1 FESEM and HRTEM analysis                                    | 86          |
|            | 5.3.1.2 Powder X-ray diffraction study                              | 88          |
|            | 5.3.1.3 BET surface area and basic strength study                   | 88          |
|            | 5.3.1.4 XPS study   | 89          |
|            | 5.3.2 Influence of reaction conditions on ethanolysis of WCO        | 90          |
| <b>5.4</b> | <b>Effect of FFA on catalyst activity</b>                           | 93          |
| <b>5.5</b> | <b>Evaluation of the recyclability and homogeneous contribution</b> | 94          |
| <b>5.6</b> | <b>Kinetic study</b>  | 97          |
| <b>5.7</b> | <b>Proposed mechanism for transesterification</b>                   | 97          |
| <b>5.8</b> | <b>Conclusions</b>  | 99          |
|            | <b>References</b>   | 100         |

---

### **Abstract**

In order to use ethanol in place of methanol for biodiesel production, in present work, a series of  $\text{Li}^+$  impregnated NiO (Li/NiO) was prepared in nano particle form in aqueous medium without adding any organic solvent or templates. The structure of the catalyst was established by powder X-ray diffraction study, surface morphology by field emission scanning electron microscopy and particle size by high resolution transmission electron microscopy. Basic strengths of the catalysts were measured by Hammett indicators and found to be maximum in case of catalyst prepared with 5 wt%  $\text{Li}^+$  in NiO followed by calcination at 600 °C (5-Li/NiO-600). Catalyst characterization supported the oxidation of  $\text{Ni}^{2+}$  into  $\text{Ni}^{3+}$  upon lithium impregnation. Finally, the Li/NiO was employed as heterogeneous catalyst for the ethanolysis of waste cottonseed oil. Under optimized reaction condition of 5wt% catalyst, ethanol to oil molar ratio of 12:1 and at 65 °C reaction temperature, > 98% fatty acid ethyl ester yield was obtained in 3 h. The catalyst was found to be effective for the ethanolysis of vegetable oils having up to 8.4 wt% free fatty acids. During reusability experiments, Li/NiO catalyst was able to catalyze seven reaction cycles without major loss in activity. Thus present work has demonstrated the development of a greener and completely renewable biofuel, fatty acid ethyl esters, using waste cottonseed oil as feedstock.

## 5.1 Introduction

Heterogeneous catalysts for the methanolysis of triglycerides are quite frequent in literature, however, fewer catalysts are reported for the ethanolysis. Literature reported work on ethanolysis was mainly performed in presence of homogeneous catalysts and use of solid catalysts for this reaction is not frequent. Rashid and Anwar (2008), have reported the ethanolysis of cottonseed oil using sodium hydroxide, potassium hydroxide, sodium methoxide and potassium methoxide as homogeneous catalysts. Although, they reported > 96.9% FAEEs yield in 90 min, however, the ethyl esters were contaminated with catalyst and hence ester formed must be washed to remove the catalyst contamination. Most of the literature reported heterogeneous catalysts demand relatively high temperature, pressure and longer reaction time. Li et al., (2009) have reported the ethanolysis of canola oil in presence of  $Mg_2CoAl$  solid catalyst (2 wt%) with 16:1 ethanol to oil molar ratio at 200 °C and 25 atm pressure to obtain 97% FAEEs yield in 5 h.

Thus preparation of a reusable heterogeneous catalyst, which could catalyze the ethanolysis of high FFA containing VOs under ambient conditions, is still a challenge. In present chapter, lithium doped nickel oxide (Li/NiO) has been prepared and employed as solid reusable catalyst for the ethanolysis of waste cottonseed oil. The catalyst was prepared in a single step in the form of nano particles using water as a solvent and without employing any harmful solvent or organic template.

## 5.2 Experimental section

### 5.2.1 Catalyst preparation

The NiO used as a support for the catalyst was prepared by ceramic method *via* calcination of commercial nickel nitrate at 500 °C for 5 h. Then, nickel oxide was impregnated with lithium by wet chemical method. In a typical preparation, 10 g of NiO was stirred with 80 mL of deionized water, and to this 10 mL aqueous solution of  $LiNO_3$  of desired concentration was added. The resulted slurry was stirred for 7 h, evaporated to dryness, initially heated at 140 °C for 24 h and finally calcined at desired temperature for 3 h to obtain  $x$ -Li/NiO-T, where  $x$  and T represents the wt% of lithium and calcination temperature (°C), respectively.

The prepared catalysts were characterized by powder XRD, BET surface area measurements, FESEM and HRTEM techniques.

### 5.2.2 Transesterification reaction

To study the catalytic activity of prepared catalyst, all transesterification reactions were carried out in a 250 ml, two necked round bottom flask equipped with water cooled reflux condenser, thermometer, oil bath and a magnetic stirrer. In a typical run, the flask was charged with 10 g vegetable oil, desired molar concentrations of ethanol, and desired amount of catalyst. To monitor the progress of the reaction, the aliquots were collected from the reaction mixture after every 30 min with the help of glass dropper and subjected to the  $^1\text{H}$  NMR study for FAEEs quantification.

## 5.3 Results & Discussion

### 5.3.1 Catalyst Characterization

#### 5.3.1.1 FESEM and HRTEM analysis

The surface morphology and structure of the 5-Li/NiO-600 was studied by FESEM imaging. As shown in Fig.5.1a, the catalyst has formed as 3D hexagonal or oval shaped particles of  $\sim 2.4\ \mu\text{m}$  size. The HRTEM image (Fig. 5.1b) suggested that these particles were formed due to the agglomeration of smaller hexagonal particles of  $\sim 150\ \text{nm}$  size.

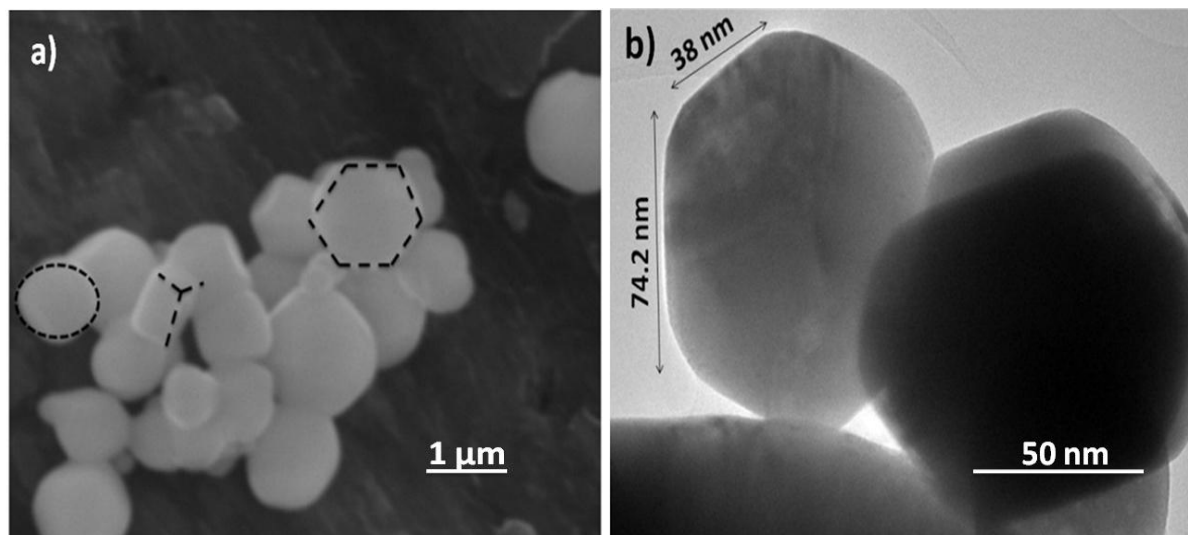


**Fig. 5.1. a) FESEM image and b) HRTEM image of 5-Li/NiO-600 catalyst.**

### 5.3.1.2 Powder X-ray diffraction study

To establish the impact of lithium impregnation and calcination temperature on NiO structure, Li/NiO was prepared either by varying lithium concentration or calcination temperature. As evident from the XRD diffraction patterns shown in Fig. 5.2a, lithium doping (1-6 wt%) in NiO followed by calcination at 600 °C besides regular cubic structure of NiO (JCPDS file no. 47-1049), appearance of new peaks at  $2\theta = 38.4^\circ$  and  $66.1^\circ$ , supported the formation of cubic-Li<sub>2</sub>O (JCPDS file no. 77-2144) and at  $2\theta = 33.1^\circ$ ,  $56.3^\circ$ ,  $62.6^\circ$  indicate the formation of hexagonal-Ni<sub>2</sub>O<sub>3</sub> (JCPDS file no. 14-0481). The crystal structure of NiO adopts the NaCl structure, in which Ni<sup>2+</sup> is present in octahedral sites created by O<sup>2-</sup>. Octahedral Ni<sup>2+</sup> in high spin state possess two unpaired electrons and oxidation of Ni<sup>2+</sup> to Ni<sup>3+</sup>, due to Li doping, lead to increase the number of unpaired electrons from 2 to 3 (Wei-Luen et al., 2010). An increase in specific magnetic susceptibility of NiO was observed on increasing the lithium concentration, as shown in Table 5.1, to support the oxidation of nickel. Moreover, visual color change (green to dark grey) upon lithium impregnation in NiO, also supports the oxidation of Ni<sup>2+</sup> into Ni<sup>3+</sup> upon lithium impregnation. As given in Table 5.1, the values of lattice parameters remain constant with increasing Li loading, to support that lithium is well dispersed in NiO without making any defect in regular structure.

To study the effect of calcination temperature on catalyst structure, 5 wt% Li impregnated NiO was calcined in the temperature range of 300-900 °C. As shown in Fig. 5.2b, similar diffraction patterns were observed for all the samples to maintain that a change in calcination temperature (300-900 °C) was not able to induce any major change in Li/NiO structure.

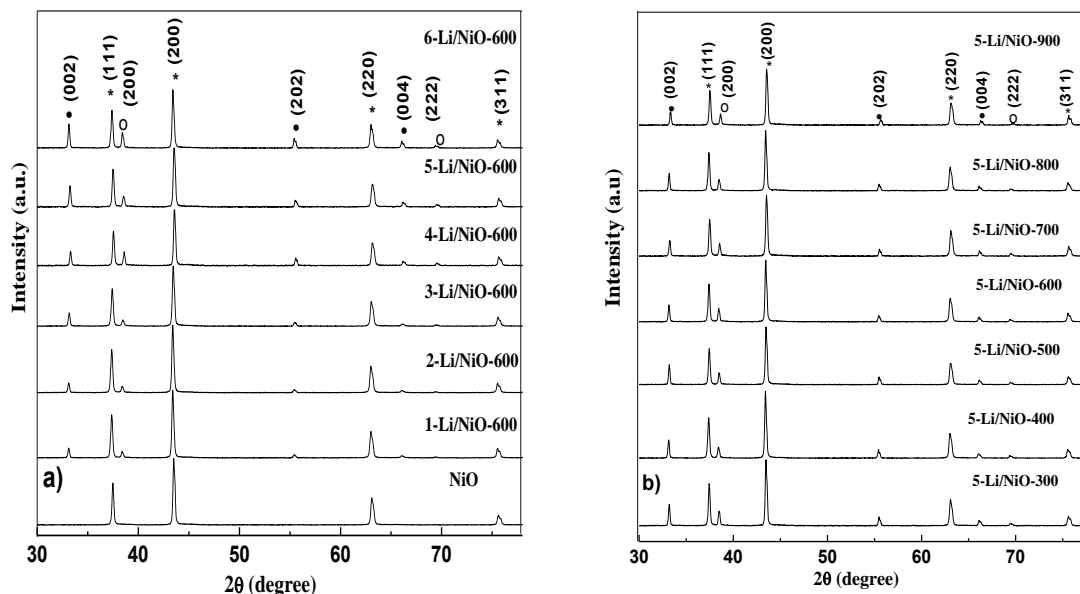


**Fig. 5.2. Comparison of powder XRD patterns of a) 0-6 wt% Li impregnated NiO calcined at 600 °C and b) 5-Li/NiO calcined in the range 300-900 °C [ $*$  = NiO;  $\bullet$  = Ni<sub>2</sub>O<sub>3</sub>;  $\circ$  = Li<sub>2</sub>O].**

The crystallite size of Li/NiO catalysts corresponding to (200) plane was determined with the help of Debye-Scherrer equation (Qadri et al., 1999). A constant crystallite size of ~ 41 nm support that change in either lithium concentration or calcination temperature has no significant effect on the crystallite size of Li/NiO particles.

### 5.3.1.3 BET surface area and basic strength study

The specific surface area, basic strength and basicity of nickel oxide and Li/NiO-600 are compared in Table 5.1. The surface area gradually decreases with the increase in lithium concentration due to the pore plugging of the NiO upon lithium impregnation. The basicity of Li/NiO gradually increases with the increase in lithium concentration, this could be attributed to the formation of Li<sub>2</sub>O (a strong Lewis base).

**Table.5.1. Comparison of BET surface area, lattice parameters, magnetic susceptibility, basic strength ( $H_-$ ), basicity and turn over frequency (TOF) of prepared catalysts.**

| Catalyst     | BET surface area ( $m^2 g^{-1}$ ) | Lattice parameters ( $\text{\AA}$ ) |                       |   | $\chi_g$ ( $m^3/kg$ ) $\times 10^{-2}$ | Basic Strength <sup>a</sup> ( $H_-$ ) | Basicity <sup>b</sup> (mmoles of HCl $g^{-1}$ of catalyst) | TOF ( $\times 10^{-2}$ ) ( $min^{-1}$ ) |
|--------------|-----------------------------------|-------------------------------------|-----------------------|---|--|---------------------------------------|--|---|
|              |                                   | NiO (a)                             | Li <sub>2</sub> O (a) | Ni <sub>2</sub> O <sub>3</sub> (a = b $\neq$ c) |  |                                       |  |   |
| NiO          | 6.86                              | 4.16                                | 4.61                  | 4.84, 5.3                                       | 4.1                                    | $9.8 < H_- < 10.1$                    | 4.4  | NF                                      |
| 1-Li/NiO-600 | 5.96                              | 4.15                                | 4.60                  | 4.83, 5.3                                       | 4.3                                    | $9.8 < H_- < 10.1$                    | 8.5  | 2.04                                    |
| 2-Li/NiO-600 | 5.66                              | 4.14                                | 4.62                  | 4.82, 5.2                                       | 4.6                                    | $9.8 < H_- < 10.1$                    | 9.3  | 2.23                                    |
| 3-Li/NiO-600 | 4.86                              | 4.14                                | 4.61                  | 4.83, 5.4                                       | 5.1                                    | $10.1 < H_- < 11.1$                   | 9.7  | 2.39                                    |
| 4-Li/NiO-600 | 4.04                              | 4.13                                | 4.62                  | 4.82, 5.2                                       | 5.2                                    | $11.1 < H_- < 15.0$                   | 10.8   | 2.40                                    |
| 5-Li/NiO-600 | 3.51                              | 4.12                                | 4.60                  | 4.82, 5.3                                       | 8.5                                    | $15.0 < H_- < 18.4$                   | 12.0   | 2.43                                    |
| 6-Li/NiO-600 | 3.17                              | 4.11                                | 4.60                  | 4.81, 5.2                                       | 9.9                                    | $15.0 < H_- < 18.4$                   | 13.1   | 2.27                                    |

$\chi_g$  is magnetic susceptibility, <sup>a</sup> basic strength of the catalyst calculated by Hammett indicators, <sup>b</sup> total basicity of the catalysts calculated by acid-base titrations.

#### 5.3.1.4 XPS study

The electronic state of the metal ions present in catalysts was determined by using XPS as shown in Fig. 5.3. The peaks corresponding to Ni<sup>2+</sup> 2p<sub>3/2</sub> and Ni<sup>3+</sup> 2p<sub>3/2</sub> were observed at 855.1 and 872.8 eV respectively, to support the oxidation of Ni<sup>2+</sup> into Ni<sup>3+</sup> upon lithium impregnation. The presence of lithium in Li/NiO was supported by the presence of a peak at 58.5 eV corresponding to Li<sup>+</sup> 1s. The peak appeared at 531.7 eV, attributes to O 1s in LiOH on the surface and the peak at 529.5 eV to O 1s in Li<sub>2</sub>O (Tanaka et al., 2000).

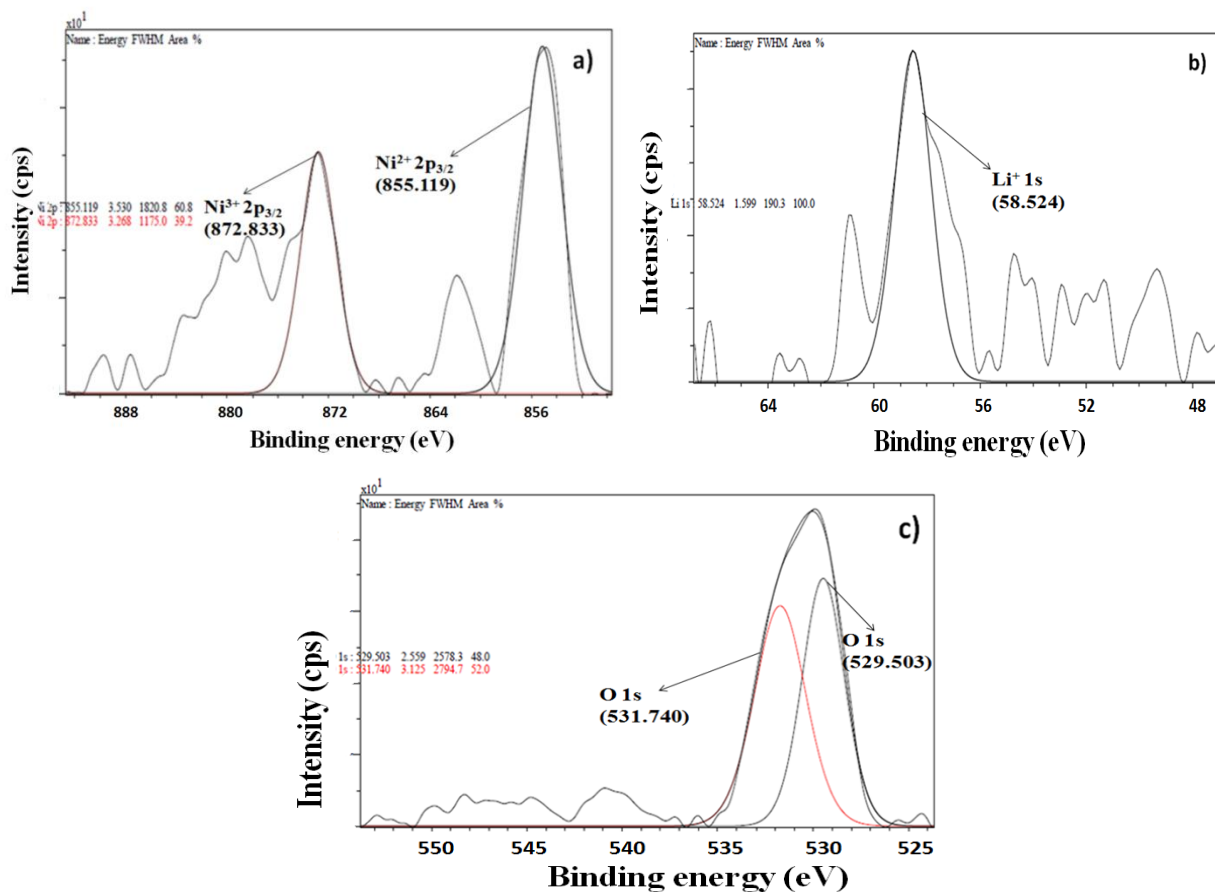


Fig. 5.3. XPS spectra for a) nickel b) lithium and c) oxygen in 5-Li/NiO-600.

### 5.3.2 Influence of reaction conditions on ethanolysis of WCO

The prepared Li/NiO has been employed for the ethanolysis of WCO, KO and JO. To optimize the reaction conditions for the favorable catalytic activity, transesterification reactions have been carried out at 550 rpm by varying one parameter at a time out of the followings: (i) impregnated lithium ion concentration, (ii) catalyst concentration, (iii) reaction temperature, and (iv) ethanol to oil molar ratio. Apart from this study, the FFA tolerance and reusability of the catalyst have also been studied under optimized reaction conditions.

Pure nickel oxide remains silent towards the transesterification reaction and lithium impregnation was found to activate NiO towards ethanolysis as shown in Table 5.1. In order to determine the optimum lithium concentration in NiO, a series of Li/NiO catalyst was prepared by varying Li amount in the range of 1-6 wt% and calcining at 600 °C. The Li impregnation has

formed strong basic sites ( $\text{Li}_2\text{O}$ ) as well as  $\text{Ni}^{3+}$  centers in NiO support. Basic sites act as catalytic centers for the transesterification reaction and  $\text{Ni}^{3+}$  being electron deficient may hold the substrate molecules during the reaction.

In order to study the effect of Li concentration catalytic activity, a series of Li/NiO was prepared by varying the Li concentration in range 1-6 wt%. Transesterification reaction was performed at 65 °C in presence of 5 wt% catalyst (oil/catalyst) and employing a 12:1 ethanol to oil molar ratio. The time required for the complete transesterification of WCO was found to reduce from 9 to 3 h as the Li concentration in NiO was increased from 1 to 5 wt%. A further increase in Li concentration (from 5 to 6 wt %) was not found to reduce the reaction time significantly as shown in Fig. 5.4a. Hence, 5-Li/NiO-600 catalyst was employed to optimize other parameters to achieve the minimum time for the complete ethanolysis of WCO.

The catalyst amount required for any chemical process has major economical and environmental implications. In general, higher catalyst concentrations provide more number of surface active sites which may increase the reaction rate to significant extent. However, in order to make the process economically viable and greener, it is preferable to use the minimum possible amount of catalyst. To determine the optimum catalyst concentration, transesterification reactions were performed at 65 °C, employing a 12:1 ethanol to oil molar ratio in presence of 5-Li/NiO-600 catalyst by varying its concentration from 1 to 6 wt% (catalyst/oil). Time required for the complete conversion of WCO into FAEEs was found to reduce on increasing the catalyst amount upto 5 wt%. Further increase in catalyst concentration (5 to 6 wt%) doesn't reduce the reaction time significantly as shown in Fig. 5.4b. Hence, transesterification reactions were studied with 5 wt% catalyst concentration (oil/catalyst) for optimizing other reaction parameters.

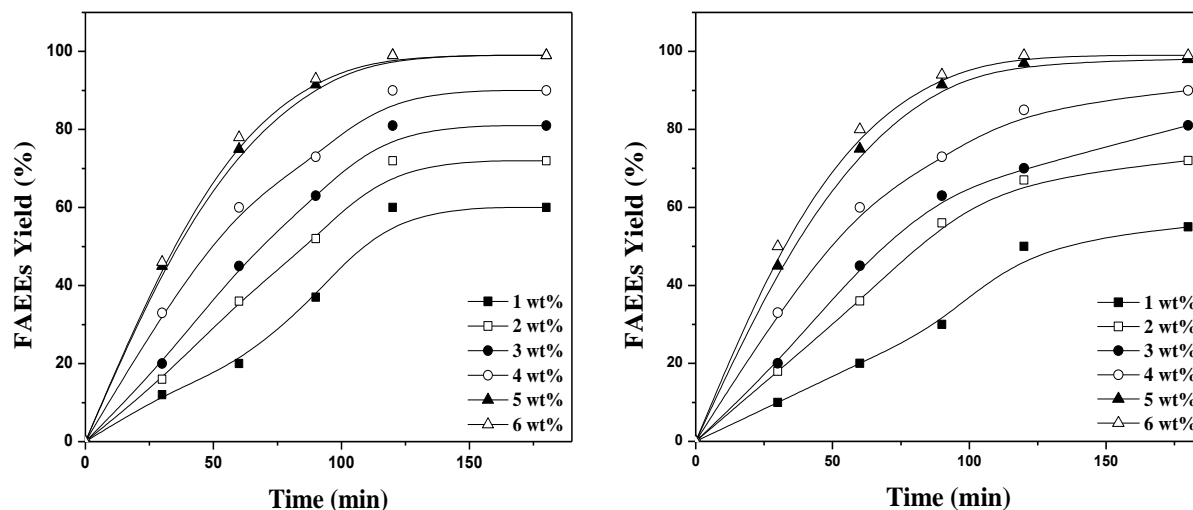


**Fig. 5.4. Effect of a) lithium ion concentration in Li/NiO and b) catalyst concentration on ethanolysis of WCO**

Ethanolysis reactions with WCO were performed in the temperature range of 35-75 °C to determine the reaction temperature for the optimum catalytic activity. Heterogeneous catalysts due to the phase difference usually demand high temperature and pressure to catalyze the reaction to vital extent. Moreover, activity of the literature reported heterogeneous catalysts were mainly studied towards methanolysis reaction (Omar and Amin, 2011; Sree et al., 2009; Desmartin-Chomel et al., 2010; Babu et al., 2008). Thus development of a heterogeneous catalyst working under ambient conditions for the ethanolysis reaction is still a challenge. Although, 5-Li/NiO-600 catalyst was able to complete the transesterification of WCO even at room temperature (35 °C), but required longer reaction duration (24 h). The time required for the complete transesterification decreases from 24 to 3 h on increasing the temperature from 35 to 65 °C. A further increase in reaction temperature was not found to reduce the reaction time to significant extent as shown in Fig. 5.5a, and hence, ethanolysis of vegetable oils were performed at 65 °C.

To determine the optimum ethanol/oil molar ratio for the better catalytic activity, a series of reactions were performed in presence of 5 wt% 5-Li/NiO-600 catalyst, at 65 °C employing 3:1 to 15:1 ethanol to oil molar ratio. The maximum rate of transesterification reaction was observed with 12:1 molar ratio of ethanol to oil as shown in Fig. 5.5b.

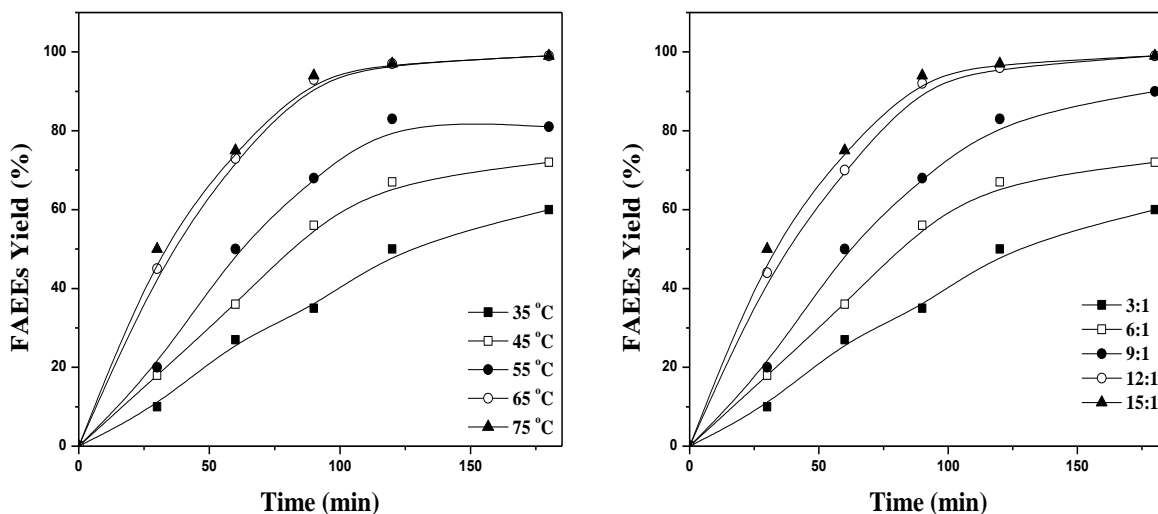


**Fig. 5.5. Effect of a) reaction temperature and b) ethanol/oil molar ratio on ethanolsis of WCO.**

Thus, under optimized reaction conditions of 12:1 ethanol to oil molar ratio, 5 wt% of 5-Li/NiO-600 and 65 °C reaction temperature, a maximum FFAEs yield (> 98%) was achieved in 3 h of reaction duration.

#### 5.4 Effect of FFA on catalyst activity

The ethanolsis of WCO (with 2.8 wt% FFA) was also performed in presence of homogeneous catalyst (NaOH). However, reaction catalyzed by NaOH catalyst didn't yield biodiesel due to the deactivation of the catalyst *via* saponification reaction. On the other hand, 5-Li/NiO-600 leads to the completion of transesterification of WCO, and hence, prepared catalyst is clearly advantageous over the homogeneous one. In order to find out the maximum FFA tolerance of the catalyst, ethanolsis of other oils having high FFA content *viz.*, karanja oil (3.4 wt% FFA) and jatropha oil (8.3 wt% FFA), were also performed. As shown in Fig. 5.6, 5-Li/NiO-600 catalyst was found to be effective even for the complete ethanolsis of JO having FFA as high as 8.3 wt%. However, oil with higher FFA concentration found to reduce the activity of the catalyst and hence, complete ethanolsis (> 98% FFAEs yield) of JO and KO was achieved in longer reaction duration of 6.5 h and 9 h, respectively. The high FFA tolerance of Li/NiO catalyst could be

attributed to the immobilization of the active (basic) sites within the solid catalyst, which did not react with FFA present in VOs and hence, saponification is prevented.

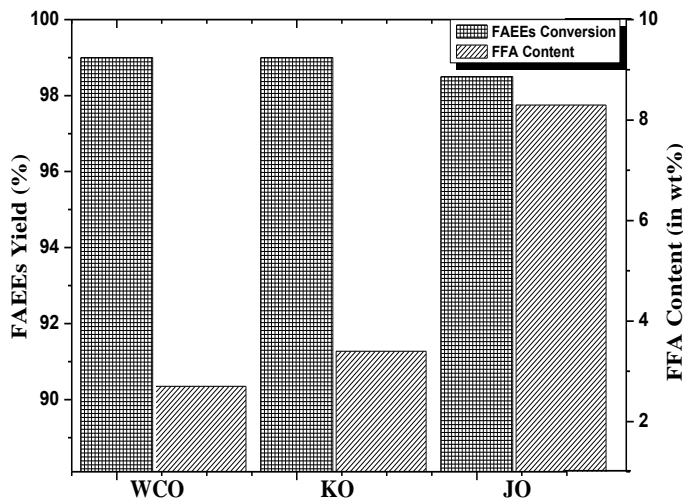


**Fig. 5.6. Effect of FFAs on Li/NiO catalyzed ethanolysis of WCO, KO and JO (Reaction conditions: Catalyst amount = 5 wt%; Temperature = 65 °C).**

### 5.5 Evaluation of the recyclability and homogeneous contribution

Heterogeneous catalysts could make a process economically viable as they could be recovered easily from the reaction mixture and reused. To demonstrate the reusability of 5-Li/NiO-600 catalyst, the ethanolysis of WCO was performed and after the completion of the reaction the catalyst was recovered by filtration, washed with hexane and dried initially at 140 °C and finally calcined at 600 °C. The recovered catalyst was reused in eight successive runs, under the same experimental condition and regeneration method. The catalyst was found to catalyze seven reaction cycles without major loss in activity as shown in Fig. 5.7. Partial loss in activity was observed in 8<sup>th</sup> cycle as ~ 65 % FAEEs yield was obtained.

The Li/NiO catalyst found to be more active towards ethanolysis reaction as compare to Li/CaO catalyst reported in previous chapter, this may be due to the less leaching of active species present in reaction mixture which was confirmed by ICP-OES and XRD patterns. Upto 8<sup>th</sup> cycle ~65% FAEEs yield was observed. The Li/NiO catalyst found to show higher tolerance towards FFA (up to 8.3 wt%) in comparison to the Li/CaO catalyst (up to 3.4 wt %). Similarly, Li/NiO catalyst was found to catalyze seven reaction cycles, thus demonstrate a better reusability than Li/CaO catalyst which was able to catalyze only four cycles.

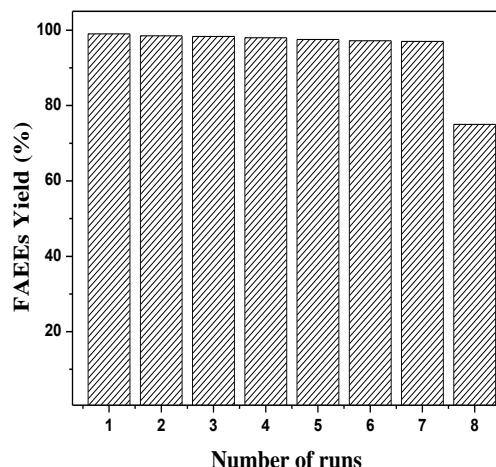


**Fig. 5.7. Reusability of 5-Li/NiO-600 catalyst (Reaction conditions: EtOH/oil molar ratio = 12:1; Catalyst amount = 5 wt% of oil; Temperature = 65 °C).**

Upon metal analysis, Li (7.6 ppm) as well as Ni (3.2 ppm) were found in FAEEs. The leaching of alkali metal ions from catalyst support is also frequently reported in literature (Sivasamy et al., 2009; Serio et al., 2008), and primarily found responsible for the loss in activity of alkali metal supported catalysts. The comparison of diffraction patterns of fresh and reused catalyst was shown in Fig.5.8. The disappearance of  $\text{Ni}_2\text{O}_3$  and  $\text{Li}_2\text{O}$  peaks from the diffraction pattern (Fig. 5.8b) of reused catalysts also supports the leaching of Li into the product which resulted in reduced catalytic activity after 7<sup>th</sup> cycle.

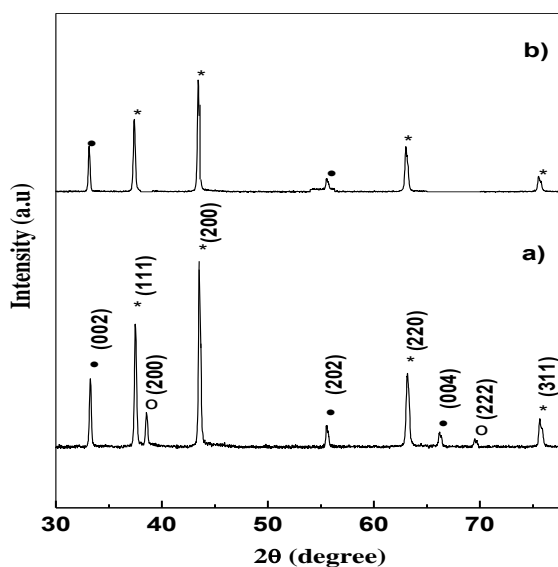


**Fig. 5.8. Comparison of powder XRD patterns of 5-Li/NiO-600 a) fresh and, b) after 8<sup>th</sup> cycle [\* = NiO; ● =  $\text{Ni}_2\text{O}_3$ ; ○ =  $\text{Li}_2\text{O}$ ].**

The leached metal ions from a heterogeneous catalyst could catalyze the reaction similar to the homogeneous catalyst. In order to determine the homogeneous contribution in catalytic activity, 5-Li/NiO-600 (500 mg), was refluxed with appropriate amount of ethanol for 3 h at 65 °C. Then catalyst was separated by centrifugation and recovered ethanol was employed for transesterification of WCO. Even, after 3 h of reaction duration negligible FAEs yield was obtained to support that leached Li from catalyst remain silent towards the reaction.

Only few reports are available in literature for the ethanolysis of triglycerides in presence of heterogeneous catalyst. A comparison of reaction conditions for ethanolysis of various triglycerides in presence of literature reported heterogeneous catalysts is given in Table 5.2.

**Table 5.2. Comparison of reaction conditions of literature reported heterogeneous catalysts used for ethanolysis with present catalyst.**

| Catalyst  | EtOH:oil<br>Molar<br>ratio | Catalyst<br>amount | Temp<br>(°C) | Time<br>(h) | Yield<br>(%)   | Reusability<br>(cycles) | Ref.   |
|---|----------------------------|--------------------|--------------|-------------|----------------|-------------------------|--|
| Ion-exchange<br>resin-sulfonated<br>polystyrene<br>SPS#218                                | 100:1                      | 20 mol%            | 64           | 18          | <b>70</b>      | 3                       | Soldi et al.,<br>2009                        |
| Heteropolyacid<br>H <sub>3</sub> PW <sub>12</sub> O <sub>40</sub> ,<br>24H <sub>2</sub> O | 6:1                        | 1.7 mol%           | 85           | 3           | <b>27</b>      | NR                      | Morin et al.,<br>2007; Hamad<br>et al., 2008 |
| Calcined calcium<br>zincate   | 20:1                       | 3 wt%              | 78           | 3           | <b>&gt; 90</b> | 3                       | Rubio-<br>Caballero et<br>al., 2013          |
| MgO/SBA-15  | 6:1                        | 2 wt%              | 220          | 5           | <b>96</b>      | NR                      | Li et al., 2008                              |
| SO <sub>4</sub> <sup>2-</sup> /ZrO <sub>2</sub>   | 20:1                       | 5 wt%              | 120          | 1           | <b>92</b>      | 4                       | Garcia et al.,<br>2008                       |
| CaO   | 18:1                       | 20 wt%             | 75           | 75          | <b>100</b>     | N.R                     | Stamenkovic<br>et al., 2011                  |
| CaO-La <sub>2</sub> O <sub>3</sub>  | 10:1                       | 8 wt%              | 65           | 65          | <b>71.6</b>    | N.R                     | Kim et al.,<br>2010                          |
| Ca(OCH <sub>2</sub> CH <sub>3</sub> )   | 12:1                       | 3 wt%              | 75           | 75          | <b>91.8</b>    | N.R                     | Liu et al., 2008                             |
| Zr/CaO  | 21:1                       | 5 wt%              | 75           | 75          | <b>&gt; 99</b> | N.R.                    | Kaur and Ali,<br>2014                        |
| Li/CaO  | 12:1                       | 5 wt%              | 65           | 2.5         | <b>&gt; 98</b> | 4                       | Chapter 4                                    |
| Li/NiO  | 12:1                       | 5 wt%              | 65           | 3           | <b>&gt; 98</b> | 7                       | Present study                                |

A comparison between the ethanolsis activity of present catalyst with literature reports is given in Table 5.2. As could be seen from the comparison, the use of present catalyst for ethanolsis is valuable as it requires lesser alcohol to oil molar ratio, lower reaction temperature and also gives better stability and reusability (seven cycles).

## 5.6 Kinetic study

To study the kinetics, Li/NiO catalyzed ethanolsis reaction of WCO was performed under optimized conditions at 35, 45, 55 and 65 °C reaction temperature. As shown in Fig. 5.9a,  $-\ln(1-X_{ee})$  versus 't' plots were found to be linear to maintain that reaction has followed (pseudo) first order kinetic equation.

The  $E_a$  and A values from the Arrhenius plot (Fig. 5.9b) were found to be  $74.2 \text{ kJ mol}^{-1}$  and  $1.9 \times 10^9 \text{ min}^{-1}$ , respectively.

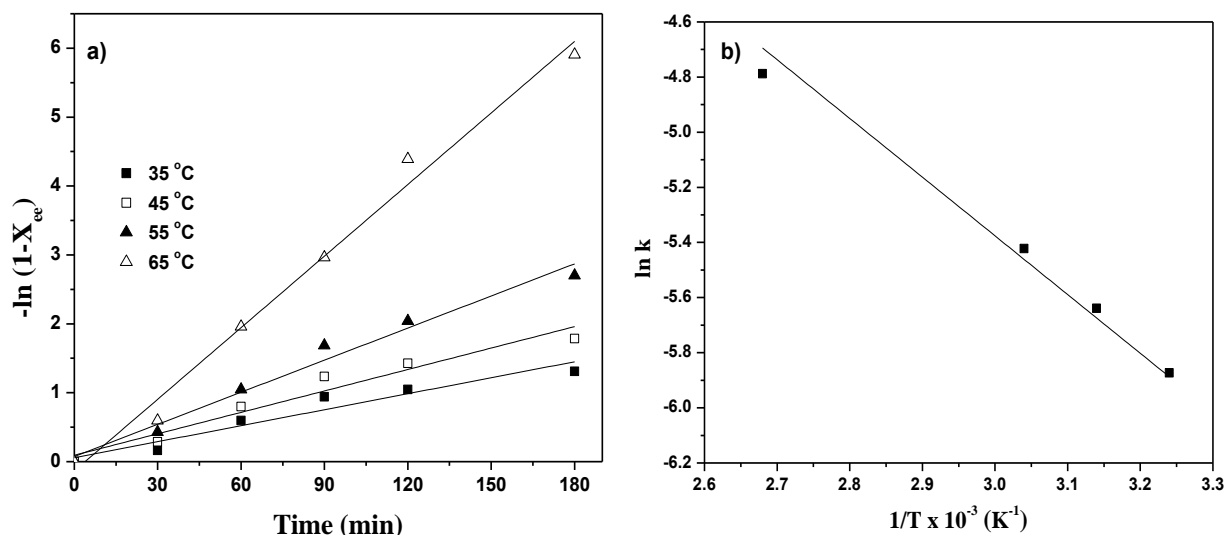


**Fig. 5.9.** Plots of a)  $-\ln(1-X_{ee})$  versus reaction time 't' at different temperatures (Reaction conditions: EtOH/oil molar ratio = 12:1; catalyst amount = 5 wt%) and b) The Arrhenius plot for the ethanolsis of WCO.

## 5.7 Proposed mechanism for transesterification

In literature, transesterification reaction catalyzed by heterogeneous catalyst was proposed to undergo in three steps (Fig. 5.10a). The first step involves the physisorption and/or chemisorption of triglyceride onto the catalyst surface. The carbonyl oxygen atom of triglyceride interacts with the acidic site ( $M^+$ ) of catalyst. As could be seen from Fig. 5.10b, the FTIR

spectrum of triglyceride adsorbed on catalyst surface show the carbonyl band at  $1649\text{ cm}^{-1}$ , in comparison to  $1742\text{ cm}^{-1}$  for free triglyceride molecule, to support the chemisorptions of triglyceride over catalyst surface. Similarly  $-\text{OH}$  group of  $\text{C}_2\text{H}_5\text{OH}$  also show strong interaction with catalyst surface as  $\text{C}-\text{O}$  band upon adsorption over catalyst shifts to  $1379\text{ cm}^{-1}$  from  $1455\text{ cm}^{-1}$  for neat ethanol.

The second step is the attack on electrophilic carbon by alkoxide from alcohol to form a tetrahedral intermediate. Finally in third step, this intermediate would cleave in fatty acid ester and diglyceride which would desorb from the catalyst surface (Yan et al., 2009). Diglyceride molecule will further undergo transesterification; yield two more FAEE and glycerol molecule.

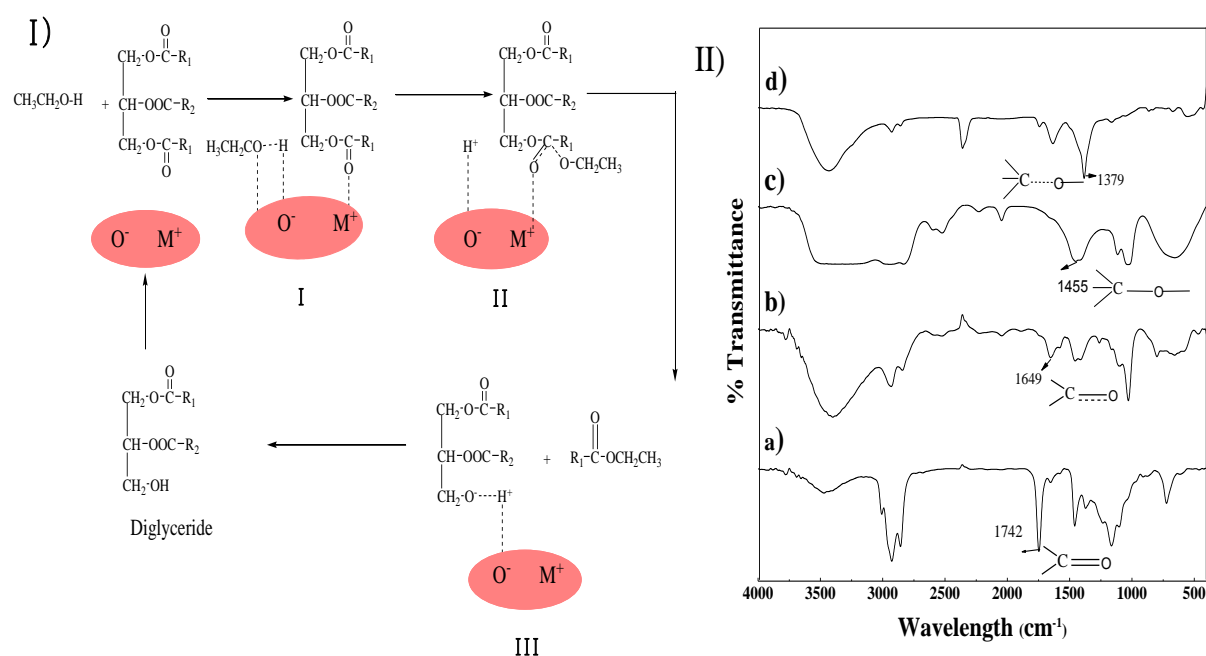


**Fig. 5.10. I) Proposed mechanism for Li/NiO transesterification of WCO and II) Comparison of FTIR spectra of a) neat WCO b) WCO absorbed over Li/NiO c) neat ethanol and d) ethanol adsorbed over Li/NiO.**

### 5. 8 Conclusions

Present work has demonstrated the preparation and application of Li/NiO as heterogeneous catalyst for the production of greener diesel fuel substitute, fatty acid ethyl esters, utilizing waste cottonseed oil as feedstock. The prepared 5-Li/NiO-600 catalyst required 3 h for the complete transesterification of WCO with ethanol (1:12 molar ratio) at 65 °C. The catalyst activity was not found to be affected adversely by the presence of high free fatty acid contents (up to 8.3 wt%) in vegetable oils. The catalyst has demonstrated reasonably good reusability as it remains active in seven catalytic runs. Leaching of the lithium from the catalyst was established as major reason for the loss of activity, although, leached metal ions was not found to show any homogeneous contribution.

### References

Achten, W. M. J.; Verchot, L.; Franken, Y. J.; Mathijs, E.; Singh, V. P.; Aerts R.; Muys, B.; Jatropha bio-diesel production and use. *Biomass Bioenerg.*; **2008**, 32, 1063-1084.

Babu, N. S.; Sree, R.; Prasad P. S. S.; Lingaiah, N.; Room-Temperature Transesterification of Edible and Nonedible Oils Using a Heterogeneous Strong Basic Mg/La Catalyst. *Energ. Fuel*; **2008**, 22, 1965–1971.

Balat, M.; Balat, H.; Progress in biodiesel processing. *Appl. Energ.*; **2010**, 87, 1815–1835.

Caballero, J. M. R.; Gonzalez, J. S.; Robles, J. M.; Tost, R. M.; Castillo, M. L. A.; Alonso, E. V.; Lopez, A. J.; Torres, P. M.; Calcium zincate derived heterogeneous catalyst for biodiesel production by ethanolysis, *Fuel*; **2013**, 105, 518-522.

Cernoch, M.; Hájek, M.; Skopal, F.; Ethanolysis of rapeseed oil – Distribution of ethyl esters, glycerides and glycerol between ester and glycerol phases. *Bioresour. Technol.*; **2010**, 101, 2071-2075.

Desmartin-Chomel, A.; Hamad, B.; Palomeque, J.; Essayem, N.; Bergeret, G.; Figueras, F.; Basic properties of MgLaO mixed oxides as determined by microcalorimetry and kinetics. *Catal. Today*; **2010**, 152, 110–114.

Garcia, C. M., Teixeira, S., Marciniuk, L. L., Schuchardt, U., Transesterification of soybean oil catalyzed by sulfated zirconia, *Bioresour. Technol.*, **2008**, 99, 6608-6613.

Ghesti, G. F.; de Macedo, J. L.; Resck, I. S.; Dias, J. A.; Dias, S. C. L.; FT-Raman spectroscopy quantification of biodiesel in a progressive soybean oil transesterification reaction and its correlation with <sup>1</sup>H NMR spectroscopy methods. *Energ. Fuel*; **2007**, 21, 2475–2480.

Hamad, B. , de Souza, R. O. L.; Sapaly, G.; Rocha, M. G. C.; de Oliveira, P. G. P.; Gonzalez, W. A.; Sales, E. A.; Essayem, N.; Transesterification of rapeseed oil with ethanol over heterogeneous heteropolyacids. *Catal. Commun.*; **2008**, 10, 92-97.

Kaur, N.; Ali, A.; Kinetics and reusability of Zr/CaO as heterogeneous catalyst for the ethanolysis and methanolysis of *Jatropha crucas* oil, *Fuel Process. Technol.*; **2014**, 119,173-184.

Knothe, G.; Determining the blend level of mixtures of biodiesel with conventional diesel fuel by fiber optic NIR spectroscopy and <sup>1</sup>H NMR spectroscopy. *J. Am. Oil Chem. Soc.*; **2011**, 78, 1025–1028.

Kwon, E. E.; Seo, J.; Yi, H.; Transforming animal fats into biodiesel using charcoal and CO<sub>2</sub>. *Green Chem.*; **2012**, 14, 1799–1804.

Lam, M. K.; Lee K. T.; Mohamed, A. R.; Homogeneous, heterogeneous and enzymatic catalysis for transesterification of high free fatty acid oil (waste cooking oil) to biodiesel: A review. *Biotechnol. Adv.*; **2010**, 28, 500-518.

Leung, D. Y. C.; Wu, X.; Leung, M. K. H.; A review on biodiesel production using catalyzed transesterification. *Appl. Energ.*; **2010**, 87, 1083-1095.

Li, E.; Xu, Z. P.; Rudolph, V.; MgCoAl–LDH derived heterogeneous catalysts for the ethanol transesterification of canola oil to biodiesel. *Appl. Catal. B: Environ.*; **2009**, 88, 42-49.

Morin, P.; Hamad, B.; Sapaly, G.; Rocha, M. G. C.; de Oliveira, P. G. P.; Gonzalez, W. A.; Sales, E. A.; Essayem, N.; Transesterification of rapeseed oil with ethanol: I. Catalysis with homogeneous Keggin heteropolyacids. *Appl. Catal. A: Gen.*; **2007**, 330, 69-76.

Omar, W. N. N. W.; Amin, N. A. S.; Biodiesel production from waste cooking oil over alkaline modified zirconia catalyst. *Fuel Process Technol.*; **2011**, 92, 2397–2405.

Qadri, S. B.; Skelton, E. F.; Hsu, D.; Dinsmore, A. D.; Yang, J.; Gray, H. F.; Ratna, B. R.; Size-induced transition-temperature reduction in nanoparticles of ZnS. *Phys. Rev. B*; **1999**, 60, 9191–9193.

Rubio-Caballero, J. M.; Santamaria-Gonzalez, J.; Merida-Robles, J.; Moreno-Tost, R.; Alonso-Castillo, M. L.; Vereda-Alonso, E.; Jimenez-Lopez A.; Maireles-Torre, P.; Calcium zincate derived heterogeneous catalyst for biodiesel production by ethanolysis. *Fuel*; **2013**, 105, 518–522.

Serio, M. D.; Tesser, R.; Pengmei, L.; Santacesaria, E.; Heterogeneous Catalysts for Biodiesel Production. *Energ. Fuel*; **2008**, 22, 207–217.

Singh, A. K.; Fernando, S. D.; Preparation and Reaction Kinetics Studies of Na-based Mixed Metal Oxide for Transesterification. *Energ. Fuel*; **2009**, 23, 5160–5164.

Silva, N. L.; Batistella, C. B.; Filho, R. M.; Maciel, M. R. W.; Biodiesel Production from Castor Oil: Optimization of Alkaline Ethanolysis. *Energ. Fuel*; **2009**, 23, 5636–5642.

Sivasamy, A.; Cheah, K. Y.; Fornasiero, P.; Kemausuor, F.; Zinoviev, S.; Miertus, S.; Catalytic applications in the production of biodiesel from vegetable oils. *Chem. Sus. Chem.*; **2009**, 2, 278–300.

Soldi, R. A.; Oliveira, A. R. S.; Ramos, L. P.; César-Oliveira, M. A. F.; Soybean oil and beef tallow alcoholysis by acid heterogeneous catalysis. *Appl. Catal. A: Gen.*; **2009**, 361, 42–48.

Sree, R.; Babu, N. S.; Prasad, P. S. S.; Lingaiah, N.; Transesterification of edible and non-edible oils over basic solid Mg/Zr catalysts. *Fuel Process. Technol.*; **2009**, 90, 152–157.

Stamenkovic, O. S.; Velickovic, A. V.; Veljkovic, V. B.; The production of biodiesel from vegetable oils by ethanolysis: Current state and perspectives, *Fuel*; **2011**, 90, 3141–3155.

Tanaka, S.; Taniguchi, M.; Tanigawa, H.; XPS and UPS studies on electronic structure of Li<sub>2</sub>O. *J. Nucl. Mater.*; **2000**, 283-287, 1405-1408.

Wei-Luen, J.; Yang-Ming, L.; Weng-Sing H.; Wei-Chien, C.; Electrical properties of Li-doped NiO films. *J. Eur. Ceram. Soc.*; **2010**, 30, 503–508.

Yan, S.; Kim, M.; Salley, S. O.; Ng, K. Y. S.; Oil transesterification over calcium oxides modified with lanthanum. *Appl. Catal. A: Gen.*; **2009**, 360, 163–170.

---

**Tungsten Supported Ti/SiO<sub>2</sub> Nanoflowers: Mesoporous Solid Catalyst for Biodiesel Production**

---

|            | <b>Contents</b>   | <b>Page</b> |
|------------|---|-------------|
| <b>6.1</b> | <b>Introduction</b>   | 104         |
| <b>6.2</b> | <b>Experimental section</b>   | 105         |
|            | 6.2.1 Catalyst preparation  | 105         |
|            | 6.2.2 Transesterification reaction                                  | 105         |
| <b>6.3</b> | <b>Results and discussion</b>                                       | 106         |
|            | 6.3.1 Catalyst characterization                                     | 106         |
|            | 6.3.1.1 Powder X-ray diffraction study                              | 106         |
|            | 6.3.1.2 BET surface area study                                      | 107         |
|            | 6.3.1.3 FESEM analysis  | 109         |
|            | 6.3.1.4 HRTEM analysis  | 110         |
|            | 6.3.1.5 XPS study   | 111         |
|            | 6.3.1.6 TPD analysis  | 112         |
|            | 6.3.2 Catalytic activity  | 113         |
| <b>6.4</b> | <b>Effect of FFA on catalyst activity</b>                           | 116         |
| <b>6.5</b> | <b>Evaluation of the recyclability and homogeneous contribution</b> | 117         |
| <b>6.6</b> | <b>Kinetic study</b>  | 120         |
| <b>6.7</b> | <b>Conclusions</b>  | 121         |
|            | <b>References</b>   | 122         |

---

### **Abstract**

Present chapter demonstrated a convenient method for the synthesis of flower shaped tungsten supported  $\text{TiO}_2/\text{SiO}_2$  by sol-gel method without using any template. The prepared  $\text{W}/\text{Ti}/\text{SiO}_2$  catalyst has been employed as heterogeneous catalyst for the transesterification of waste cotton seed oil with methanol. The structure of the catalyst was established by powder X-ray diffraction and surface morphology and particle size by field emission scanning and high resolution transmission electron microscopy studies. The oxidation state of tungsten by X-ray photoelectron spectroscopy was found to be +6. Acidic strengths of the catalysts were measured by temperature programmed desorption study and found to be maximum in case of catalyst prepared with 20 wt% tungsten in  $\text{TiO}_2/\text{SiO}_2$  at 700 °C calcination temperature. The same catalyst being highest in catalytic activity among the prepared catalysts has been selected to study the transesterification reaction of waste cotton seed oil with methanol. The variables for the methanolysis were; percentage of tungsten in  $\text{TiO}_2/\text{SiO}_2$ , catalyst concentration, reaction temperature and methanol to oil molar ratio. Under optimized reaction condition of 5wt% of 20- $\text{W}/\text{TiO}_2/\text{SiO}_2$ -700 catalyst, 30:1 methanol to oil molar ratio and at 65 °C reaction temperature, > 98% fatty acid ethyl ester yield was obtained in 4 h. The catalyst was also found to be stable, as < 5 ppm metal concentration was observed in FAMES and reused successfully in four catalytic cycles without any significant loss in activity.

---

## 6.1 Introduction

Mesoporous based material due to the inert nature and tunable surface properties have been used as a versatile support material for the immobilization of active species. Recent studies have found mesoporous silica, such as tin-oxide-modified mesoporous SBA-15 (Martin et al., 2010), titanium-grafted mesoporous silica (Gao et al., 1999), and magnesium supported MCM-41 (Dai et al., 2014) effective for catalyzing transesterification reactions using a variety of triglycerides. However, for complete conversion of vegetable oils into fatty acid esters, most of the mesoporous based catalysts require high temperature and pressure conditions along with longer reaction duration. From economical point of view such reaction conditions are not very favorable as they could increase the biodiesel product cost to significant extent (Kiss et al., 2010). In literature molybdenum and tungsten based solid acid catalysts are extensively investigated for many reactions *viz.* oxidation, amidation, esterification and transesterification (Hattori et al., 1978; Xia et al., 2000; Davis, 1978; Furuta et al., 2004). Among tungsten catalysts, sodium tungstate, tungstate supported mesoporous silica/alumina,  $\text{WO}_3/\text{ZrO}_2$  and hetero-polyacid of tungsten are extensively studied for the transesterification of vegetable oils (Kiss et al., 2010). Furuta et al., (2004) have reported transesterification of soybean oil at 250 °C to obtain > 90% yield in presence of tungstated  $\text{Zr}/\text{Al}_2\text{O}_3$  catalyst. Ramu et al., (2004) has also investigated the same mesoporous catalyst for the esterification of palmitic acid with methanol and found maximum activity upon activation at 400-500 °C. Shao et al., (2013) reported that sulfated mixed oxides ( $\text{SO}_4^{2-}/\text{TiO}_2\text{-SiO}_2$ ), gave 90% yield upon transesterification of waste cooking oil at 200 °C in 6 h.

Mesoporous silica based tungstate catalysts have been reported to show poor reactivity; stability and reusability in comparison to the sodium tungstate for the transesterification of soybean oil (Nakagaki et al., 2008). On the other hand major problem with the use of pure sodium tungstate is its higher mass (~ 10 wt%) in every reaction cycles (Santos et al., 2011). In order to prepare tungsten based effective solid catalyst, in present chapter a mixed oxide of titanium and silicon ( $\text{Ti}/\text{SiO}_2$ ) has been used as support for the immobilization of tungstate species. The prepared flower shaped tungsten supported  $\text{Ti}/\text{SiO}_2$  was found to be an efficient heterogeneous and reusable catalyst for biodiesel production from waste cottonseed oil.

---

## 6.2 Experimental section

### 6.2.1 Catalyst preparation

Flower shaped tungsten impregnated Ti/SiO<sub>2</sub> catalyst was prepared in a two step method involving (i) preparation of Ti/SiO<sub>2</sub> as catalyst support and followed by (ii) impregnation of tungsten over Ti/SiO<sub>2</sub> support

#### *Step I: Preparation of Ti/SiO<sub>2</sub>*

Catalyst support, Ti/SiO<sub>2</sub>, was prepared by the chemical method in a 250 mL round bottom flask equipped with an oil bath, magnetic stirrer, and water cooled condenser. Flask was charged with 20 ml of titanium isopropoxide and 10 ml of isopropanol and stirred for 20 min at room temperature (38 °C) to obtain a transparent sol. To this, 80 ml distilled water was added and pH 2 was maintained with the help of 0.1 M HCl. The resulted mixture was stirred at 700 rpm for 5 h followed by the addition of 3 g silica gel. The pH at this stage was raised to 3 by adding 0.1 M NaOH and suspension was stirred for another 2 h, followed by successive centrifugation and washing to obtain the pH neutral solid. The obtained solid was initially dried at 80 °C for 8 h and finally calcined at 550 °C for 3 h to obtain Ti/SiO<sub>2</sub>.

#### *Step II: Tungsten impregnated Ti/SiO<sub>2</sub> supported catalyst*

A series of tungsten impregnated Ti/SiO<sub>2</sub> (W/Ti/SiO<sub>2</sub>) catalyst was prepared by wet chemical method by varying the amount of tungsten in the range of 5-25 wt%. In a typical preparation 10 g of prepared Ti/SiO<sub>2</sub> was suspended in 40 mL of deionized water, and to this 10 mL aqueous solution of Na<sub>2</sub>WO<sub>4</sub>·2H<sub>2</sub>O of desired concentration was added to obtain 5-25 wt% tungsten supported Ti/SiO<sub>2</sub>. The resulted slurry was stirred for 5 h at room temperature (38 °C), dried at 120 °C for 24 h and finally calcined at 700 °C for 3 h. The prepared catalysts were designated as x-W/Ti/SiO<sub>2</sub>, where x is the wt% of tungsten.

### 6.2.2 Transesterification reaction

The transesterification reactions were performed in a 100 mL, two-neck, round bottom flask equipped with a water-cooled reflux condenser, oil bath, and magnetic stirrer. In a typical transesterification reaction, 10 g of vegetable oil was mixed with desired molar concentrations of

---

methanol and catalyst and stirred at a desired temperature to accomplish the complete conversion (> 98%) of feedstock into corresponding FAMEs.

## 6.3 Results and discussion

### 6.3.1 Catalyst characterization

#### 6.3.1.1 Powder X-ray diffraction study

The powder XRD patterns of Ti/SiO<sub>2</sub>, WO<sub>3</sub> and 5-25 wt% W impregnated Ti/SiO<sub>2</sub> are compared in Fig 6.1. The diffraction pattern of Ti/SiO<sub>2</sub> shows a broad peak at 25.7°, to support the existence of long range order in Ti/SiO<sub>2</sub> structure. The diffraction patterns of tungsten impregnated (up to 15 wt%) Ti/SiO<sub>2</sub> mainly shows the diffraction peaks corresponding to the anatase-TiO<sub>2</sub> phase. Absence of diffraction patterns corresponding to WO<sub>3</sub> supports the high degree of dispersion of tungsten over Ti/SiO<sub>2</sub>. On increasing tungsten concentration > 20 wt%, formation of WO<sub>3</sub> in monoclinic phase over Ti/SiO<sub>2</sub> support was observed as supported by the appearance of diffraction peaks at  $2\theta = 22.90^\circ, 23.71^\circ, 24.13^\circ, 34.21^\circ, 41.69^\circ, 49.91^\circ$  and  $50.55^\circ$  (ICDD-01-075-2072). The peaks observed at  $37.10^\circ, 38.68^\circ$  and  $47.3^\circ$  indicate the presence of sodium titanium silicate (Na<sub>2</sub>TiSi<sub>4</sub>O<sub>11</sub>) in tetragonal form (ICDD-01-011-0478) and peaks at  $25.2^\circ, 37.9^\circ$  and  $49.9^\circ$  support the presence of TiO<sub>2</sub> in anatase form in minor amount in 20-W/Ti/SiO<sub>2</sub>. Crystallite size of the catalyst particles were determined by the Debye–Scherer method (Qadri et al., 1999) and found to be ~ 50 nm for 20-W/Ti/SiO<sub>2</sub>.

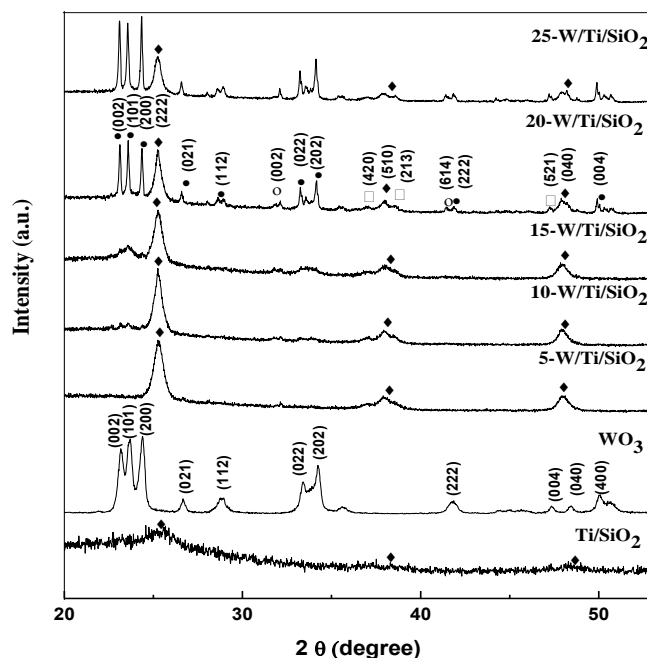


**Fig. 6.1.** Comparison of the powder XRD patterns of  $\text{Ti/SiO}_2$ ,  $\text{WO}_3$  and 5-25 wt% W impregnated  $\text{Ti/SiO}_2$ -700 (○ =  $\text{SiWO}_2$ ; ● =  $\text{WO}_3$ ; ◆ =  $\text{TiO}_2$  (anatase phase); □ =  $\text{Na}_2\text{TiSi}_4\text{O}_{11}$ ).

### 6.3.1.2 BET surface area study

During the catalyst preparation, pH of the reaction mixture was maintained in acidic range. At acidic pH, the isopolytungstates ( $[\text{H}_x\text{W}_q\text{O}_y]^{n-}$ ) formation has been reported in literature (Santos et al., 2011) according to the following equation 1:



These large sized isopolytungstate ions may occupy the pores of the catalyst support to result the pore expansion. As evident from Table 6.1, the pore size of  $\text{W/Ti/SiO}_2$  was found to be larger than the pore size of bare  $\text{Ti/SiO}_2$ , to support the occupancy of tungstate ions inside the support. The surface area as well as pore volume, upon tungsten impregnation, was found to decrease due to the pore plugging of  $\text{Ti/SiO}_2$  by isopolyanions.

**Table 6.1. Comparison of BET surface area, pore volume, pore size and crystallite size of 0-25 wt% tungsten impregnated Ti/SiO<sub>2</sub>.**

| Catalyst                      | BET surface area (m <sup>2</sup> g <sup>-1</sup> ) | Pore volume (cm <sup>3</sup> g <sup>-1</sup> ) | Pore size (nm) | Crystallite size at (222) plane (nm) |
|-------------------------------|--|--|----------------|--------------------------------------|
| Ti/SiO <sub>2</sub> -700      | 180.3  | 0.61   | 15.39          | 55.2                                 |
| 5-W/Ti/SiO <sub>2</sub> -700  | 110.9  | 0.52   | 34.82          | 52.1                                 |
| 10-W/Ti/SiO <sub>2</sub> -700 | 90.0   | 0.43   | 30.40          | 49.9                                 |
| 15-W/Ti/SiO <sub>2</sub> -700 | 85.1   | 0.40   | 34.72          | 50.1                                 |
| 20-W/Ti/SiO <sub>2</sub> -700 | 77.64  | 0.34   | 30.73          | 50.0                                 |
| 25-W/Ti/SiO <sub>2</sub> -700 | 70.12  | 0.10   | 30.23          | 51.2                                 |

The nitrogen adsorption-desorption isotherms (Fig. 6.2a) indicate a type IV isotherm profile for Ti/SiO<sub>2</sub> and W/Ti/SiO<sub>2</sub> with a clear hysteresis at a relative pressure of about 0.75-1.0; characteristic to mesoporous materials (Dacquin et al., 2012). The Barrett-Joyner-Halenda (BJH) method was applied to calculate the pore size distribution. The support material Ti/SiO<sub>2</sub> shows pores of 3.4 nm diameter with narrow pore size distribution and 15 nm diameter with relatively broad pore size distribution (Fig. 6.2b). Tungsten impregnation over this support leads to increase the pore size diameter in the range of 30-35 nm. This increase in pore diameter further supports the Ti/SiO<sub>2</sub> pore opening due to the tungsten impregnation.

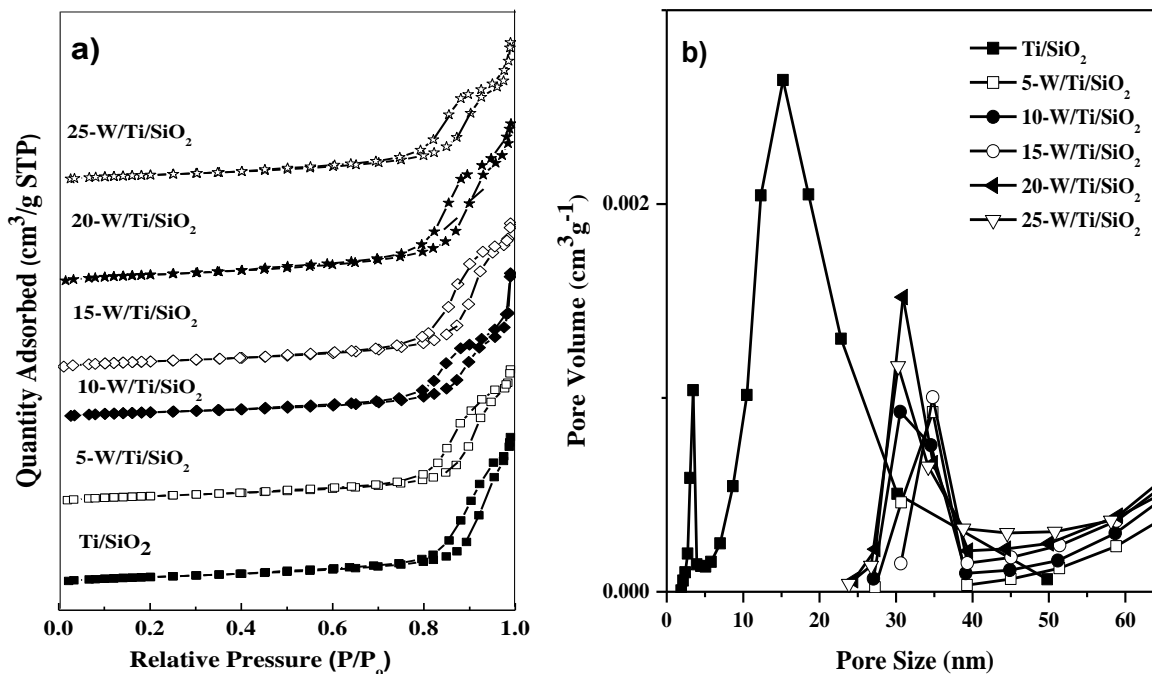


**Fig. 6.2.** a)  $N_2$  adsorption-desorption isotherms and b) pore size distribution curve of 0-25 wt% W impregnated  $Ti/SiO_2$ -700.

### 6.3.1.3 FESEM analysis

The FESEM images of 20-W/ $Ti/SiO_2$  calcined in the temperature range of 500-700 °C are compared in Fig. 6.3. At 500 °C calcination temperature, W/ $Ti/SiO_2$  flakes have formed which start to aggregate as flowered shaped particles at 600 °C and complete flower formation took place at 700 °C calcination temperature. The pH of the preparation media was found to have the significant role on the formation of flower shaped particles, as deviation from pH 3 leads to the formation of particles of irregular geometries. The petals of these flowers appear to have pointed ends with an average length of ~ 226 nm and width of 80 nm. As could be seen from Fig. 6.3d, EDS analysis support the presence of ~ 22 wt% tungsten in 20-W/ $Ti/SiO_2$  particles.

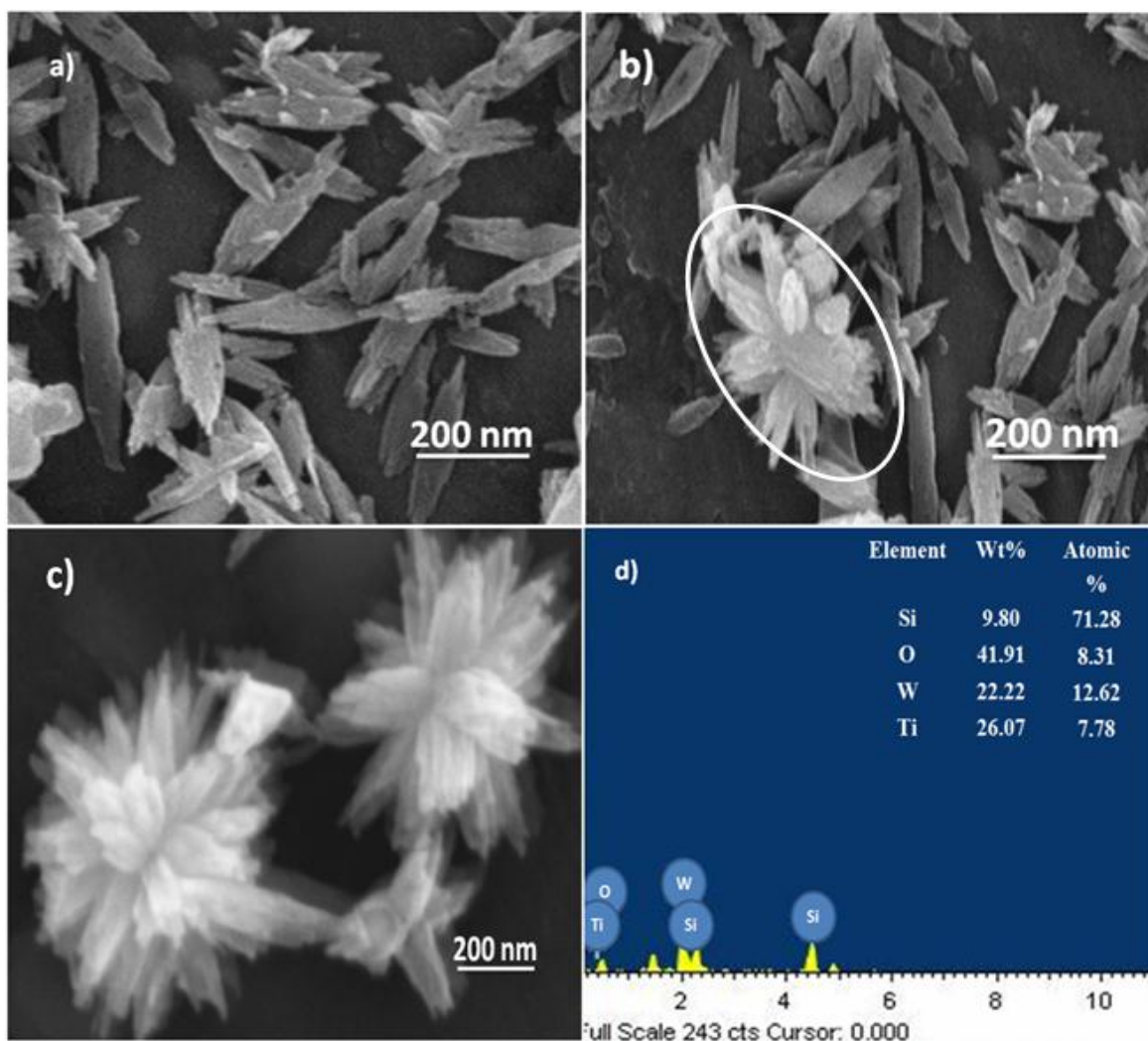


**Fig. 6.3.** FESEM images of 20-W/Ti/SiO<sub>2</sub> prepared at a) 500 °C b) 600 °C and c) 700 °C calcination temperature, and d) EDS pattern of 20-W/Ti/SiO<sub>2</sub>.

#### 6.3.1.4 HRTEM analysis

To further confirm the mesoporous nature of nanoflowers, HRTEM study was performed. The HRTEM image shows that each petal consists of thin flake like structures with few dark regions to indicate the presence of tungsten (Fig. 6.4a and 6.4b). At high magnification, the lattice fringes with a spacing of 0.2 nm corresponding to the (222) diffraction plane was observed (Fig. 6.4c). The average size of tungsten particles was found to be ~ 2 nm. The selected area electron diffraction (SAED) pattern shown in Fig. 6.4d presents four fused rings indexed as (110), (200),

(211) and (202) planes, suggesting the amorphous anisotropy of the nanoflower petals produced by self-assembly of short length nanorods.

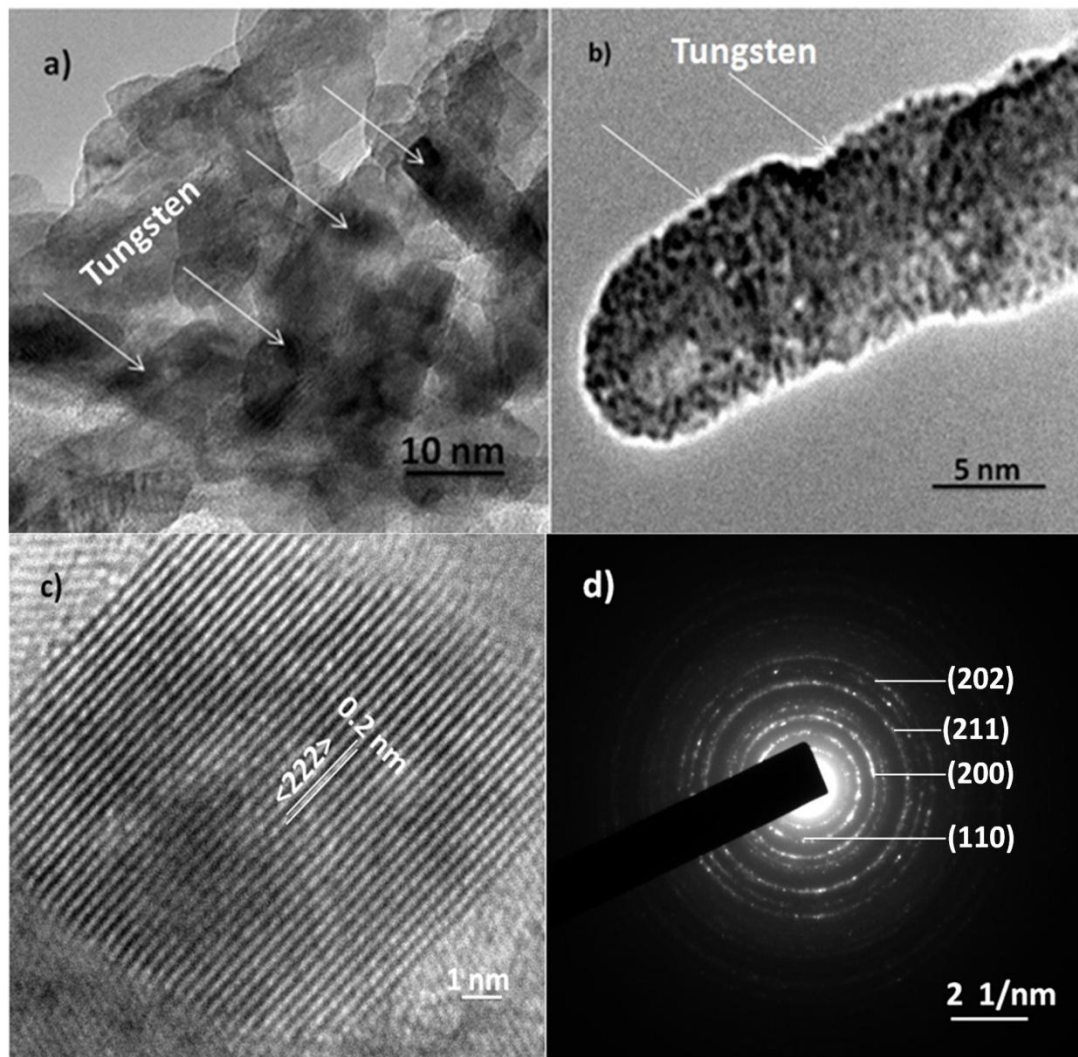


**Fig. 6.4.** HRTEM Images of 20-W/Ti/SiO<sub>2</sub> a-b) Dark spots signifies the presence of tungsten on the support c) lattice fringes of mesoporous petals and d) SAED pattern for prepared catalyst.

### 6.3.1.5 XPS study

The oxidation state of the various elements present in W/Ti/SiO<sub>2</sub> catalyst was determined by XPS spectroscopy. The peak obtained due to W 4f can be deconvoluted in two peaks at 36.3 and 38.3 eV due to the presence of W 4f<sub>7/2</sub> and W 4f<sub>5/2</sub>, states respectively (Fig. 6.5a), which are a good agreement with the presence of W(VI) state (Li et al., 2013). The spectrum obtained for

O 1s consist of two peaks located at 532.7 eV due to the presence of Si-O-Si and W-O-W bonding and at 533.9 eV corresponding to the H<sub>2</sub>O adsorbed on the silica surface (Fig. 6.5b). Fig. 6.5c shows the XPS spectrum of Ti 2p and peaks located at 458.5 and 464.4 eV could be attributed to the spin-orbit splitting of Ti 2p<sub>3/2</sub> and Ti 2p<sub>1/2</sub> states of titanium in +4 oxidation state (Cheng et al., 2005). The binding energy for Si 2p was found to be 104.1 eV (Fig. 6.5d), due to the presence of SiOH<sub>2</sub><sup>+</sup> species on the catalysts surface (Liu et al., 2012).

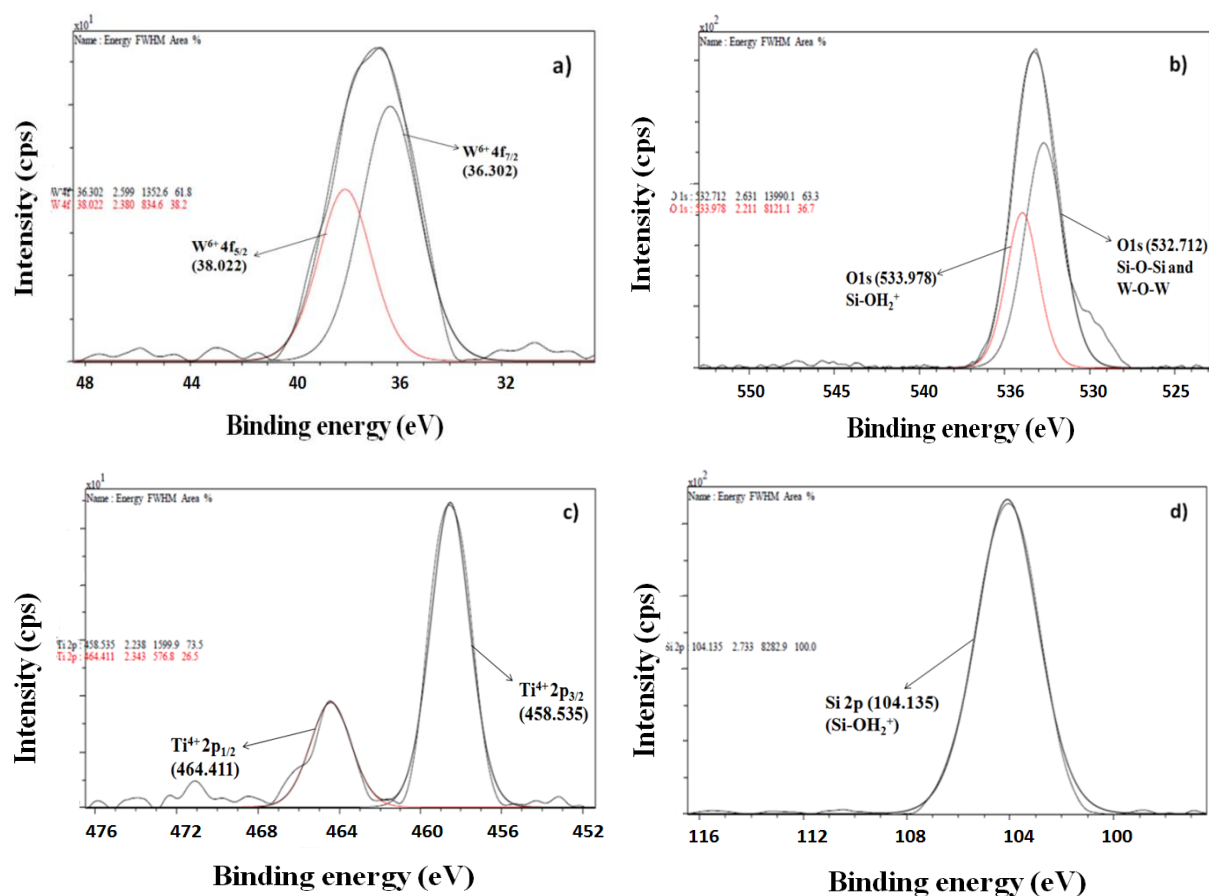


Fig. 6.5. XPS spectra of a) tungsten b) oxygen c) titanium and d) silicon in W/Ti/SiO<sub>2</sub> Catalyst.

### 6.3.1.6 TPD analysis

Number and strength of surface acidic sites have been reported to affect the transesterification activity of the solid catalysts (Kiss et al., 2010). To quantify the surface acid sites in prepared catalysts, the NH<sub>3</sub> TPD was performed. According to ammonia desorption temperature (Td)

acidic sites could be classified as weak (< 200 °C), medium (200-600 °C), and strong (> 600 °C) sites (Wang et al., 2011). The prepared Ti/SiO<sub>2</sub> demonstrated four desorption peaks at ~ 160 °C, 470 °C and 800 °C, to support the presence of weak, medium and strong acidic sites, respectively. As could be seen from Table 6.2, an increase in tungsten amount over Ti/SiO<sub>2</sub> was found to enhance the concentration as well as strength of strong acidic sites and at 25 wt% W impregnation, maximum amount of acidic sites was observed.

**Table 6.2. NH<sub>3</sub>-TPD measurements of 0-25 wt% tungsten impregnated Ti/SiO<sub>2</sub> catalysts.**

| Catalyst                 | Weak                |                                   | Medium              |                                   | Strong              |                                   | Total NH <sub>3</sub> (mmol/g) |
|--------------------------|---------------------|-----------------------------------|---------------------|-----------------------------------|---------------------|-----------------------------------|--------------------------------|
|                          | T <sub>1</sub> (°C) | NH <sub>3</sub> desorbed (mmol/g) | T <sub>2</sub> (°C) | NH <sub>3</sub> desorbed (mmol/g) | T <sub>3</sub> (°C) | NH <sub>3</sub> desorbed (mmol/g) |                                |
| Ti/SiO <sub>2</sub>      | 167.6               | 0.23                              | 489.4               | 0.07                              | 804.1               | 0.62                              | 0.92                           |
| 5-W/Ti/SiO <sub>2</sub>  | 168.9               | 0.19                              | 464.7               | 0.05                              | 784.3               | 0.63                              | 0.87                           |
| 10-W/Ti/SiO <sub>2</sub> | 178.7               | 0.20                              | 466.3               | 0.04                              | 773.8               | 1.15                              | 1.39                           |
| 15-W/Ti/SiO <sub>2</sub> | 236.2               | 0.16                              | 458.0               | 0.04                              | 803.8               | 1.24                              | 1.44                           |
| 20-W/Ti/SiO <sub>2</sub> | 184.2               | 0.15                              | 454.2               | 0.08                              | 801.8               | 1.26                              | 1.49                           |
| 25-W/Ti/SiO <sub>2</sub> | 272.2               | 0.16                              | 481.8               | 0.10                              | 789.8               | 1.26                              | 1.52                           |

### 6.3.2 Catalytic activity

The prepared *x*-W/Ti/SiO<sub>2</sub> has been employed for the methanolysis of waste cottonseed oil. To optimize the reaction conditions for the favorable catalytic activity, transesterification reactions have been carried out at 600 rpm by varying one parameter at a time out of the following: (i) impregnated tungsten ion concentration, (ii) catalyst concentration, (iii) reaction temperature, and (iv) methanol to oil molar ratio. Apart from this study, the FFA tolerance and reusability of the catalyst have also been studied under optimized reaction conditions.

In order to study the effect of tungsten concentration on catalytic activity, a series of W/Ti/SiO<sub>2</sub> was prepared by varying the tungsten concentration in the range of 5-25 wt%. Transesterification reaction was performed at 65 °C in presence of 5 wt% catalyst (oil/catalyst) and employing a 30:1 methanol to oil molar ratio. The complete conversion (> 98%) of WCO was achieved in 4 h with the catalyst having 20wt% tungsten in Ti/SiO<sub>2</sub>. The increase in reaction

rate on increasing the tungsten concentration in Ti/SiO<sub>2</sub> could be due to the increase in acidic sites (shown in Table 6.2) on the catalyst surface. A further increase in tungsten concentration (from 20 to 25 wt %) was not found to reduce the reaction time significantly as shown in Fig.6.6a. Hence, 20-W/Ti/SiO<sub>2</sub>-700 catalyst was employed to optimize other parameters to achieve the minimum time for the complete methanolysis of WCO. The catalytic activity of tungsten supported Ti/SiO<sub>2</sub> catalysts directly related to the presence of tungsten species, which are acting as Lewis sites and may interact with triglyceride molecule through carbonyl group.

In order to make the process economically viable and greener, it is preferable to use the minimum possible amount of catalyst. To determine the optimum catalyst concentration, transesterification reactions were performed at 65 °C, employing a 30:1 methanol to oil molar ratio in presence of 20-W/Ti/SiO<sub>2</sub> catalyst by varying its concentration from 1 to 6 wt% (catalyst/oil). Time required for the complete conversion of WCO into FAMEs was found to reduce on increasing the catalyst amount from 1 to 5 wt%. Further increase in catalyst concentration (5 to 6 wt%) doesn't reduce the reaction time significantly as shown in Fig. 6.6b. Hence, transesterification reactions were studied with 5 wt% catalyst concentration (oil/catalyst) for optimizing other reaction parameters.

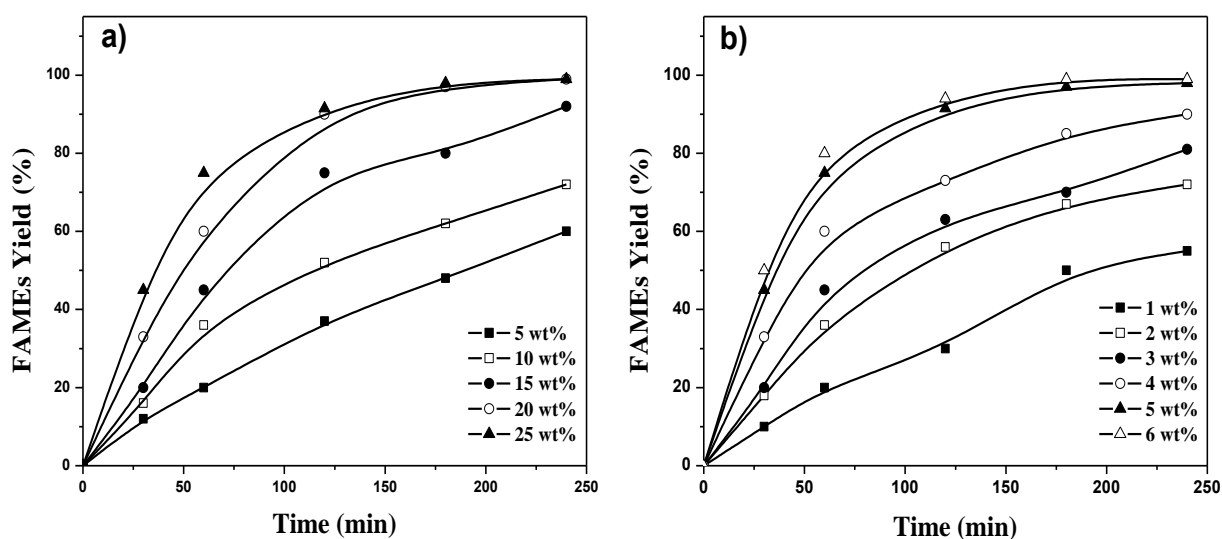


**Fig. 6.6.** Effect of a) tungsten concentration in Ti/SiO<sub>2</sub> and b) catalyst concentration on methanolysis of WCO.

Methanolysis reactions with WCO were performed in the temperature range of 35-75 °C to determine the reaction temperature for the optimum catalytic activity. Heterogeneous catalysts due to the phase difference usually demand high temperature and pressure to catalyze the reaction to vital extent. Although, W/Ti/SiO<sub>2</sub> was able to complete the transesterification of WCO even at room temperature (35 °C), but required longer reaction duration (48 h). The time required for the complete transesterification decreases from 48 to 4 h on increasing the temperature from 35 to 65 °C. A further increase in reaction temperature was not found to reduce the reaction duration to significant extent as shown in Fig. 6.7a, and hence, methanolysis of vegetable oils were performed at 65 °C.

Transesterification, being a reversible reaction, is usually performed with excess amount of methanol to shifts the equilibrium in forward direction and to achieve the maximum methyl ester yield. The effect of alcohol/oil molar ratio on transesterification reaction is one of the important parameter which affects the ester yield as well as cost of biodiesel production. Further, in case of heterogeneous catalysts, excess of alcohol not only to shift the equilibrium towards the forward direction but also regenerate the acidic site by removing the product molecule from the catalyst surface.

To determine the optimum methanol/oil molar ratio for the better catalytic activity, a series of reactions were performed in presence of 5 wt% 20-W/Ti/SiO<sub>2</sub> catalyst, at 65 °C employing 10:1 to 35:1 methanol to oil molar ratio. The maximum rate of transesterification reaction was observed with 30:1 molar ratio of methanol to oil as shown in Fig. 6.7b.

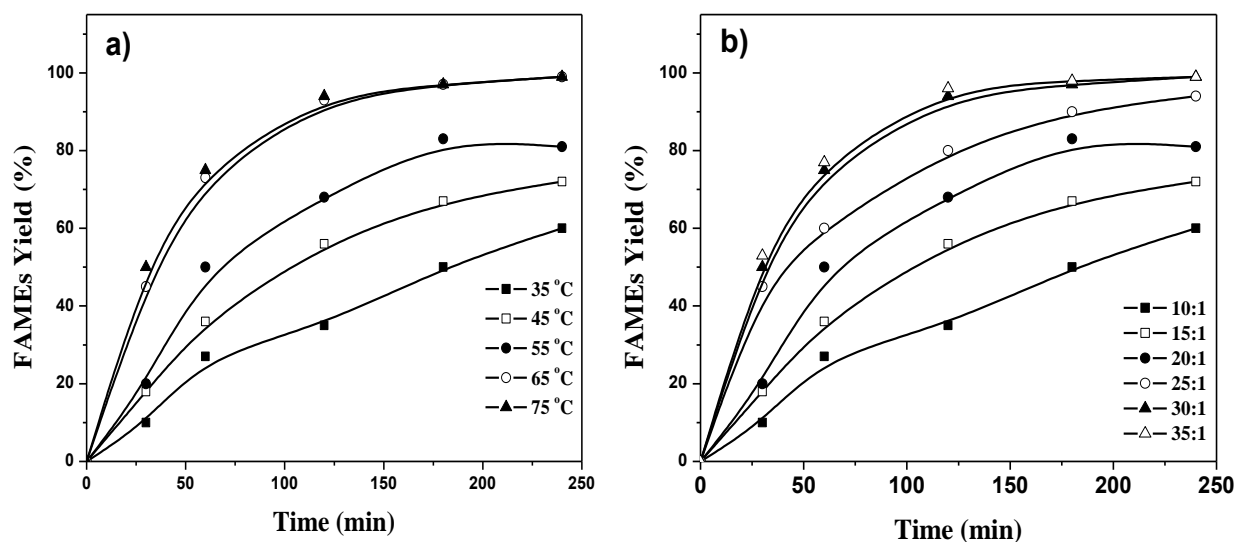


**Fig. 6.7. Effect of a) reaction temperature and b) methanol/oil molar ratio on methanolysis of WCO.**

Thus, a 5 wt% of 20-W/Ti/SiO<sub>2</sub> catalyst with respect to oil, 30:1 methanol to oil molar ratio and reaction temperature of 65 °C, were the optimized reaction conditions to achieve the complete transesterification (> 98 % FAMES yield) of WCO in 4 h.

#### 6.4 Effect of FFA on catalyst activity

The methanolysis of WCO (with 2.8 wt% FFA) was also performed in presence of homogeneous catalyst (NaOH). However, reaction catalyzed by NaOH catalyst didn't yield biodiesel due to the deactivation of the catalyst *via* saponification reaction. On the other hand, 20-W/Ti/SiO<sub>2</sub> leads to the completion of WCO transesterification, and hence, prepared catalyst is clearly advantageous over the homogeneous one.

In order to find out the maximum FFA tolerance of the catalyst, methanolysis of WCO was performed in presence of palmitic acid (up to 4 wt%). Under optimized reaction conditions, the catalyst 20-W/Ti/SiO<sub>2</sub> was found to resist the presence of up to 4 wt% added FFA and yielded complete transesterification (> 98%) of WCO (as shown in Fig. 6.8). The high FFA tolerance of 20-W/Ti/SiO<sub>2</sub> catalyst could be attributed to the immobilization of the active sites within the solid catalyst, which did not react with FFA present in WCO and hence, saponification is prevented.

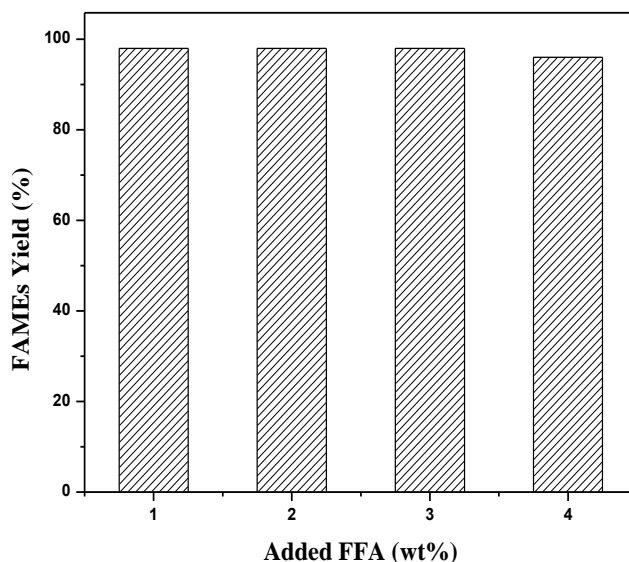


**Fig. 6.8. Effect of added FFA (Palmitic acid) on W/Ti/SiO<sub>2</sub> catalyzed methanolysis of WCO (Reaction conditions: MeOH/oil molar ratio = 30:1; Catalyst amount = 5 wt% of oil; Temperature = 65 °C).**

### 6.5 Evaluation of the recyclability and homogeneous contribution

Reusability is an attractive feature of the heterogeneous catalysts as it could make the post reaction processing easier and reduce the effective production cost of a molecule. To reveal the reusability of 20-W/Ti/SiO<sub>2</sub> catalyst, the methanolysis of WCO was performed under optimized reaction conditions and upon completion of reaction the catalyst was recovered by filtration, washed with hexane and dried initially at 140 °C and finally calcined at 700 °C. The recovered catalyst was reused in five successive runs, under the same experimental condition and regeneration method. The catalyst was able to complete (> 98 %) the transesterification of oil in 4 successive cycles as shown in Fig. 6.9. However, in fifth catalytic run, ~ 50% conversion was achieved.

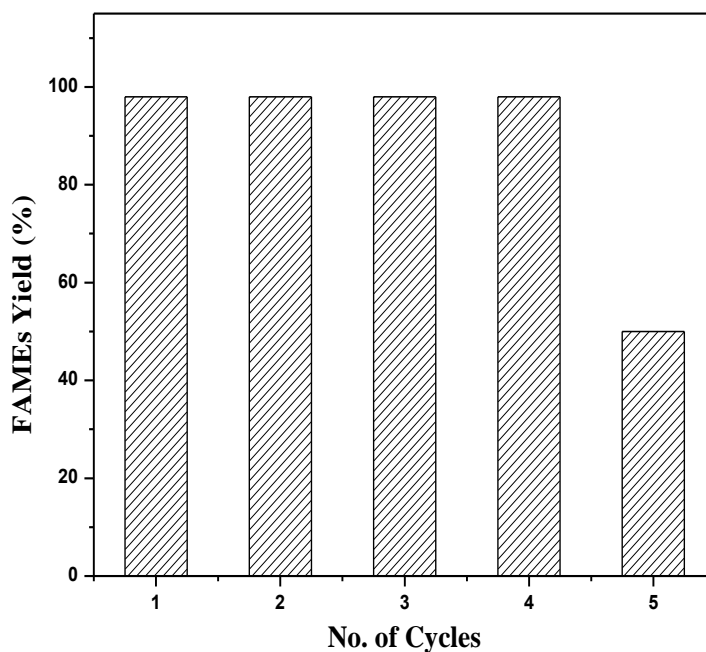


**Fig. 6.9. Reusability of 20-W/Ti/SiO<sub>2</sub> (Reaction conditions: MeOH/oil molar ratio = 30:1; Catalyst amount = 5 wt% of oil; Temperature = 65 °C).**

This gradual loss in catalytic activity, after every successive cycle, could be due to the partial leaching of the active species from the catalyst support. The leached tungstate species from the catalyst could catalyze the transesterification reaction similar to the homogeneous catalyst. In order to quantify the homogeneous contribution, the catalyst 20-W/Ti/SiO<sub>2</sub> (500 mg), was refluxed with methanol for 4 h at 65 °C. After the specific time the catalyst was filtered out, and methanol thus obtained has been employed for the transesterification of WCO (MeOH/oil = 30:1) at 65 °C for 4 h. Under these experimental conditions negligible conversion of the WCO into FAMES was achieved to rule out the possibility of homogeneous contribution in W/Ti/SiO<sub>2</sub> activity.

In order to quantify the leached metal, the concentration of W, Ti and Si was analyzed in FAMES, by ICP-OES, after every cycle. As could be seen from Table 6.3, the maximum metal leaching was observed after 4<sup>th</sup> cycle, although overall metal leaching was not found very high.

**Table 6.3. Metal ion concentration (ppm) in FAMES after every catalytic cycle.**

| Catalytic cycle | Metal concentration (ppm) |     |     |
|-----------------|---------------------------|-----|-----|
|                 | W                         | Ti  | Si  |
| <b>I</b>        | 0.2                       | NF  | NF  |
| <b>II</b>       | 1.1                       | NF  | NF  |
| <b>III</b>      | 1.5                       | NF  | 0.9 |
| <b>IV</b>       | 2.2                       | 0.1 | 1.2 |
| <b>V</b>        | 3.2                       | 0.4 | 1.5 |

\* *NF= Not found*

The XRD patterns of fresh and reused catalyst (after 4<sup>th</sup> cycle) were compared in Fig. 6.10. As could be seen from the comparison, peaks of  $\text{Na}_2\text{TiSi}_4\text{O}_{11}$  and few peaks of  $\text{SiWO}_2$  at  $2\theta = 36.9^\circ$ ,  $38.7^\circ$ ,  $47.2^\circ$  and  $42.5^\circ$  were no longer found in the diffraction patterns of reused catalyst. Thus loss in activity after 4<sup>th</sup> run could be attributed to the change in catalyst structure.

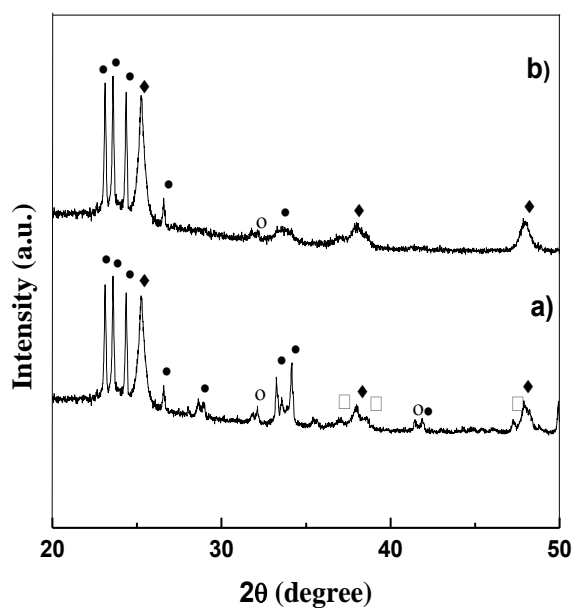


**Fig. 6.10. Comparison of the powder XRD patterns of a) fresh and b) reused 20-W/Ti/SiO<sub>2</sub>, (o = SiWO<sub>2</sub>; ● = WO<sub>3</sub>; ◆ = TiO<sub>2</sub> (anatase phase); □ = Na<sub>2</sub>TiSi<sub>4</sub>O<sub>11</sub>).**

## 6.6 Kinetic study

In order to study the kinetics of the methanolysis of WCO in presence of 20-W/Ti/SiO<sub>2</sub> catalyst, reaction has been performed under optimized reaction conditions and the FAMEs yield obtained at various time intervals (after every 30 min) was fitted in equation (1) as mentioned in chapter 3. Linear nature of the  $-\ln(1-X_{me})$  versus time plot suggest that pseudo first order kinetic equation is followed by 20-W/Ti/SiO<sub>2</sub> catalyzed methanolysis.

The Arrhenius model was employed, as discussed in chapter 3, to estimate the activation energy ( $E_a$ ) and pre-exponential factor ( $A$ ) for methanolysis of WCO. A plot between  $\ln k$  versus  $1/T$  is shown in Fig. 6.11b, and the values of  $E_a$  and  $A$  from the graph was found to be 46.2 kJ mol<sup>-1</sup> and  $2.9 \times 10^{10}$  min<sup>-1</sup>, respectively. The value of  $E_a$  was found within the range (33-84 kJ mol<sup>-1</sup>) of reported values (Sun et al., 2010) for the methanolysis of vegetable oils.

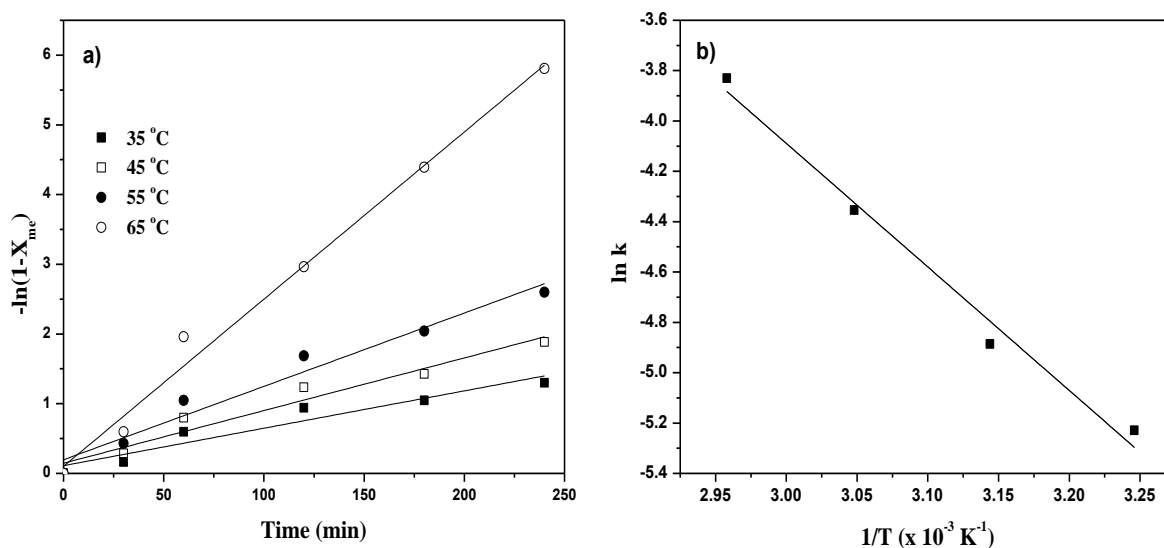


**Fig. 6.11.** a) A plot of  $-\ln(1-X_{me})$  versus reaction time ( $t$ ) at different temperatures (Reaction conditions: MeOH/oil molar ratio = 30:1; catalyst amount = 5 wt% of oil) and b) Arrhenius plot for methanolysis of WCO in presence of 20-W/Ti/SiO<sub>2</sub>

## 6.7 Conclusions

Present work has demonstrated the preparation and application of flower shaped W/Ti/SiO<sub>2</sub>-700 mixed metal oxide as heterogeneous catalyst for the production of greener diesel fuel substitute, fatty acid methyl esters, using waste cottonseed oil as feedstock. The flower shape morphology of the prepared catalyst (at pH=3, and 700 °C calcination temperature) was observed as supported by FESEM study. The N<sub>2</sub> adsorption-desorption curves validate the presence of catalyst in mesoporous form which is further confirmed by HRTEM study. The prepared 20-W/Ti/SiO<sub>2</sub>-700 catalyst required 4 h for the complete transesterification of WCO with methanol (1:30 molar ratio) at 65 °C. The catalyst has demonstrated reasonably good reusability as it remains active in four catalytic runs, without significant loss in activity. Metal analysis in FAMEs demonstrated no significant metal leaching from catalyst during successive runs. Few changes in W/Ti/SiO<sub>2</sub> structure were observed, upon repeated use, which could be the foremost reason for the partial loss of catalytic activity.

---

## References

Cheng, L.; Zhang, X.; Liu, B.; Wang, H.; Li, Y.; Huang, Y.; Du, Z.; Template synthesis and characterization of WO<sub>3</sub>/TiO<sub>2</sub> composite nanotubes. *Nanotech.*; **2005**, 16, 1341–1345.

Dacquin, J. P.; Lee, A. F.; Pireza, C.; Wilson, K.; Pore-expanded SBA-15 sulfonic acid silicas for biodiesel synthesis. *Chem. Commun.*; **2012**, 48, 212–214.

Dai, Z.; Guo, M. Q.; Wang, X. J.; Wang, H. F.; Chen, W. Y.; Development of Amperometric Laccase Biosensor through Immobilizing Enzyme in Magnesium-Containing Mesoporous Silica Sieve (Mg-MCM-41)/Polyvinyl Alcohol Matrix. *J. Nanomaterial.*; **2014**, (In press).

Davis, B. H.; Catalytic conversion of alcohols: VII. Alkene selectivity of tungsten oxides. *J. Catal.*; **1978**, 55, 158–165.

Delfort, B.; Le Pennec, D.; Lendresse, C.; *United state Patent B2*; **2006**, 7, 151, 187.

Furuta, S.; Matsushashi, H.; Arata, K.; Biodiesel fuel production with solid superacid catalysis in fixed bed reactor under atmospheric pressure. *Catal. Commun.*; **2004**, 5, 721–723.

Gao, X.; Wachs, I.; Titania–silica as catalysts: molecular structural characteristics and physico-chemical properties. *J. Catal.*; **1999**, 51, 233–254.

Hattori, H.; Asada, N.; Tanabe, K.; Acidic Property and Catalytic Activity of Tungsten Oxide. *Bull. Jpn. Chem. Soc.*; **1978**, 51, 1704–1707.

Kiss, F. E.; Jovanovic, M.; Boskovic, G. C.; Economic and ecological aspects of biodiesel production over homogeneous and heterogeneous catalysts. *Fuel Process. Technol.*; **2010**, 91; 1316–1320.

Li, M.; Hu, M.; Jia, D.; Ma, S.; Yan, W.; NO<sub>2</sub>-sensing properties based on the nanocomposite of n-WO<sub>3-x</sub>/n-porous silicon at room temperature. *Sensor. Actuat. B: Chem.*; **2013**, 186, 140–147.

Li, Y.; Zhang, X. D.; Sun, L.; Zhang, J.; Xu, H. P.; Fatty acid methyl ester synthesis catalyzed by solid superacid catalyst SO<sup>2</sup>/ZrO<sub>2</sub>-TiO<sub>2</sub>/La<sup>3+</sup>. *Appl. Energ.*; **2010**, 87, 156-159.

Li, Y.; Zhang, X. D.; Sun, L.; Xu, M.; Zhou, W. G.; Liang, X. H.; Solid superacid catalyzed fatty acid methyl esters production from super oil. *Appl. Energ.*; **2010**, 87, 2369-2373.

Liu, G.; Wang, X.; Wang, X.; Han, H.; Li, C.; Photocatalytic H<sub>2</sub> and O<sub>2</sub> evolution over tungsten oxide dispersed on silica. *J. Catal.*; **2012**, 293, 61–66.

Martin, A.; Morales, G.; Martinez, F.; van Grieken, R.; Cao, L.; Kruk, M.; Acid hybrid catalysts from poly(styrenesulfonic acid) grafted onto ultra-large-pore SBA-15 silica using atom transfer radical polymerization. *J. Matter Chem.*; **2010**, 20, 8026-8035.

Nakagaki, S.; Bail, A.; dos Santos, V. C.; de Souza, V. H. R.; Vrubel, H.; Nunes, F. S.; Ramos, L. P.; Use of anhydrous sodium molybdate as an efficient heterogeneous catalyst for soybean oil methanolysis. *Appl. Catal. A: Gen.*; **2008**, 351, 267–274.

Peng, B. X.; Shu, Q.; Wang, J. F.; Wang, G. R.; Wang, D. Z.; Han, M. H.; *Process. Saf. Environ. Prot.*; **2008**, 86, 441-447.

Qadri, S. B.; Skelton, E. F.; Hsu, D.; Dinsmore, A. D.; Yang, J.; Gray, H. F.; Ratna, B. R.; Size-induced transition-temperature reduction in nanoparticles of ZnS. *Phys. Rev. B*; **1999**, 60, 9191–9193.

Ramu, S.; Lingaiah, N.; Devi, B. L. A. P.; Prasad, R. B. N.; Suryanarayana, I.; Prasad, P. S. I.; Esterification of palmitic acid with methanol over tungsten oxide supported on zirconia solid

acid catalysts: effect of method of preparation of the catalyst on its structural stability and reactivity. *Appl. Catal. A: Gen.*; **2004**, 276, 163–168.

Santos, V. C.; Bail, A.; Okada, H. O.; Ramos, L. P.; Ciuffi, K. J.; Lima, O. J.; Nakagaki, S.; Methanolysis of soybean oil using tungsten- containing heterogeneous catalysts. *Energ. Fuel*; **2011**, 25, 2794-2802.

Shao, G. N.; Sheikh, R.; Hilonga, A.; Lee, J. E.; Park, Y-H; Kim, H. T.; Biodiesel production by sulfated mesoporous titania–silica catalysts synthesized by the sol–gel process from less expensive precursors. *Chem. Eng. J.*; **2013**, 215–216, 600–607.

Sun, P.; Sun, J.; Yao, J.; Zhang, L.; Xu, N.; Continuous production of biodiesel from high acid value oils in microstructured reactor by acid-catalyzed reactions. *Chem. Eng. J.*; **2010**, 162, 364–370.

Wang, L.; Ma, Y.; Wang, Y.; Liu, S.; Deng, Y.; Efficient synthesis of glycerol carbonate from glycerol and urea with lanthanum oxide as a solid base catalyst. *Catal. Commun.*; **2011**, 12, 1458–1462.

Xia, X.; Jin, R.; He, Y.; Deng, J.; Li, H.; Surface properties and catalytic behaviors of  $\text{WO}_3/\text{SiO}_2$  in selective oxidation of cyclopentene to glutaraldehyde. *Appl. Surf. Sci.*; **2000**, 165, 255–259.

---

**Na/CaO/Fe<sub>3</sub>O<sub>4</sub> as Nano Magnetic Catalyst for the Ethanolysis and Methanolysis of Waste Cottonseed oil**

---

|            | <b>Contents</b>  | <b>Page</b> |
|------------|--|-------------|
| <b>7.1</b> | <b>Introduction</b>                                      | 125         |
| <b>7.2</b> | <b>Experimental section</b>                              | 125         |
|            | 7.2.1 Catalyst preparation                               | 125         |
|            | 7.2.2 Transesterification reaction                       | 126         |
| <b>7.3</b> | <b>Results and discussion</b>                            | 126         |
|            | 7.3.1 Catalyst characterization                          | 126         |
|            | 7.3.1.1 BET surface area and Basic strength              | 126         |
|            | 7.3.1.2 Powder XRD study                                 | 127         |
|            | 7.3.1.3 FESEM and HRTEM study                            | 128         |
| <b>7.4</b> | <b>Catalytic activity</b>                                | 130         |
| <b>7.5</b> | <b>Effect of FFA on catalyst activity</b>                | 133         |
| <b>7.6</b> | <b>Catalyst Reusability and Homogeneous contribution</b> | 134         |
| <b>7.7</b> | <b>Kinetic study</b>                                     | 136         |
| <b>7.8</b> | <b>Conclusions</b>                                       | 138         |
|            | <b>References</b>  | 139         |

---

### **Abstract**

In present chapter, 3 wt % CaO was impregnated over Fe<sub>3</sub>O<sub>4</sub> to prepare a magnetic support of CaO/Fe<sub>3</sub>O<sub>4</sub> for sodium immobilization. Varying amount of sodium (1-5 wt%) was impregnated over CaO/Fe<sub>3</sub>O<sub>4</sub> support and catalysts (Na/CaO/Fe<sub>3</sub>O<sub>4</sub>) were characterized by powder X-ray diffraction, field emission scanning electron, high resolution transmission electron microscopy and Brunauer-Emmett-Teller surface area studies, in order to establish the structure and surface morphology of the catalyst. The prepared Na/CaO/Fe<sub>3</sub>O<sub>4</sub> catalyst has been employed as heterogeneous catalyst for the transesterification of WCO (having 2.8 wt% free fatty acid contents) with methanol and ethanol. Under the optimal reaction conditions of 9:1 alcohol/oil molar ratio, catalyst to oil weight fraction of 5 % and 65 °C reaction temperature, > 98 % fatty acid alkyl ester yield was obtained. The catalysts was removed from the reaction mixture by magnetic separation and reused in seven catalytic runs without significant loss in the activity.

## 7.1 Introduction

As discussed in previous chapter the major problem associated with the use of homogeneous catalysts is their separation from the reaction mixture. Even in case of heterogeneous catalysts time consuming decantation or filtration process is required. To overcome the difficulties in catalysts isolation and to avoid the loss of catalyst in the process, development of magnetically active catalyst may be a better alternative. Magnetic catalysts have been frequently applied in the fields of photocatalysis (Beydoun et al., 2000), biocatalysis (Gao et al., 2003), and phase transfer catalysis (Wen et al., 2008). However, few reports are available on magnetic catalysts employed for transesterification reaction. Ying and Chen (2007) have stabilized lipase producing bacteria *Bacillus subtilis* on hydrophobic carrier having  $\text{Fe}_3\text{O}_4$  magnetic particles. These magnetic particles were employed for the transesterification of waste cottonseed oil with methanol to obtain 90% conversion levels. Hu et al., (2011) have prepared 25 wt% KF on  $\text{CaO}/\text{Fe}_3\text{O}_4$  to prepare  $\text{KF}/\text{CaO}/\text{Fe}_3\text{O}_4$  magnetic nano catalyst. The magnetic catalyst was used as reusable solid catalysts for biodiesel production from stillingia oil.

In the present chapter,  $\text{Na}/\text{CaO}/\text{Fe}_3\text{O}_4$  magnetic catalyst was prepared by wet impregnation method and employed for the methanolysis as well as ethanolysis of waste cottonseed oil. The catalyst demonstrates excellent activity (> 98% fatty acid alkyl ester yield), reusability (up to seven runs) and easy magnetic separation from the reaction mixture.

## 7.2 Experimental

### 7.2.1 Catalyst preparation

The magnetic support was prepared by co-precipitation method by following the literature reported scheme with slight modification (Hu et al., 2011). In a 500 ml beaker, equipped with hot plate and magnetic stirrer, 7 g of  $\text{FeSO}_4 \cdot 7\text{H}_2\text{O}$  and 20 g of  $\text{Fe}_2(\text{SO}_4)_3$  were dissolved in 250 ml deionized water. To this solution, ammonia was added drop wise at 65 °C with vigorous stirring to maintain the final pH of 12. The mixture was stirred for 2 h to obtain  $\text{Fe}_3\text{O}_4$  as black powder which was washed with distilled water until the pH of the supernatant become 7 and finally dried at 60 °C for 24h.

To prepare  $\text{CaO}/\text{Fe}_3\text{O}_4$ , 10 g  $\text{Fe}_3\text{O}_4$  was added in 40 ml deionized water to form a slurry and to this 10 ml aqueous solution of calcium nitrate (12.3 g/l) was added to obtain 3 wt% Ca over

Fe<sub>3</sub>O<sub>4</sub>. The slurry was stirred for 2 h, evaporated to dryness, dried at 120° C for 24 h and finally calcined at 400 °C for 4 h to yield CaO/Fe<sub>3</sub>O<sub>4</sub>.

Sodium was incorporated over this magnetic support by impregnation method. CaO/Fe<sub>3</sub>O<sub>4</sub> (10 g) was suspended in 40 ml deionized water, and to this sodium nitrate solution of desired concentration was added. The resulted slurry was stirred for 4 h, initially dried at 120° C for 24 h and finally calcined at 600 °C for 4 h. The prepared catalysts were designated as *x*-Na/Ca/Fe<sub>3</sub>O<sub>4</sub>, where *x* is the Na wt%.

### 7.2.2 Transesterification reaction

All transesterification reactions were carried out in 250 ml, three necked round bottom flask equipped with a water cooled reflux condenser, thermometer, oil bath and a magnetic stirrer. In a typical run, the flask was charged with 10 g vegetable oil, desired amount of alcohol and catalyst and heated at required temperature (35-75 °C). To monitor the progress of the reaction, the aliquots were collected from the reaction mixture after every 30 min with the help of glass dropper and subjected to the <sup>1</sup>H NMR study.

## 7.3 Results and discussion

### 7.3.1 Catalyst characterization

#### 7.3.1.1 BET surface area and basic strength

In present chapter, Fe<sub>3</sub>O<sub>4</sub> is used as magnetic support for the easy separation of catalyst from the reaction mixture. To introduce the basic sites in Fe<sub>3</sub>O<sub>4</sub> it is further infused with calcium nitrate and sodium nitrate salts. The basic strength of CaO supported Fe<sub>3</sub>O<sub>4</sub> was found to be in the range of 9.8-10. In order to further increase the basicity as well as activity, CaO/Fe<sub>3</sub>O<sub>4</sub> was later supported with 1-5 wt % of sodium. An increase in sodium concentration was found to enhance the basic strength as well as activity of the Na/CaO/Fe<sub>3</sub>O<sub>4</sub> catalyst as given in Table 7.1. One wt% sodium incorporation over CaO/Fe<sub>3</sub>O<sub>4</sub> was found to increase the surface area, due to increase in interparticle spacing. A further increase in sodium concentration ( $\geq 2$ wt%) was found to reduce the surface area may be due to the pore plugging of catalyst by Na as given in Table 7.1. The activity of the various catalysts was compared by calculating the turn over frequency (methanolysis and ethanolysis of WCO) as given in Table 7.1. Increase in Na

concentration was found to enhance catalyst basic sites which impart the higher activity (TOF) to the catalyst.

**Table 7.1. Comparisons of the BET surface area, basic strength, basicity and TOF for 0-5 wt% Na impregnated CaO/Fe<sub>3</sub>O<sub>4</sub>.**

| Catalyst                                     | Basic strength             | Basicity<br>(mmoles g <sup>-1</sup> ) | BET<br>surface<br>area<br>(m <sup>2</sup> /g) | Methanolysis                                   | Ethanolysis                                    |
|--|----------------------------|---------------------------------------|---|--|--|
|  |                            |                                       |   | TOF<br>(× 10 <sup>-4</sup> min <sup>-1</sup> ) | TOF<br>(× 10 <sup>-5</sup> min <sup>-1</sup> ) |
| CaO/Fe <sub>3</sub> O <sub>4</sub> -400      | 9.8<H_ <sub>+</sub> <10.1  | 5.22                                  | 27.6  | 0.46   | 0.35   |
| 1-Na/CaO/Fe <sub>3</sub> O <sub>4</sub> -600 | 10.1<H_ <sub>+</sub> <11.1 | 6.41                                  | 38.2  | 1.16   | 3.48   |
| 2-Na/CaO/Fe <sub>3</sub> O <sub>4</sub> -600 | 10.1<H_ <sub>+</sub> <11.1 | 6.52                                  | 35.6  | 2.91   | 4.45   |
| 3-Na/CaO/Fe <sub>3</sub> O <sub>4</sub> -600 | 11.1<H_ <sub>+</sub> <15.0 | 6.80                                  | 30.1  | 4.82   | 6.21   |
| 4-Na/CaO/Fe <sub>3</sub> O <sub>4</sub> -600 | 15.0<H_ <sub>+</sub> <18.4 | 7.41                                  | 29.2  | 7.81   | 9.21   |
| 5-Na/CaO/Fe <sub>3</sub> O <sub>4</sub> -600 | 15.0<H_ <sub>+</sub> <18.4 | 7.75                                  | 22.6  | 10.3   | 11.3   |

### 7.3.1.2 Powder XRD studies

The powder XRD study of Fe<sub>3</sub>O<sub>4</sub> and 1-5 wt% Na impregnated CaO/Fe<sub>3</sub>O<sub>4</sub> have been performed and respective diffraction patterns are compared in Fig. 7.1. The diffraction patterns of Fe<sub>3</sub>O<sub>4</sub> supported the formation of cubic phase (JCPDS-00-65-3107) with lattice constant of 8.3 Å. The XRD study of 1-5 wt% Na impregnated CaO/Fe<sub>3</sub>O<sub>4</sub> show the diffraction patterns corresponding to the orthorhombic phase of CaFeO<sub>4</sub> (JCPDS-00-03-0804), orthorhombic phase of NaCaFe<sub>3</sub>O<sub>4</sub> (JCPDS-00-48-0388) and monoclinic phase of Na<sub>3</sub>Fe<sub>5</sub>O<sub>9</sub> (JCPDS-00-18-1213). A gradual increase in NaCaFe<sub>3</sub>O<sub>4</sub> phase was observed with the increase in Na concentration. Formation of these new phases has supported the chemical bonding between Na and CaO/Fe<sub>3</sub>O<sub>4</sub>.

The crystallite size of 4-Na/CaO/Fe<sub>3</sub>O<sub>4</sub>-600 catalyst corresponding to (311) plane by the Debye-Scherrer method (Qadri et al., 1999) was found to be 44.2 nm.

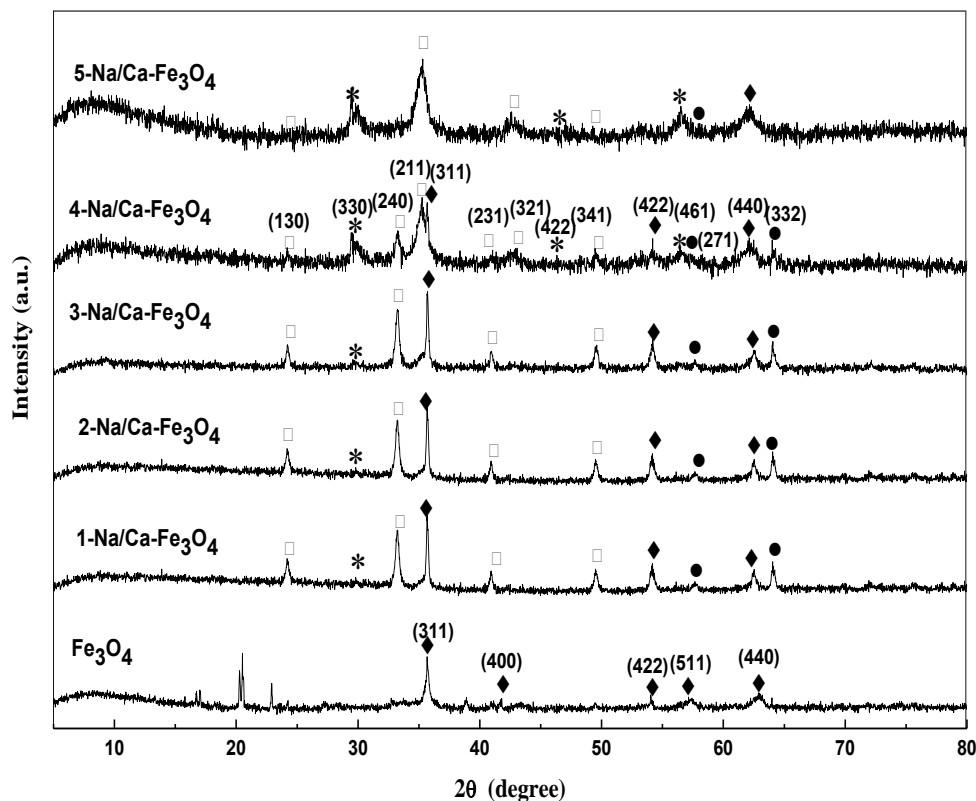


**Fig. 7.1.** Comparative powder XRD patterns of Fe<sub>3</sub>O<sub>4</sub>, 1-5 wt% Na impregnated CaO/Fe<sub>3</sub>O<sub>4</sub>-600 [CaFeO<sub>4</sub> (●), Fe<sub>3</sub>O<sub>4</sub> (◆), NaCaFe<sub>3</sub>O<sub>4</sub> (□), Na<sub>3</sub>Fe<sub>5</sub>O<sub>9</sub> (\*)].

### 7.3.1.3. FESEM and HRTEM study

The surface morphology of Fe<sub>3</sub>O<sub>4</sub> and 4-Na/CaO/Fe<sub>3</sub>O<sub>4</sub>-600 was studied by FESEM imaging. As shown in Fig.7.2a, the catalyst particles have formed in cuboid geometry of  $\sim 1.8 \times 1.5 \times 1.1 \mu\text{m}$  dimensions with smooth surfaces. Upon Ca and Na impregnation followed by calcination at 600 °C, the catalyst particles adopted the irregular shapes (grain size of 0.5-3  $\mu\text{m}$ ) with rough surface (Fig. 7.2b). This may be due to the agglomeration of the Fe<sub>3</sub>O<sub>4</sub> particles during Na and Ca impregnation.

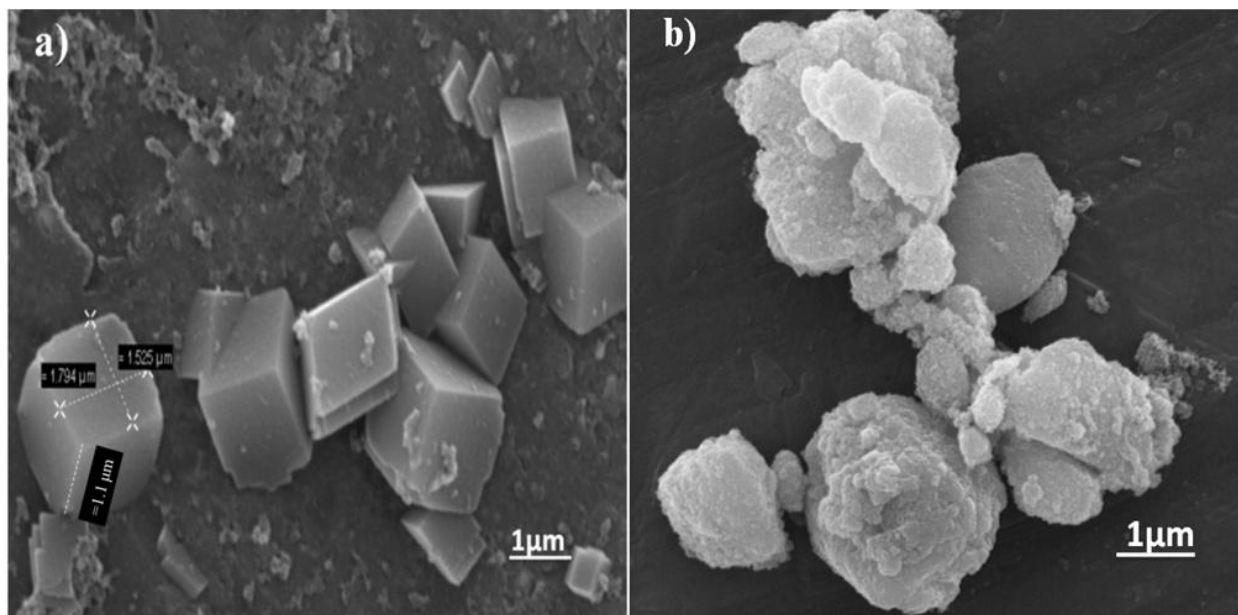


**Fig. 7.2. FESEM images of a)  $\text{Fe}_3\text{O}_4$  and b) 4-Na/CaO/ $\text{Fe}_3\text{O}_4$ -600**

The HRTEM study reveals that,  $\text{Fe}_3\text{O}_4$  cuboid particles further consists of small cuboid particles (Fig. 7.3a) with an average particle size of  $\sim 11.5$  nm and lattice fringe width of 0.22 nm. Upon Na and Ca impregnation agglomeration of  $\sim 15$  nm sized particles has formed as shown in Fig. 7.3b. The lattice fringe width in 4-Na/CaO/ $\text{Fe}_3\text{O}_4$ -600 found to be 0.12 nm, which is roughly half of the fringe width observed for  $\text{Fe}_3\text{O}_4$  support.

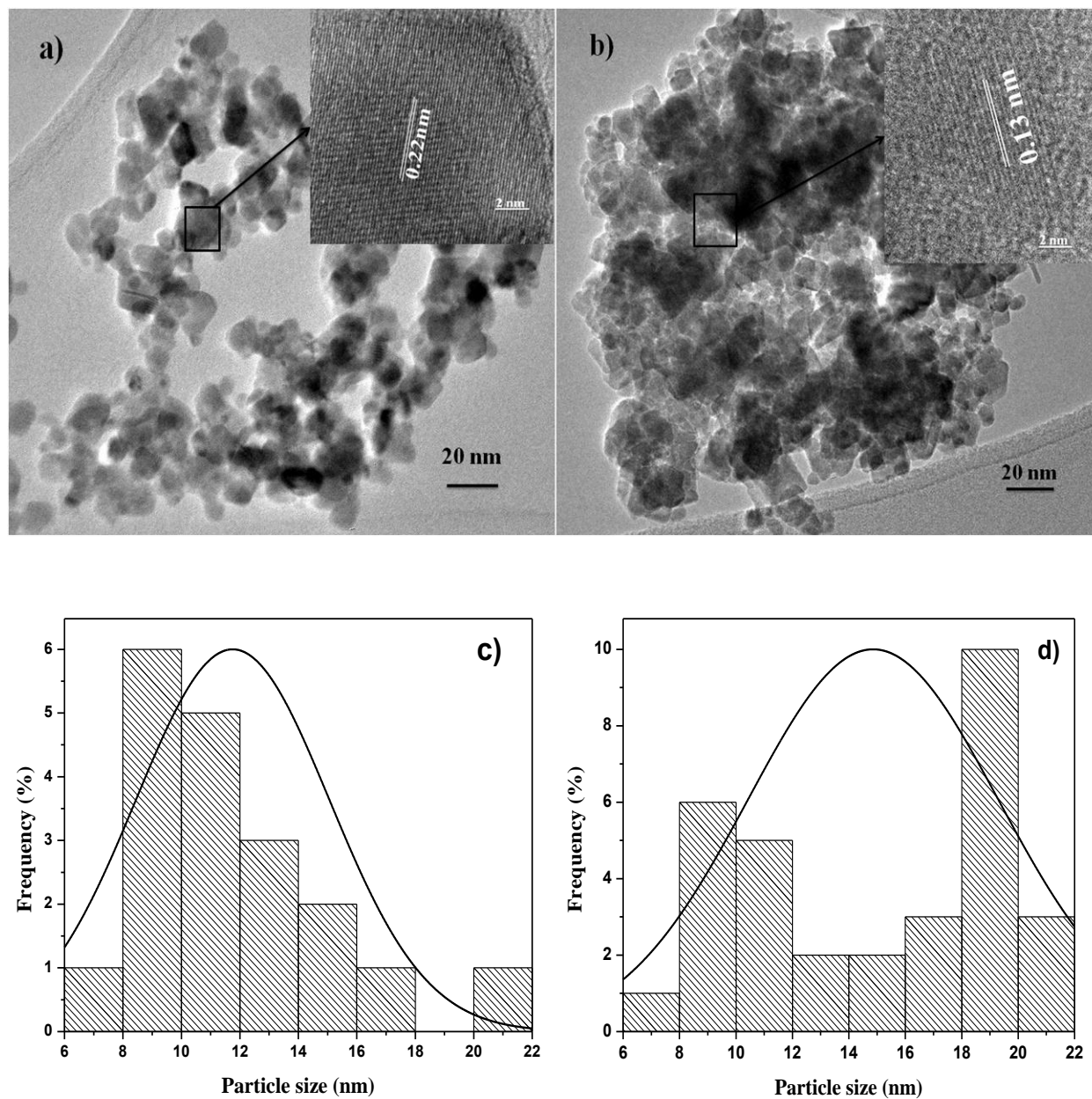


**Fig. 7.3.** HRTEM images of a) Fe<sub>3</sub>O<sub>4</sub> and b) 4-Na/CaO/Fe<sub>3</sub>O<sub>4</sub>-600 particles and particle size distribution for c) Fe<sub>3</sub>O<sub>4</sub> and d) 4-Na/CaO/Fe<sub>3</sub>O<sub>4</sub>-600.

#### 7.4 Catalytic activity

In order to optimize the reaction conditions for the catalytic activity, transesterification reactions have been carried out at fixed stirring speed of 600 rpm in presence of Na/CaO/Fe<sub>3</sub>O<sub>4</sub>-600 and varying one parameter at a time out of the followings: (i) catalyst amount with respect to oil, (ii) reaction temperature, and (iii) alcohol to oil molar ratio.

Under optimized reaction conditions effect of FFA, the reusability of the catalyst and kinetics of the 4-Na/CaO/Fe<sub>3</sub>O<sub>4</sub>-600 catalyzed transesterification has also been studied.

In order to find the optimum catalyst concentration, a series of transesterification reactions of WCO with methanol and ethanol (9:1 molar ratio) was performed in presence of 1-6 wt% (with respect to oil) of 4-Na/CaO/Fe<sub>3</sub>O<sub>4</sub>-600 catalyst. Time required for the complete conversion (> 98%) of WCO with methanol and ethanol to biodiesel was found to be 1.5 and 2.5 h, respectively, when 5 wt% of the catalyst was used. Further increase in catalyst concentration ( $\geq 5$  wt%) does not reduce the reaction time significantly as shown in Fig. 7.4a and 7.4b. This could be due to the fact that at higher catalyst loading reaction mixture becomes more viscous which could resist the mass transfer in the system.

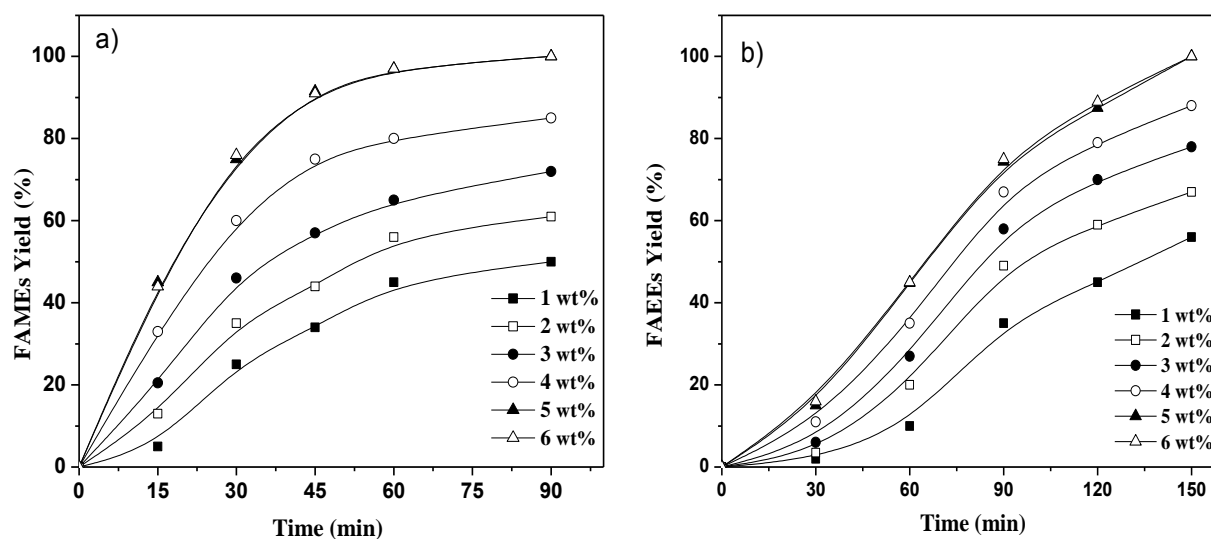


**Fig.7.4. Effect of catalyst concentration on 4-Na/CaO/Fe<sub>3</sub>O<sub>4</sub>-600 catalyzed a) methanolysis and b) ethanolysis of WCO.**

The optimum reaction temperature for 4-Na/CaO/Fe<sub>3</sub>O<sub>4</sub>-600 was determined by performing the transesterification of WCO with ethanol and methanol in the temperature range of 35-75 °C. The methanolysis and ethanolysis of WCO were found to give complete conversion (> 98%) in 1.5 and 2.5 h respectively, on increasing the temperature from 35 to 65 °C. A further increase in reaction temperature was not found to reduce the reaction duration to significant extent as shown in Fig. 7.5a and 7.5b, and hence, transesterification reaction of vegetable oils with methanol and ethanol were performed at 65 °C.

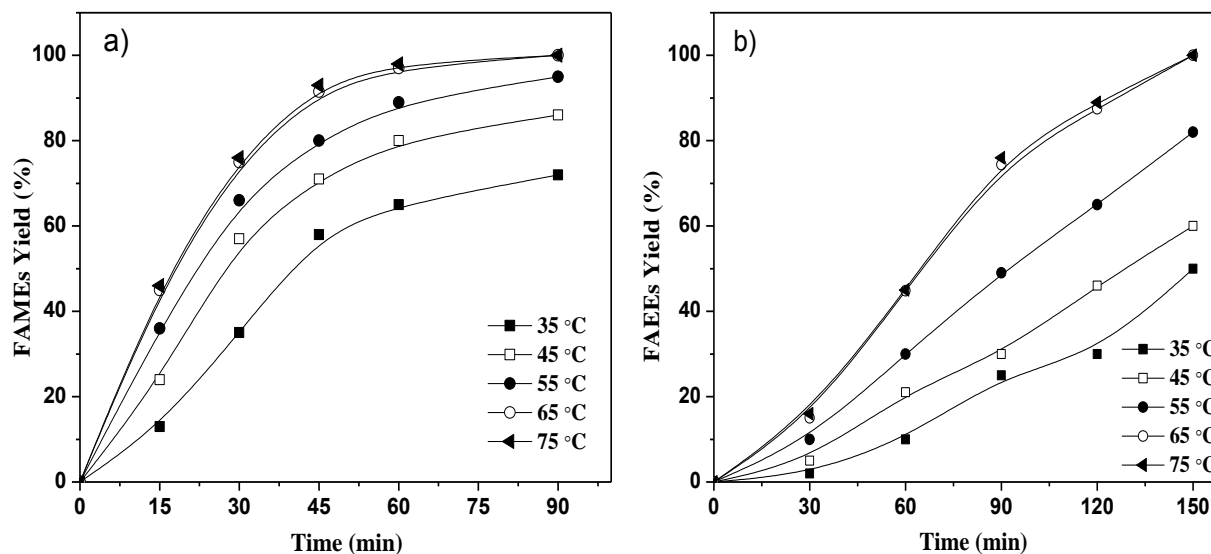


**Fig.7.5. Effect of reaction temperature on 4-Na/CaO/Fe<sub>3</sub>O<sub>4</sub>-600 catalyzed a) methanolysis and b) ethanolysis of WCO.**

To determine the optimum alcohol/oil molar ratio for 4-Na/CaO/Fe<sub>3</sub>O<sub>4</sub>-600, the reactions were performed by varying the alcohol/oil molar ratio from 3:1 to 12:1 for both alcohols. An optimum molar ratio of 9:1 (alcohol/oil) was required to yield the complete methanolysis and ethanolysis of WCO as shown in Fig.7.6a and 7.6b. The rate of ethanolysis was found to be slower than methanolysis owing to the low mobility of ethoxide nucleophile than methoxide (Kim et al., 2010).

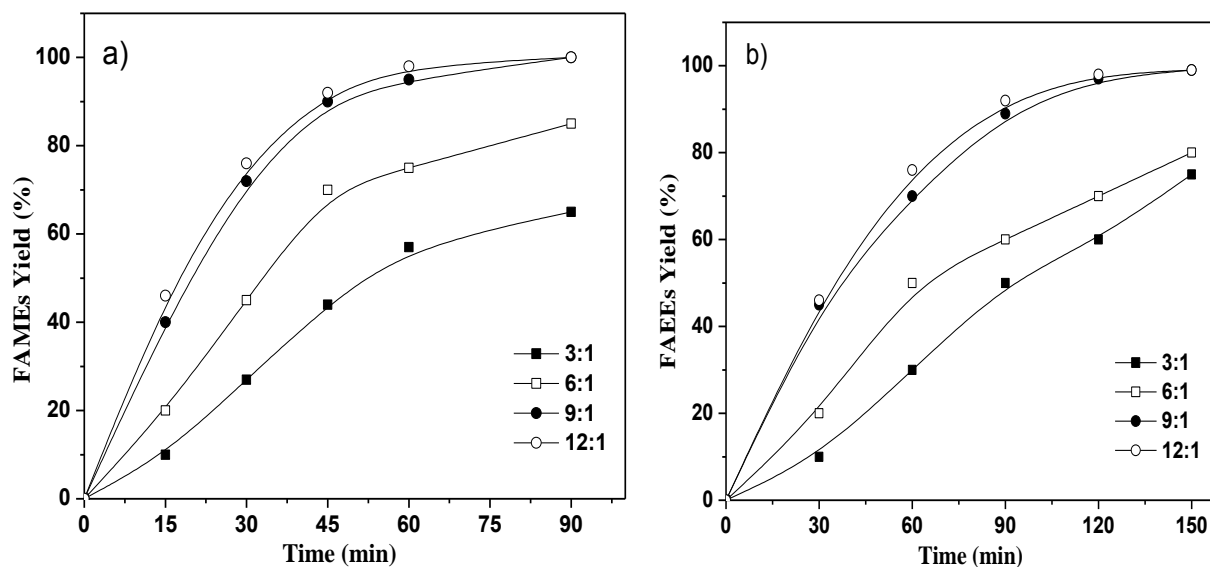


**Fig.7.6. Effect of alcohol to oil molar ratio on 4-Na/CaO/Fe<sub>3</sub>O<sub>4</sub>-600 catalyzed a) methanolysis and b) ethanolysis of WCO.**

### 7.5 Effect of FFA on catalyst activity

In order to test the efficacy of 4-Na/CaO/Fe<sub>3</sub>O<sub>4</sub>-600 catalyst towards the transesterification of few commonly available vegetable oils (having various amount of FFA) in the locality, it has been employed for the ethanolysis and methanolysis of FCO, SO, WCO, KO and JO. All reactions were performed in presence of 5 wt% catalyst at 65 °C using ethanol or methanol with oil in 9:1 molar ratio. The time required for conversion of various feedstocks to fatty acid methyl/ethyl esters is shown in Fig. 7.7. The activity of catalyst was found to be adversely affected with the increase in FFA in feedstock. Slow rate of reaction in presence of high FFA concentration suggest that fatty acids have strong interactions with the basic sites and thus, may partially block their participation in catalytic process.

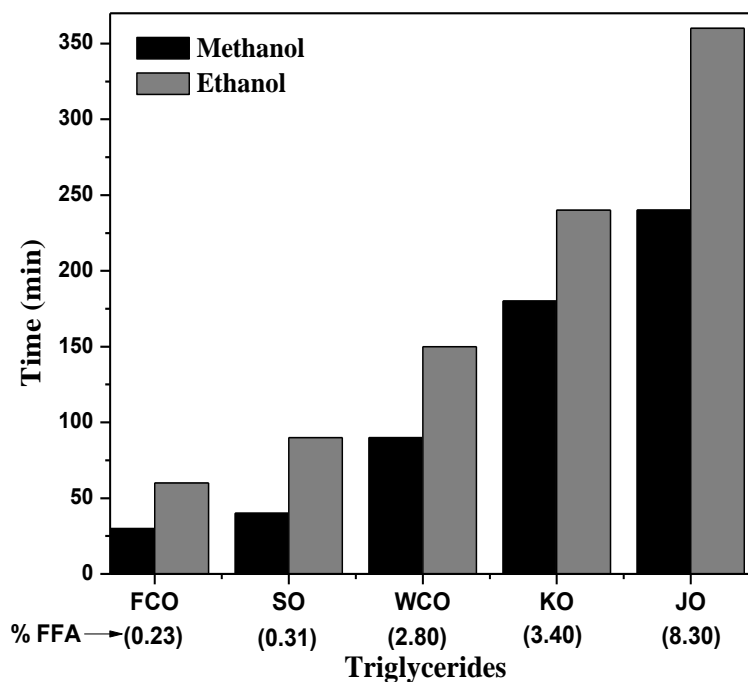


**Fig. 7.7.** Effect of FFA on 4-Na/CaO/Fe<sub>3</sub>O<sub>4</sub>-600 catalyzed methanolysis and ethanolysis of various triglycerides.

### 7.6 Catalyst Reusability and Homogeneous contribution

To demonstrate the reusability of 4-Na/CaO/Fe<sub>3</sub>O<sub>4</sub>-600 catalyst, the methanolysis and ethanolysis of WCO has been performed under the optimized reaction condition. The catalyst show magnetic property due to the presence of Fe<sub>3</sub>O<sub>4</sub> and was recovered from the reaction mixture with the help of magnet (Fig. 7.8), after the completion of reaction.

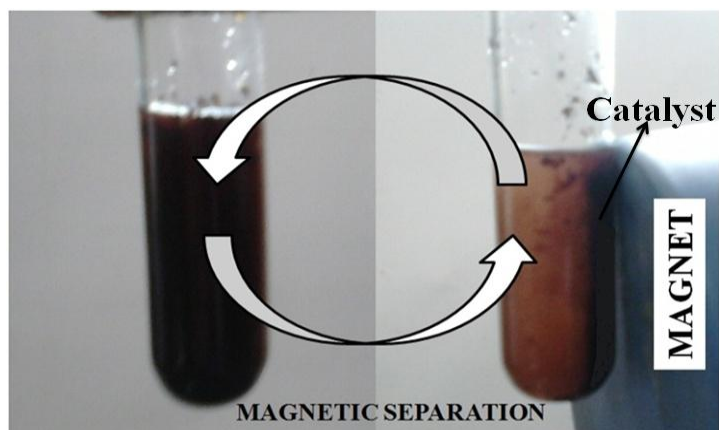


**Fig. 7.8.** Separation of Na/CaO/Fe<sub>3</sub>O<sub>4</sub>-600 catalyst from product using magnet.

The recovered catalyst was washed with hexane in order to remove the adsorbed organic molecules from its surface and initially dried at 120 °C and further calcined at 600 °C. The recovered catalyst was reused in seven runs under the optimized reaction conditions and similar regeneration method. As could be seen from Fig. 7.9, more than 90% alkyl ester yield was obtained up to 5<sup>th</sup> cycle. However, a partial drop in activity was observed in 6<sup>th</sup> and 7<sup>th</sup> catalytic cycle.

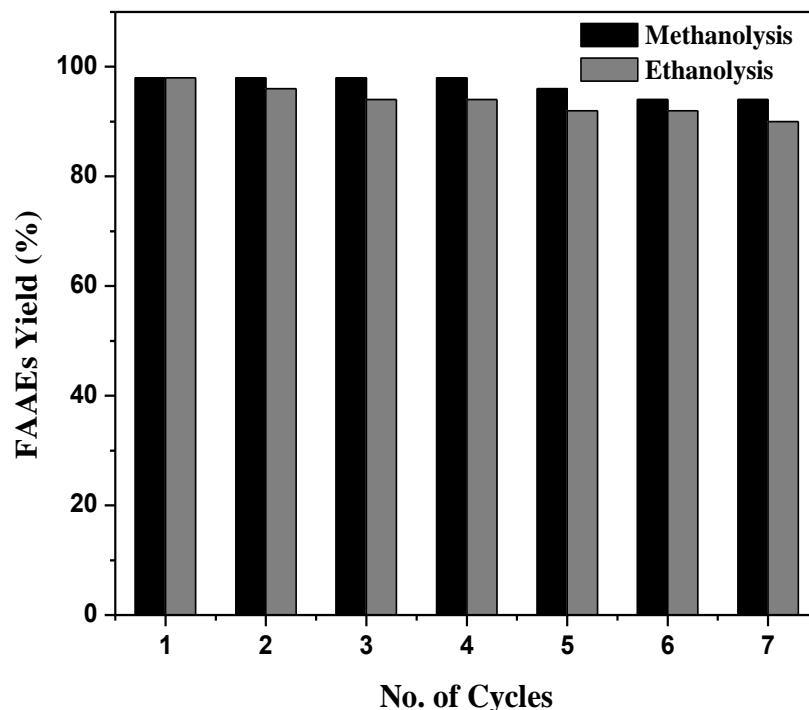


**Fig. 7.9. Reusability of 4-Na/CaO/Fe<sub>3</sub>O<sub>4</sub>-600 catalyst (Reaction conditions: alcohol to oil molar ratio = 9:1; Catalyst amount = 5 wt% of oil; Temperature = 65 °C).**

To establish the reason behind the loss in catalytic activity, the XRD patterns (Fig. 7.10) of the fresh and reused catalyst were compared. As evident from the diffraction patterns no peak corresponding to the Na<sub>3</sub>Fe<sub>5</sub>O<sub>9</sub> (at 2θ ~ 29.6°, 46.4° and 56.5°) was observed in reused catalyst. This study supports the partial leaching of the active species from the catalyst support and could be the reason behind the partial loss of catalytic activity.

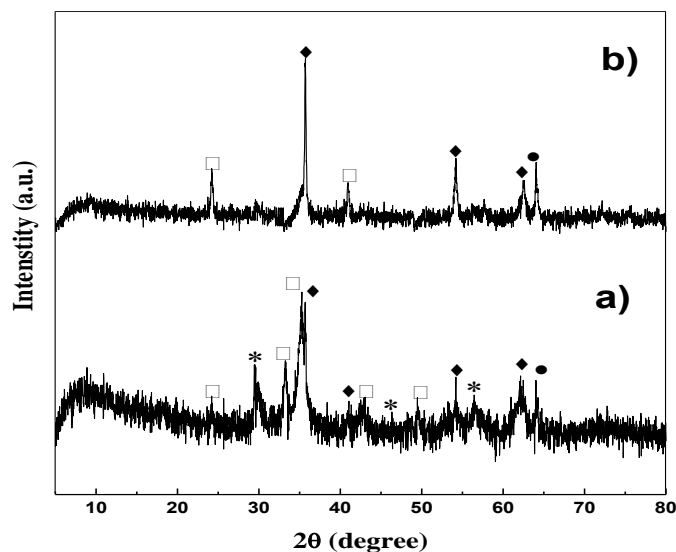


**Fig. 7.10.** Comparative powder XRD patterns of a) fresh and b) reused (after 7<sup>th</sup> cycle) Na/CaO/Fe<sub>3</sub>O<sub>4</sub>-600 catalyst [CaFeO<sub>4</sub> (●), Fe<sub>3</sub>O<sub>4</sub> (◆), NaCaFe<sub>3</sub>O<sub>4</sub> (□), Na<sub>3</sub>Fe<sub>5</sub>O<sub>9</sub> (\*)].

The leached metal ions from the support may catalyze the reaction similar to homogeneous catalyst. To quantify the homogeneous contribution, the catalyst 4-Na/CaO/Fe<sub>3</sub>O<sub>4</sub>-600 (500 mg), was refluxed separately with methanol for 1.5 h at 65 °C. After the specific time the catalyst was separated from methanol with the help of magnet, and methanol was employed for the transesterification of WCO (alcohol/oil = 9:1) at 65 °C. Under these experimental conditions negligible conversion of the WCO into FAMAs was achieved to rule out the possibility of significant homogeneous contribution in catalyst activity.

## 7.7 Kinetic study

The transesterification of triglycerides in presence of excess alcohol has been reported to follow pseudo-first order kinetics (Freedman et al., 1986). The kinetics of the 4-Na/CaO/Fe<sub>3</sub>O<sub>4</sub>-600 catalyzed transesterification of WCO has been studied at different temperatures and plotting the graph between  $-\ln(1-X_{me})$  or  $-\ln(1-X_{ee})$  versus 't' as given in Fig. 7.11a and 7.11b by following the equation 1 as described in chapter 3.

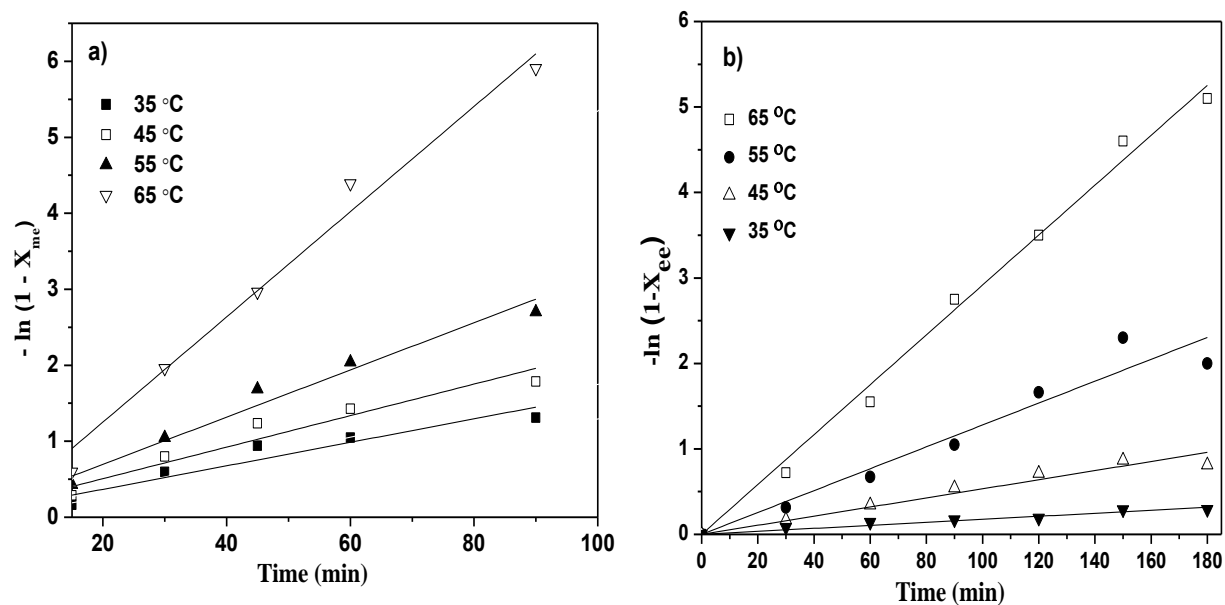


**Fig.7.11.** Plots of a)  $-\ln(1-X_{me})$  and b)  $-\ln(1-X_{ee})$  versus time at different temperatures. (Reaction conditions: alcohol to oil molar ratio of 9:1 and 5 wt% of 4-Na/CaO/Fe<sub>3</sub>O<sub>4</sub>-600 with respect to oil,  $X_{me}$  and  $X_{ee}$  = FAMES and FAEEs yield, respectively).

A plot between  $\ln k$  versus  $1/T$  is shown in Fig. 7.12, and the activation energy ( $E_a$ ) and pre-exponential factor ( $A$ ) from the plot was found to be  $37.8 \text{ kJ mol}^{-1}$  and  $1.9 \times 10^3 \text{ min}^{-1}$ , respectively for methanolysis and  $39.5 \text{ kJ mol}^{-1}$  and  $2.6 \times 10^4 \text{ min}^{-1}$ , respectively for ethanolysis.

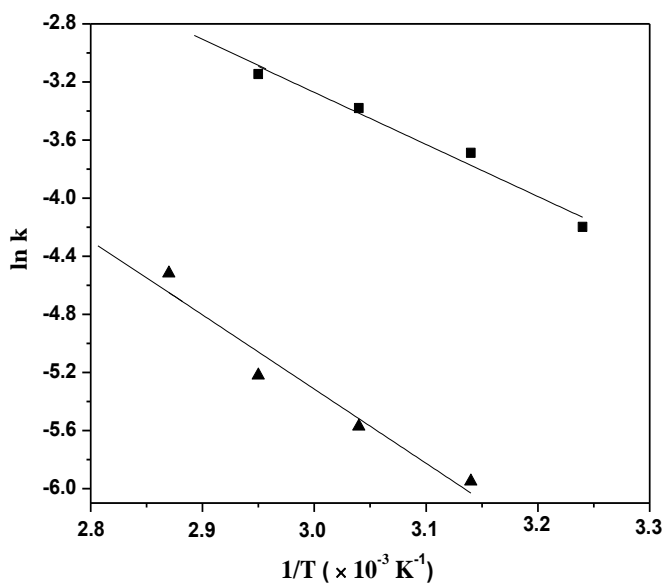


**Fig. 7.12.** Arrhenius plot for the transesterification of WCO with methanol (■) and ethanol (▲).

### 7.7 Conclusions

Present chapter has demonstrated the preparation of Na/CaO/Fe<sub>3</sub>O<sub>4</sub>-600 as magnetic catalyst for methanolysis as well as ethanolysis of waste cottonseed oil. Under the optimal reaction conditions of 9:1 alcohol/oil molar ratio, catalyst to oil weight fraction of 5 % and 65 °C reaction temperature, > 98 % fatty acid alkyl ester yield was obtained. Following the pseudo first order kinetic equation, activation energy for the methanolysis and ethanolysis of WCO was found to be 37.8 and 39.5 kJ mol<sup>-1</sup>, respectively. The main advantage of this catalyst was its ease of separation from the reaction mixture with the help of permanent magnet. The catalyst has demonstrated reasonably good reusability as it remains active in seven catalytic runs. Leaching of the active species from the catalyst was established as major reason for the loss in activity, although, leached species were not found to show any significant homogeneous contribution in catalytic activity.

---

## References

Beydoun, D.; Amal, R.; Low, G. K. C.; McEvoy S.; Novel photocatalyst: titania-coated magnetite: activity and photo dissolution. *J. Phys. Chem. B*; **2000**, 104, 4387–4396.

Freedman, B.; Butterfield, R.O.; Pryde, E.H.; Transesterification kinetics of soybean oil, *J. Am. Oil. Chem. Soc.*; **1986**, 63, 1375–1380.

Gao, X.; Yu, K. M. K.; Tam, K. Y.; Tsang, S. C.; Colloidal stable silica encapsulated nanomagnetic composite as a novel bio-catalyst carrier. *Chem. Commun.*; **2003**, 24, 2998–2999.

Hu, S.; Guan, Y.; Wang, Y.; Han, H.; Nano-magnetic catalyst KF/CaO–Fe<sub>3</sub>O<sub>4</sub> for biodiesel production. *Appl. Energ.*; **2011**, 88, 2685–2690.

Qadri, S. B.; Skelton, E. F.; Hsu, D.; Dinsmore, A. D.; Yang, J.; Gray, H. F.; Ratna, B. R.; Size-induced transition-temperature reduction in nanoparticles of ZnS. *Phys. Rev. B*; **1999**, 60, 9191–9193.

Wen, M.; Qi, H.; Zhao, W.; Chen, J.; Li, L.; Wu, Q.; Phase transfer catalysis: synthesis of monodispersed Fe-Pt nanoparticles and its electro catalytic activity. *Colloids. Surf. A*; **2008**, 312, 73–78.

Ying, M.; Chen, G. Y.; Study on the production of biodiesel by magnetic cell biocatalyst based on lipase-producing *Bacillus subtilis*. *Appl. Biochem. Biotechnol.*; **2007**, 137, 793–803.

**Conclusions, Future Perspective and Scope**

---

|            | <b>Contents</b>                         | <b>Page</b> |
|------------|---|-------------|
| <b>8.1</b> | <b>Introduction</b>                     | 140         |
| <b>8.2</b> | <b>Conclusions from present studies</b> | 140         |
| <b>8.3</b> | <b>Futuristic aspects</b>               | 143         |

---

### **Abstract**

The results given in chapter 3-7 have been concluded, compared and correlated in this chapter. A future studies possible with the prepared catalysts is also discussed.

---

## 8.1 Introduction

In the present thesis, work was carried out for the preparation and characterization of mixed metal oxide and their application as solid catalysts for the transesterification of a variety of triglycerides. The transesterification reaction is mainly reported in literature with methanol because of high reaction rate and good yield. However, only few reports are available with ethanol.

## 8.2 Conclusions from the present thesis

- i. **In chapter 3**, a series of KF impregnated CaO/NiO catalyst was prepared by varying the KF amount. The resulted catalysts were characterized by powder XRD, BET surface area, SEM, TEM and Hammett indicator studies.
- ii. CaO/NiO impregnated with 20 wt% KF was found to have the highest basic strength ( $15.0 < H_- < 18.4$ ) as supported by Hammett indicator tests and same catalyst required 4 h to yield the complete transesterification > 98 % yield of WCO with methanol.
- iii. The fatty acid methyl esters thus obtained was analyzed and quantified by  $^1\text{H-NMR}$  spectroscopy. The prepared fatty acid methyl esters have also been tested for few physicochemical properties and observed values were found within the acceptable limits of the European and American standards.
- iv. Reusability study suggests that catalyst could be recycled in four catalytic runs without significant loss in activity. But this catalyst was unable to catalyze ethanolysis reaction.
- v. **In chapter 4**, Li/CaO (3 wt% Li) catalyst was prepared by wet impregnation method and used for the ethanolysis as well as methanolysis of WCO. Under optimal reaction conditions viz., ethanol/oil molar ratio of 12:1, catalyst to oil weight fraction of 5 % and 65 °C reaction temperature, 98 % fatty acid ethyl ester yield was obtained in 2.5 h of reaction duration.
- vi. The prepared catalysts were characterized by powder XRD, BET surface area, SEM, TEM and Hammett indicator studies. The average size of catalyst particles by TEM study was found to be ~ 13 nm.
- vii. Under the optimized reaction conditions, the pseudo first order constant and Arrhenius activation energy was found to be  $0.03 \text{ min}^{-1}$  and  $70.0 \text{ kJ mol}^{-1}$ , respectively.

- viii. The lixiviation study suggested negligible homogeneous contribution in catalyst activity. The catalyst was also recovered and reused in four catalytic runs but with partial loss in activity during successive catalytic cycles.
- ix. **In chapter 5**, lithium impregnated NiO has been prepared in nano particle form in aqueous medium without adding any organic solvent or templates. The structure of the catalyst was established by powder X-ray diffraction, surface morphology and particle size by FESEM and HRTEM studies. The oxidation state and binding energy of the metal ions were calculated with the help of XPS study.
- x. The prepared catalyst, Li/NiO, was employed as heterogeneous catalyst for the ethanolysis of waste cottonseed oil and > 98% fatty acid ethyl ester yield was obtained in 3 h. The catalyst was found to be effective for the ethanolysis of vegetable oils having up to 8.4 wt% free fatty acids.
- xi. Prepared catalyst was able to catalyze seven reaction cycles without major loss in activity.
- xii. **In chapter 6**, flower shaped tungsten impregnated Ti/SiO<sub>2</sub> mesoporous solid catalyst has been employed for the transesterification of waste cotton seed with methanol and 98% fatty acid methyl ester yield was obtained in 4 h.
- xiii. Prepared catalyst was characterized by powder XRD, FESEM and HRTEM studies. Acidic strengths of the catalyst was measured by temperature programmed desorption and found to be maximum in case of catalyst prepared with 20 wt% tungsten loading over TiO<sub>2</sub>/SiO<sub>2</sub> followed by calcination at 700 °C. The oxidation state and binding energy of the metal ions were calculated with the help of XPS study.
- xiv. The catalyst was reused successfully for transesterification reaction in four catalytic cycles without any significant loss in activity with minimum metal ion leaching.
- xv. Leaching of the metal ion from the catalyst and structural changes was established as major reason for the loss in activity (5th cycle onward), although, leached metal ions was not found to show any homogeneous contribution.
- xvi. **In chapter 7**, sodium impregnated CaO/Fe<sub>3</sub>O<sub>4</sub> magnetic solid catalyst has been prepared and employed for the transesterification of waste cotton seed with methanol and ethanol, to obtain > 99% fatty acid alkyl ester yield.

- xvii. The structure of the catalyst was established by powder XRD study, surface morphology by FESEM and particle size by HRTEM study.
- xviii. The optimized catalyst was reused successfully for transesterification reaction in seven catalytic cycles without any significant loss in activity and partial metal ion leaching was found after every cycle.

The activity of the prepared catalysts, reported in present thesis are compared in Table 8.1.

**Table 8.1. Optimized reaction parameters<sup>#</sup> to obtain the complete transesterification (> 98% FAAEs yield) of WCO.**

| Catalyst  | Alcohol / oil molar ratio | FFA tolerance (wt %) | Reusability    | Reaction time (h) | Activation energy (kJ mol <sup>-1</sup> ) |
|---|---------------------------|----------------------|----------------|-------------------|---|
| <b>20-KF/CaO/NiO-700</b>                        | 15:1                      | 5.8                  | 4              | 4                 | 41.2                                      |
| <b>3-Li/CaO</b>                                 | 12:1                      | 8.3                  | Not calculated | 0.75              | Not calculated                            |
|   | 12:1*                     | 3.4*                 | 4              | 2.5*              | 70*                                       |
| <b>5-Li/NiO-600</b>                             | 12:1                      | 8.3                  | 5              | 1                 | 37.0                                      |
|   | 12:1*                     | 8.3*                 | 7*             | 3*                | 74.2*                                     |
| <b>20-W/Ti/SiO<sub>2</sub>-700</b>              | 30:1                      | 4                    | 5              | 4                 | 46.2                                      |
| <b>4-Na/CaO/Fe<sub>3</sub>O<sub>4</sub>-600</b> | 9:1                       | 8.3                  | 7              | 1.5               | 37.8                                      |
|   | 9:1*                      | 8.3*                 | 7*             | 2.5*              | 39.5*                                     |

<sup>#</sup>Optimized reaction temperature and catalyst concentration for all reactions are 65 °C and 5wt%, respectively; \* Ethanolysis.

Thus, all prepared catalysts have shown excellent activity and have the potential to use waste cooking oil and/or high FFA containing non-edible oil as feedstock for biodiesel preparation.

### 8.4 Futuristic aspects

In the present thesis, mixed metal oxide catalysts have been prepared and used as heterogeneous catalysts for the transesterification of triglycerides. Few futuristic suggestions related with the present work are listed below:

- i. In future, Zr, Mo and La doped mixed oxide catalysts will be prepared and used for simultaneously esterification and transesterification reactions.
- ii. Prepared mixed oxide catalyst will be tested for other organic reactions e.g. amidation, epoxidation etc.
- iii. Shape selective magnetic catalysts will be prepared for biodiesel production to simplify the separation process.
- iv. Other heating methods, such as microwave heating, will be used to reduce the reaction time and production cost.

## **List of publications**

1. **Kaur, M.; Ali, A.** “*Transesterification of waste cottonseed oil using KF Impregnated CaO/NiO as reusable solid catalyst: Reusability & Kinetics*”.  
*Euro. J. Lipid Sci. Technol.*, **2014**, 116, 80-88.
2. **Kaur, M.; Ali, A.** “*Ethanolysis of waste cottonseed oil over lithium impregnated calcium oxide: Kinetics and reusability studies*”.  
*Renew. Energ.*, **2014**, 63, 272-279.
3. **Kaur, M.; Ali, A.** “*Lithium ion impregnated calcium oxide as nano catalyst for the biodiesel production from karanja and jatropha oils*”.  
*Renew. Energ.*, **2011**, 36, 2866-2871.
4. **Ali, A.; Kaur, M.; Mehra, U.** “*Use of immobilized Pseudomonas sp. as whole cell catalyst for the transesterification of used cottonseed oil*”.  
*J. Oleo. Sci.*, **2011**, 60(1), 7-10.
5. **Kaur, M.; Ali, A.** “*An Efficient and Reusable Li/NiO Heterogeneous Catalyst for the Ethanolysis of Waste Cottonseed oil*”.  
*Euro. J. Lipid Sci. Technol.* (Just Accepted)

## **Patent filed**

**Kaur, M.; Ali, A.**, A solid catalyst for biodiesel production and a process for its preparation (*patent application no 2358/DEL/2012*).

## **Manuscripts under preparation**

1. **Kaur, M.; Ali, A.** “*Synthesis of Novel flower shaped Tungsten Supported Ti/SiO<sub>2</sub> Mixed Oxide Catalyst for Biodiesel production and polymerization of Triglycerides*”.
2. **Kaur, M.; Ali, A.** “*Preparation of alkali metal impregnated Cube shaped Fe<sub>3</sub>O<sub>4</sub> nanoparticles for Biodiesel Production*”.
3. **Kaur, M.; Ali, A.** “*Tungsten and Molybdenum Impregnated Nano Silica for Transesterification of waste cooking oil*”.
4. **Kaur, M.; Ali, A.** “*Application of Sulphonic acid functionalised nano silica as catalyst for biodiesel production*”.

## **Papers in proceedings**

1. **Kaur, M.; Kumar, D.; Ali A.**, “*Physicochemical properties of biodiesel prepared from Jatropha and used cottonseed oil in the presence of Li/CaO solid catalyst*” *Advances in Chemical Engineering* 2011, Macmillan 2<sup>nd</sup> edition, 315-323.
2. **Kaur, M.; Ali A.**, “*Molybdenum impregnated nano silica used as heterogeneous catalyst for biodiesel production*” *International conference on Bioenergy, Environment & Sustainable Technologies (BEST-2013)* (ISBN 978-81-926424-0-6).